UNCLASSIFIED

AD NUMBER

AD821476

NEW LIMITATION CHANGE

TO

Approved for public release, distribution
unlimited

FROM

Distribution authorized to U.S. Gov't.
agencies and their contractors;
Administrative/Operational Use; Feb 1967.
Other requests shall be referred to Naval
Air Systems Command, Washington, DC 20360.

AUTHORITY

US Naval Air Systems Command ltr dtd 26
Oct 1971

STUDIES OF CERAMIC PROCESSING (U)

FINAL REPORT

December 15, 1965 to February 15, 1967

by

E. J. Smoke
P. L. Fleischner
W. C. Jacobs
D. R. Mangino

by the

School of Ceramics

Rutgers, The State University

New Brunswick, New Jersey

Qualified Requesters May Obtain Copies Of This Report
Direct From the Defense Documentation Center
Station, Alexandria, Virginia

Distribution of this Report is Unlimited.

AD821476

STUDIES OF CERAMIC PROCESSING

R. J. Smoke, P. L. Fleischner, W. G. Jacobs and D. R. Mangino

School of Ceramics

RUTGERS • THE STATE UNIVERSITY

Abstract

The object of this program is to improve the structure of ceramics by processing. The overall temperature range of interest is 1800°F to above 3000°F. In the high portion of the range, 3000°F and above, spinel $MgO-Al_2O_3$ is presently under study. The parameters have been established for preparing suitable starting materials. Pure alums which by proper heat treatment result in the formation of ultra fine, pure magnesia and alumina, have been studied along with the formation of spinel. DTA, TGA, X-ray, electron microscopy, etc., have been utilized. Three compositions are of particular interest namely. $0.9MgO \cdot 1.0Al_2O_3$, $1.0MgO.1.0Al_2O_3$ and $1.0MgO \cdot 0.9Al_2O_3$. They have been studied as starting materials prereacted over the temperature range 950-1200°C and as bodies made of these prereacted materials and fired over the range 1370-1650°C. The intermediate temperature range 2600-3000°F, was studied utilizing the presintering approach to the prereacted raw materials technique and the results were reported in earlier reports. The low range, 1800-2600°F, was studied using the devitrification approach of the prereacted raw material technique. Cordierite is the crystalline phase of particular interest because of its low thermal expansion. The one-glass and the two-glass approaches have been studied. Processing, structure and properties are presented and compared.

TABLE OF CONTENTS

TABLE OF CONTENTS (Continued)

Page

LIST OF FIGURES

LIST OF FIGURES (Continued)

LIST OF TABLES

I. INTRODUCTION

This research program is directed toward a study of materials and processes by which ceramics suitable for radome applications can be processed at temperatures considerably lower than their maximum use temperature. The basis for the effort reported herein was established under Contracts NOw-64-0040-d and NOw 65-0199-d. The temperature range that can be studied is from the melting temperature of the most refractory crystalline phases showing promise of meeting the prime requirements, to as low as 1800°F.

The overall temperature range has been divided into three narrower ranges: 3000°F and above, 2600 to 3000°F, and 1800 to 2600°F. In the highest range, a sintering study of pure alumina was completed and reported in the Final Reports of the above mentioned contracts. Spinel $MgO-Al_2O_3$ which is more refractory than alumina is presently under study.

In the 2600 to 3000°F temperature range, the most promising approach is the prereacted raw materials technique using high alumina compositions. This area has been studied extensively and is reported in previous contracts. In the lowest temperature range, 1800 to 2600°F, the "two-glass system" of the devitrification approach to the prereacted raw materials technique is being studied. In this method two compositions are prepared and mixed separately on an atomic basis by melting and fritting. These frits are mixed in specific ratios, then ground to a controlled particle size distribution conducive for processing by conventional ceramic processes such as casting, pressing, etc. During firing one frit devitrifies to form the principal crystalline phase, while the second promotes sintering and supplies the bond. Some frits used in this latter manner have been designed to devitrify after performing the sintering and bonding functions. Cordierite, $2MgO.2Al_2O_3.5SiO_2$, is the crystalline phase presently under investigation and is supplied by the first frit. The second glass is of the alkaline earth (BaO, MgO, CaO) aluminosilicate type. Some preliminary results as to the microstructure resulting from this two glass approach indicates that the one glass system in which the whole composition is fritted into one glass, should result in a better structure. The one glass approach has also been studied. A comparison of the results of both approaches will be presented.

II. SINTERING STUDIES

A. Introduction

Spinel is a family of compounds of the $RO.R_2O_3$ type. It is generally identified by the compound $MgO.Al_2O_3$ which is the most stable in the family. Its melting temperature is 2135°C and exceeds that of alumina by 85°C. Its density is 3.57 gr/cc which is 10% less than that of alumina. It is chemically inert and stable, and possess good electrical and mechanical properties. Further, substitution for the divalent and trivalent ions can be accomplished quite readily, and latter parameters can be varied and thus engineering properties. Also, the binary from spinel to magnesia exhibits a rather steep rise in melting temperature. The latter factors can only be important after the sintering characteristics of pure spinel are understood.

The overall object of this phase is to study the sintering characteristics of pure spinel in an attempt to realize a find grained structure at theoretical density, and to determine the engineering properties and their uniformity. The immediate objective is to determine the parameters necessary to produce a reactive starting material or prereacted raw material, and to determine its characteristics including sinterability.

B. Literature Survey - Methods for Forming Spinel

Spinel has been prepared by a wide variety of techniques which may be divided into six categories. They are: (1) mechanically mixed oxides, (2) mechanically mixed oxide producing materials, (3) coprecipitation or chemical mixing, (4) fusion and crystal growth from melts, (5) vapor transport, and (6) hydrothermal synthesis. The first four result in a material which is formed into specimens and fired to form the spinel.

The following literature search has been arranged chronologically within each subtitle in order to indicate the development of each synthesis method.

1. Mechanically Mixed Oxides

The most direct method of producing $MgAl_2O_4$ is the combination of MgO and Al_2O_3 and reacting at elevated temperatures. Particle size, intimacy of mixing and environmental conditions were of major importance in the synethesis reaction.

Jander and Stamm [17] first made a detailed study of the synthesis of spinel in 1931 and developed a synthesis based on conductivity and diffusion measurements. In 1935 Bazilevich [2] synthesized spinel at a temperature of 1750°C by reacting coarse powders of the two oxides. Hauptmann and Novak [12] synthesized spinel from the oxides at 1200°C. They found at this temperature that long periods of time were required for reaction. Chesters and Parmelee [5] found that an addition of fluxes such as 2% B_2O_3 would lower the temperature of the synthesis of spinel. In their studies in synthesis temperature was reduced from 1500°C to 1300°C. X-ray diffraction and measurements of expansion were used to determine the formation of spinel. Huttig [15] and co-workers published two review articles and a proposal for a reaction mechanism theory in 1935. $MgAl_2O_4$ was one of many spinel compositions discussed. Synthesis of $MgAl_2O_4$ oxides in the temperature range 1000°C to 1200°C was investigated by Nakai and Fukami [20] in 1936. Jander and Pfister [16] studies the synthesis of $MgAl_2O_4$ using reactive forms of the oxides. In so doing spinel could be formed at 920°C using the oxides in the form of fine powders. One year later in 1939 Suzuki [30] prepared spinel and studied the mechanical properties, refractoriness and load bearing capacity of this material. Natural materials were used for the preparation. An enhanced rate of synthesis of spinel in alkaline environment was studied by Noda and Hosegawa [22]. In addition to the alkali and alkaline earth vapors it was found that significant spinel crystallization occurred in an atmosphere of free fluorine vapor. During a study of the corrosive resistance of $MgAl_2O_4$ refractories, Suzuki and Fujita [32] found that the formation of spinel was substantially increased in the presence of fluxes, such as H_3BO_3 and halides, such as NH_4Cl. Tenaka [33] showed that the spinel structure was maintained over a wide Mg:Al ratio in a solid reaction study. The compositions were prepared at temperatures ranging from 1000°C to 1400°C. In 1944, Castell, Dilnot and Warrington [4] investigated the formation of $MgAl_2O_4$ in the presence of metallic magnesium and found that the synthesis was 65% complete in the presence of excess Mg at 1150°C. However, only 20% yield was obtained when excess magnesium was absent. Geller, Yavorsky, Steierman and Creamer [9] synthesized spinel from large grain oxides in 1946. Their work showed that a yield of 80% to 90% spinel from the component oxides required a pre-reaction temperature of 1650°C. In an x-ray diffraction study conducted by Verwey and Heilmann [35] it was determined that several hours of heating were required at temperatures ranging from 1200°C to 1400°C to form various spinels from their respective oxides. In 1947 Rudorff and Reuter [27] using fine grain oxides, synthesized a series of magnesia spinels at temperatures ranging from 900°C to 1600°C.

Fine grained materials and a greater intimacy of mixing were indicated to enhance the synthesis. Further synthesis information was obtained by Schikore and Redlich [29], 1948, during a study in which a synthesis temperature of 1200°C was used. A review of the synthesis technique used for preparing spinels was published by Hauffe and Pschere [11] in 1950. Hanna [10] (1963) produced spinel by hot pressing. During a study of the properties of spinel in 1965, Allen [1] prepared spinel at a temperature of 1650°C from chemically pure oxides mixed either in alcohol or water. He also prepared spinel from an aqueous mixture of various salts including the sulfates.

2. Mechanically Mixed Oxide Producing Materials

Spinels have been formed from mechanical mixtures of materials which upon heating dissociate to form highly reactive oxides. Carbonates and nitrates are examples. The lowering of the synthesis temperature in procedures employing such dissociation products is related to the highly reactive state of the oxide at the time of dissociation.

Hedvall [13] was probably the first investigator to employ this technique for the preparation of spinels. A summary of this technique appears in his publication "Reaktionsfahigkeit" fester Stoffe." Based in part on Hedvall's work, Froelich [8], in 1925, prepared spinel from its sulfates for a starting material for growing gem stones. Three years later Posnjak [25] prepared spinel by reacting a mixture of aluminum oxide and magnesium carbonate. In 1930 Passerini [24] prepared spinel from a mixture of nitrates or hydorxides at 800°C.

3. Coprecipitation of Chemical Mixing

Coprecipitation or chemical mixing is a technique used to achieve a maximum of mixing between reactants. Generally salts, which form oxides when heated, are suspended or dissolved in water. Coprecipitation of the reactants is initiated by addition of a precipitating agent or by drying. The precipitate is then fired resulting in the formation of spinel.

Sullivan [30], 1953, prepared $MgAl_2O_4$ spinel by coprecipitating the hydroxides from solutions of magnesium sulfate and aluminum sulfate. Precipitation was activated by an addition of NaOH. When heated to 400°C, this mixture yielded diffuse x-ray diffraction patterns of spinel. Well defined patterns

were obtained only when the material was fired between 800°C
and 1000°C for a duration of 1 to 25 hours. Kreigel and Choi[19]
formed spinel, by coprecipitation, for feed material in a hot
pressing study. Reagent grade magnesium chloride and aluminum
chloride were mixed in aqueous solution and precipitated by
NH_4OH. The resulting gel, when heated to a temperature ranging
from 850°C to 860°C for a duration of 24 hours, yielded a fluffy
white powder with an average particle size of 40 microns.

4. Fusion and Crystal Growth from Melts

The synthesis of spinel which includes fusion of the material
may be divided into two categories. These are 1) flame fusion
and other allied processes and, 2) the drawing or growing of
crystals from melts. In 1931 Holgersson [14] used a fusion method
for growing single crystals of spinel. Verneuil [33] used his
well known flame fusion process to produce single crystal "boules."
In the case of spinel excess Al_2O_3 is generally present. In 1934,
Clark, Howe and Badger [6] formed polycrystalline spinel in vary-
ing Mg:Al ratios in a carbon arc. This material prepared by
fusion by Beregnoi and Sloneinskayn [3] and various physical pro-
perties were studied at high temperatures. In 1946-47 Noguchi [23]
also accomplished this same feat by fusion at 2200°C. Kordes and
Becker [18] did so by crystallizing from lead metaborate melt, in
1949.

5. Vapor Transport

Vapor transport mechanism has been used to form many ceramic
materials. The mechanism is dependent primarily on temperature,
pressure and atmosphere. Navias [21] apparently is the only in-
vestigator to use this technique to prepare $MgAl_2O_4$. In his
study layers of the compound were formed on both single crystal
and polycrystalline Al_2O_3 by transporting Mg vapor through various
atmospheres. Due to the diffusion mechanism a range of stoichio-
metry was obtained.

6. Hydrothermal Synthesis

A Morey 'bomb' is the reaction vessel used for hydrothermal
synthesis. Water and reactants are sealed into the 'bomb' which
is then zone heated. The reactants are preferentially deposited
in the cooler temperature zones by hydrothermal transport. Spinel
was prepared by this method in 1953 by Roy, Roy and Osborn [26].

7. Conclusions

The first two methods which entail the mechanical mixing of the raw ingredients result in rather poor mixing because of particle size, agglomeration, moisture content, etc. Vapor deposition would result in rather poor uniformity because of the mechanism in diffusion and size of initial particles or grains would be extremely important. Hydrothermal synthesis, fusion and growth from a melt would roughly result in larger crystals, and particle size reduction and accompanying contamination would cause problems. The best approach by far appears to be some ramification of coprecipitation and chemical mixing. Prereaction is a term coined at Rutgers. Its objective is to realize more intensive mixing by any means and thus to improve structure. For this spinel study it could embody chemical mixing.

C. Experimental Approach

In order to attempt to mix the ingredients to form spinel as thoroughly as possible, pure alums of magnesia and alumina were selected. Their compositions are as follows: $MgSO_4 \cdot (NH_4)_2 \cdot 6H_2O$ and $Al(SO_4)_2 NH_4 \cdot 12H_2O$. They are water soluble; thus they can mix as solutions. On heating the dried mixture, both compounds melt at relatively low temperatures and mix as liquids. They remain as liquids until dissociation into the oxides at which point the reaction should be complete and the spinel particle size extremely small and reactive. Three compositions were selected for study namely: $MgO \cdot Al_2O_3$, $0.9MgO \cdot Al_2O_3$ and $MgO \cdot 0.9Al_2O_3$. The compositions with excess Al_2O_3 and MgO over stoichiometry were evaluated to detect their effect on maturity and whether they might perform as grain growth inhibitors. These three compositions were studies as per differential thermal analysis and thermal gravimetric analysis to establish composition, and also reactions during firing. From this information the three compositions were prereacted over a temperature range and analyzed for composition and particle size. They were then studied for sinterability. Specimens were formed and fired over a temperature range, then evaluated for bulk density, moisture absorption, composition, etc. From this information the best starting material was selected for a thorough sintering study of spinel.

D. Experimental Procedures and Results - Starting Material

1. Preparation of Raw Materials and Spinel Composition

Chemically pure grades of the two alums were procured from the Amend Drug and Chemical Company of New York. The Mg alum was supplied as a rough ground aggregate with pieces of crystal ranging as large as one half inch in diameter. The alum of Al was received as uniform spheres one eighth inch in diameter. Aqueous solutions of each were prepared. Two polyethylene tanks, with lids, having a capacity of 30 gallons each were filled with approximately 25 gallons of distilled water. A 15 amp 20 watt tube type submersion heater was placed in each tank and the temperature of the water raised to 45°C. Forty five lbs. of magnesium alum was added to one of the tanks and coded "M". Fifty lbs. of aluminum alum was added to the remaining tank and coded "A". Both were held at a constant temperature of 45° and agitated with laboratory Lightin mixer (type L) until all solids were in solution and continued for an additional 24 hours. The temperature in both tanks were reduced to 25°C and held constant at this temperature ($\pm$ 1°C) and agitation continued during this cooling period. Then 24°C was reached agitation was stopped and the blenders were removed.

Upon cooling a well defined crystalline precipitate formed on the floor and walls of tank "A". The precipitate layer adhering to the floor was 1/2" thick and covered the entire area. The formations on the walls consisted of small clusters of crystals ranging in size from approximately 1/4 in. to 1/2 in. in diameter. A precipitate also formed in tank "M" but to a lesser degree. No solids were observed in suspension or lying loose in the bottom of either tank. In both cases the solutions were transparent and colorless. Both tanks were maintained at 25°C for a period of 72 hours to allow the precipitation to reach equilibrium. At that time mild agitattation was started to reduce the thermal gradient between the top and bottom of the tank. Without agitation this gradient was 4.5°C; with agitation the gradient was reduced to less than 1°C.

Approximately 40 ml of each solution was decanted into a dense alumina crucible (pre-weighed). The exact weight of each solution was determined by weighing crucible and content. Evaporation of the solution during weighing was stopped or held to a minimum by covering with a watch glass. After the crucibles were weighed they were dried for 20 hours at 100° and at 120°C

for 4 hours. Both crucibles were then covered with dense alumina setters measuring 1.5" x 2" and placed in a globar furnace for calcination. Both crucibles were calcined to a temperature of 1300°C and held at this temperature for 1 hour. After the 1 hour soak the kiln was allowed to cool to 120°C over night. This temperature was maintained until the crucibles could be removed and weighed.

The residue of solution "M" was hard, crusty and difficult to remove from the crucible. Removal was accomplished by soaking in tap water resulting in the hydration of the MgO. Examination of the crucible after removal of the residual gave no indication of reaction between MgO and the crucible. Unlike the residue of MgO, that obtained for solution "A" was a fluffy white ash which readily disintegrated into a fine powder. No adherence between this ash and the crucible was observed.

The oxide to solution weight ratio was determined to be .0512 and .0437 for solution "A" and "M" respectively. Four separate determinations were made and a variation occurred only in the 5th decimal place (beyond significance). The presence of impurities was disregarded. Using these ratios it was calculated that 1991.5 g of solution "A" would contain 1 mol. (101.96 g) of Al_2O_3 and 923.13 g of solution "M" would contain 1 mol. (40.32 g) of MgO.

The three compositions, as noted above, were prepared. The molar formulations were: S, $1MgO.1Al_2O_3$; A, $1Al_2O_3.9MgO$ and M, $1MgO.9Al_2O_3$. The batch formulas were as follows: S, 923.13 g sol. "M" + 1991.5 g sol. "A"; A, 199.15 g sol. "A" + 830.82 g sol. "M" and M, 923.13 g sol. "M" + 1792.35 g sol. "A". Three separate batches of each composition were prepared due to limited capacity of the mixing container. The compositions were mixed as solutions in plastic containers, dried at 100°C until the mixture was a thick syrup. The three batches of each composition were then combined in one container and dried at 180°C for 48 hours. The residues which formed were white granular cakes. Each cake was broken and granulated in a dense alumina mortar and pestle to pass 10 mesh screen. The granulated material of each composition was stored in plastic bags.

2. Effect of Temperature

In order to determine the effect of firing on the dissocia-
tion of the alums and their interaction to form spinels, samples
of composition S and both the starting alums were studied by
DTA and TGA. Two instruments were used to obtain DTA data.
One of these was a Robert L. Stone (Model #G-S2). The second
unit was specially designed and consisted of a platinum wound
alumina muffle powered by a Wheelco, motor driven, saturable core
reactor. Temperature was sensed with Pt vs $Pt_{90}Rh_{10}$ thermocouples
and recorded on a Brown Electronik ZPT recorder. TGA measure-
ments were made utilizing this same heating chamber. Weight
measurements were made with a 2 pan analytic Voland & Sons balance
and recorded with a Fisher Recording Balance Control unit. The
heating rate was held at 5°C/min. Deviations from this heating
rate occurred in the temperature range 100°C to 300°C where the
heating rate dropped to 3°C/min. All DTA and TGA measurements
were qualitative in nature and only the temperature at which re-
actions occurred are precise values.

The DTA, TGA curves for the alum of magnesia, shown in
Figure 1 on page 10 indicate peaks for removal of mechanically
and chemically bound water, melting on the salt and dissociation
of the salt to the oxide. Moist litmus paper was used to de-
termine the pH of the effluent at each reaction. Tests were
neutral for all effluents below 350°C. Melting appears to be the
only effect taking place. The evolved gas at 380°C gave a posi-
tive reaction with red litmus and was identified to be ammonia.
The gasses removed at 470°C and 1120°C gave positive tests with
blue litmus. At the lower temperature some SO_4 is being driven
off while the remainder comes off at the higher temperature. The
remaining residue is magnesia. DTA and TGA curves for the alum-
inum alum are shown in Figure 2 on page 11.

Mechanical and chemical water were removed from the aluminum
alum below 520°C. Inflections in both the DTA and TGA plots in-
dicate melting of the alum at 340°C. The molten state persisted
until dissociation of ammonia at 540°C. A second dissociation
follows at 830°C. SO_4 is given off at this temperature leaving
a residue of Al_2O_3. Striking differences were apparent between
the plots of the individual alums and that obtained for the mix-
ture of the two as shown in figure 3 on page 12. Four peaks
appear between 100°C and 600°C. These indicate removal of mechan-
ically and chemically bound water. An inflection at 540°C in-
dicates the melting of the mixture. The salts remain molten until
dissociation curves at 800°C. At this temperature both ammonia

Fig. 1. DTA and TGA of MAGNESIUM AMMONIUM SULFATE $[MgSO_4 \cdot (NH_4)_2SO_4 \cdot 6H_2O]$
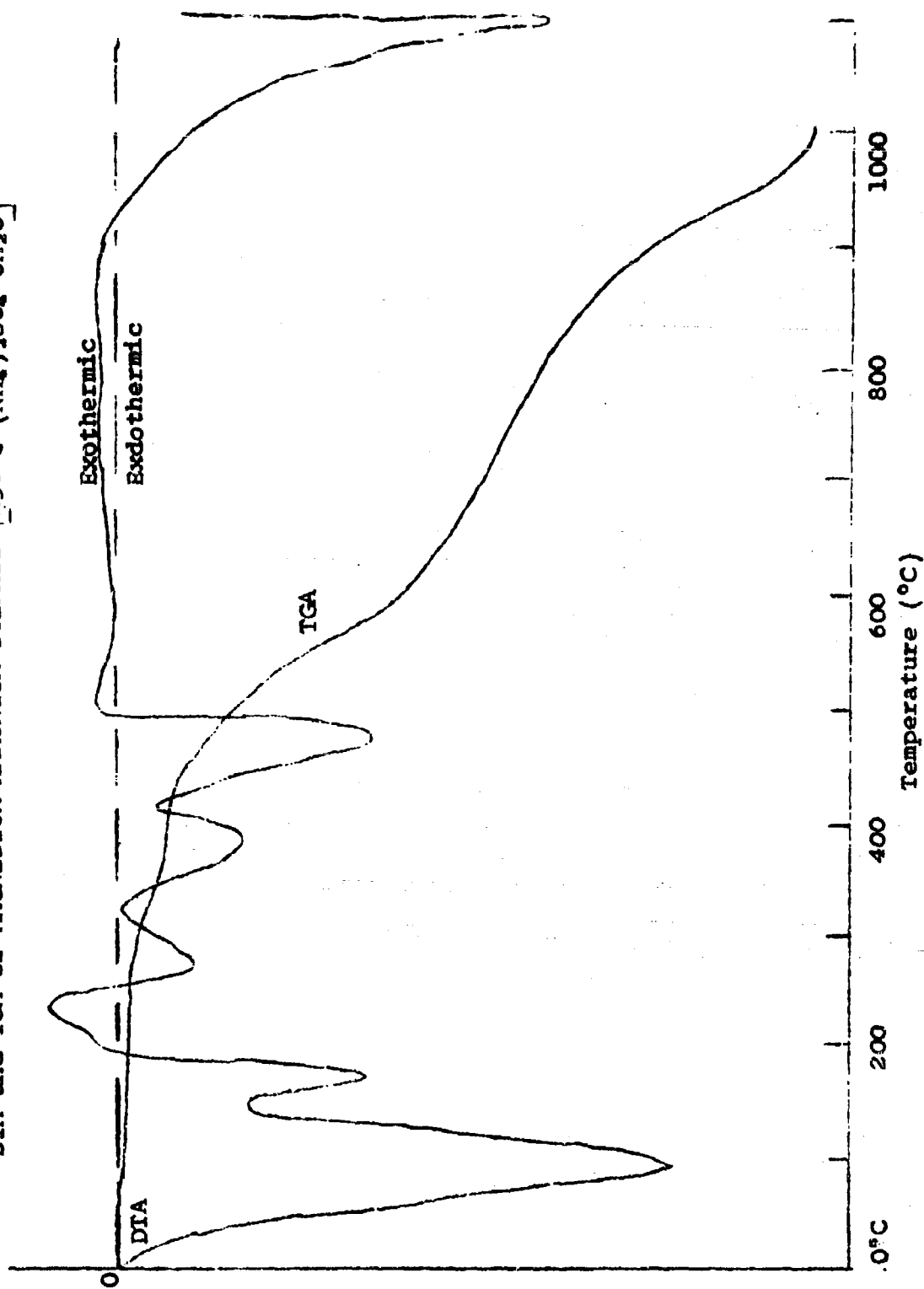
Fig. 2. DTA and TGA of ALUMINUM AMMONIUM SULFATE $[AlNH_4(SO_4)_2 \cdot 12H_2O]$

TGA

DTA

Exothermic

Endothermic

Temperature (°C)

0°C   200   400   600   800   1000
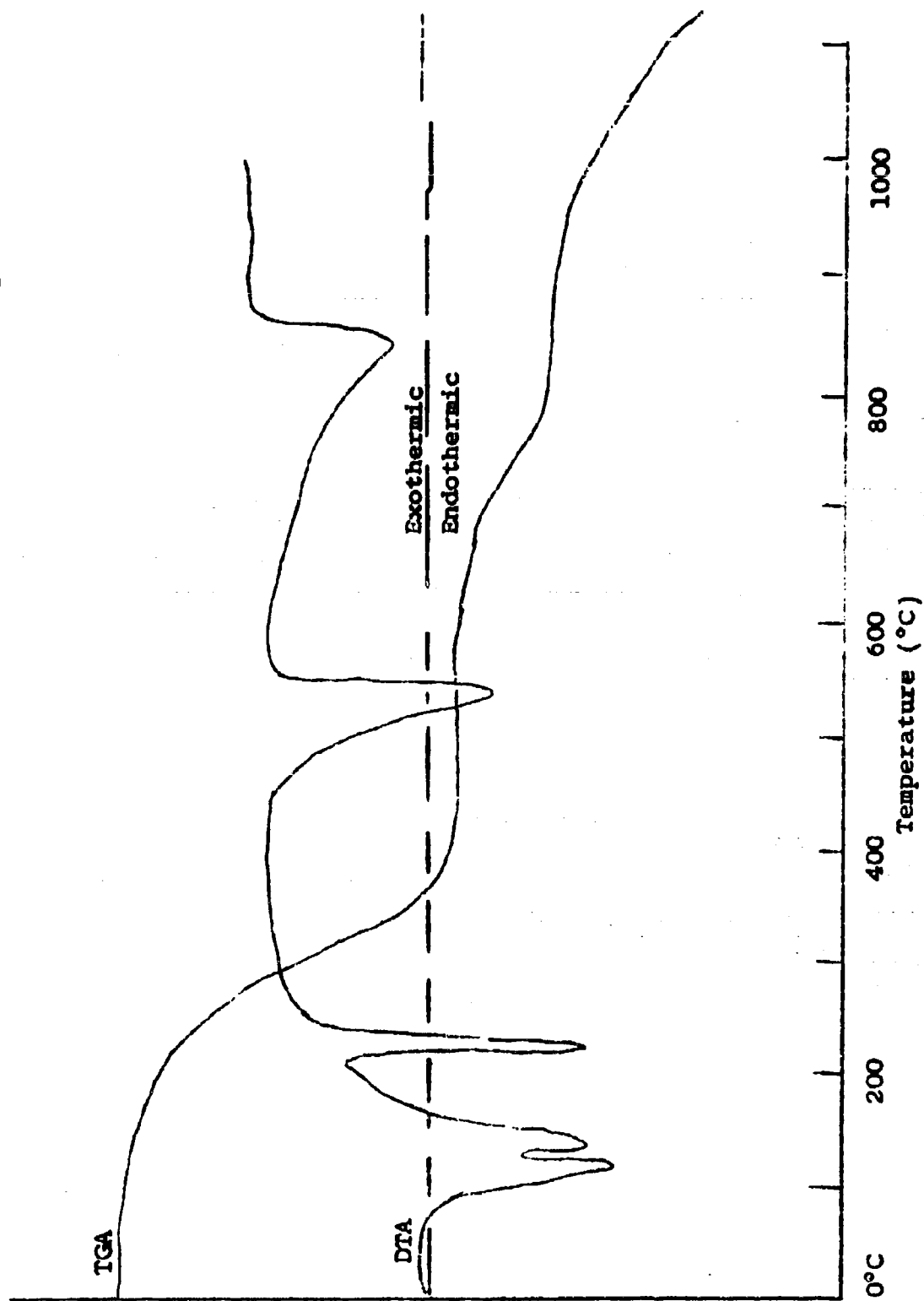
Fig. 3. DTA and TGA of MIXTURE of MAGNESIUM AMMONIUM SULFATE and ALUMINIUM AMMONIUM SULFATE which yields $MgAl_2O_4$
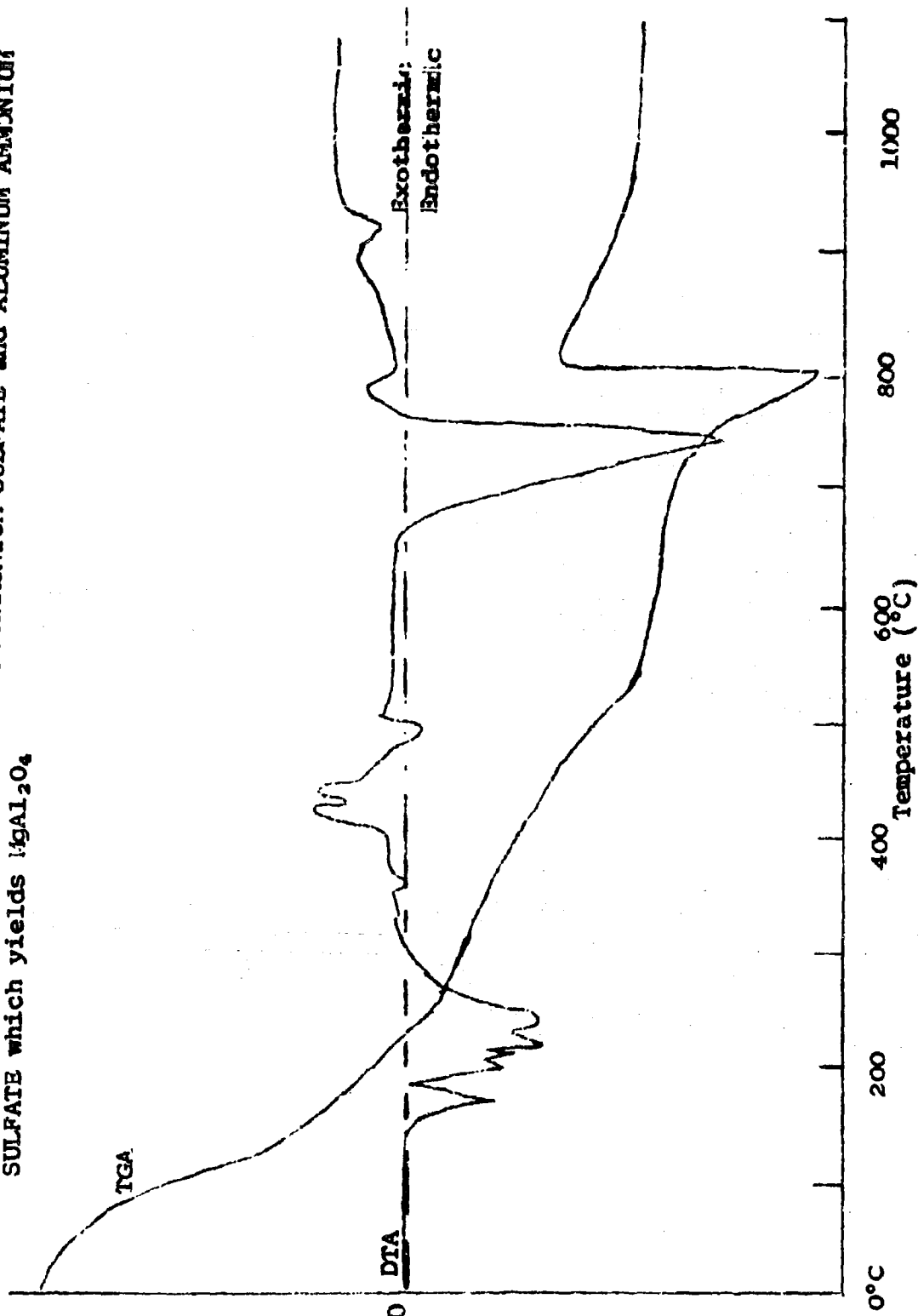
and SO_4 are given off. This dissociation is followed by a rounded peak, located at 910°C, which did not appear for either of the individual alums. This peak started while the dissociation products were being evolved from the reaction at 800°C. Neither an increase nor an inflection occurred in the TGA in this temperature region indicating no further dissociation. The peak at 910°C was identified as the formation of spinel.

Two explanations for the formation mechanism were proposed. The first of these is the spontaneous nucleation of spinel in an environment of highly reactive MgO and Al_2O_3 which were made available by dissociation at 800°C. Crystal growth continued at these nucleation sites as additional oxide material in the immediate vicinity adhered to the original nuclei. This premise is based on the assumption that the mixture of the alums dissociated into a highly reactive mixture of the individual oxides. The transformation would then be the formation of $MgAl_2O_4$ from an intimate mixture of its component oxides. The second explanation proposed is based on the assumption that a complex crystalline structure was formed during the coprecipitation of the mixture of the two alum solutions. The dissociation at 800°C removed ammonia and SO_4 leaving a metastable phase of $MgAl_2O_4$. This lattice may be characterized as being open and highly unstable. At 910°C this meta-stable structure undergoes a phase transformation to the stable face centered cubic structure of spinel.

These results indicate that the minimum temperature range for prereaction to form spinel should be 950°C. As to the maximum temperatures it is anticipated that above 1200°C the reactivity of the material will start to decrease and crystal size increase.

3. Prereaction Study

a. Procedure

Samples of the granular material of each of the three compositions were fired at 50° intervals between 950 and 1200°C. Since the reactants became liquid during the heating cycle, dense Al_2O_3 crucibles, with a capacity of 50 ml were used as reaction vessels and dense alumina setter tiles measuring 1.5" x 2" were used as crucible covers. During firing a tremendous volume expansion takes place and in order to prevent loss of material the crucibles were filled to only 2/3 capacity. Three crucibles containing composition S, A and M were fired simultaneously to each of the desired temperatures. Prereaction was carried out in the same globar kiln used to determine oxide content of the

solutions. Firing schedule, as noted in Figure 4 on page 15 was closely adhered to with a maximum variation of 20°C in the early stage of the firing schedule. The allowed variation was lessened as temperature increased to 800°C. At 800°C and continuing throughout the remainder of the firing schedules variation was within ±2°C.

b. Particulate Characteristics

The pre-reaction product was a fluffy white ash having a loosely sintered structure very similar in appearance to that of a natural sponge. This ash was readily removed from the crucible and disintegrated into a very fine powder under the slightest pressure.

Crystalline phases present were determined by x-ray diffraction using conventional powder techniques. A North American Philips X-ray diffractometer with vertical goniometer, (maximum 2-, 150°) and Brown Potentiometer (model P 53X12V-X-30y 10) strip-chart recorder, were used to obtain the diffraction patterns by scanning from 86° to 4° with instrument settings of: scalar, 1; multiplier, 8 and time constant, 1. The rate of scan was 1°/min.

Three representative x-ray diffraction patterns were obtained for the pre-reacted materials. The pattern, shown in Figure 5 on page 16 was obtained for all compositions which were fired to a pre-reaction temperature of 950°C. This pattern was compared with cards taken from the ASTM X-ray Powder Data File. All cards of compounds containing all or any of the materials known to be in the starting mixture or thought to be in the pre-reaction product, were consulted. A positive correlation was not possible. An x-ray diffraction pattern obtained for an unfired sample of the stoichiometric mixture, dried to 180°C, gave a positive correlation with the pattern of the material fired to 950°C. Identical x-ray diffraction patterns for both dried and fired samples supported the conjecture that a complex crystalline structure of the two alums had formed.

One pattern was obtained for compositions S and A pre-reacted to 1000°-1200°C. Positive correlation of this pattern was made with the pattern of (natural) spinel. Correlation was also made with synthetic spinel. The difference between these two patterns is line intensity.

Fig. 4. FIRING SCHEDULES for PRE-REACTION
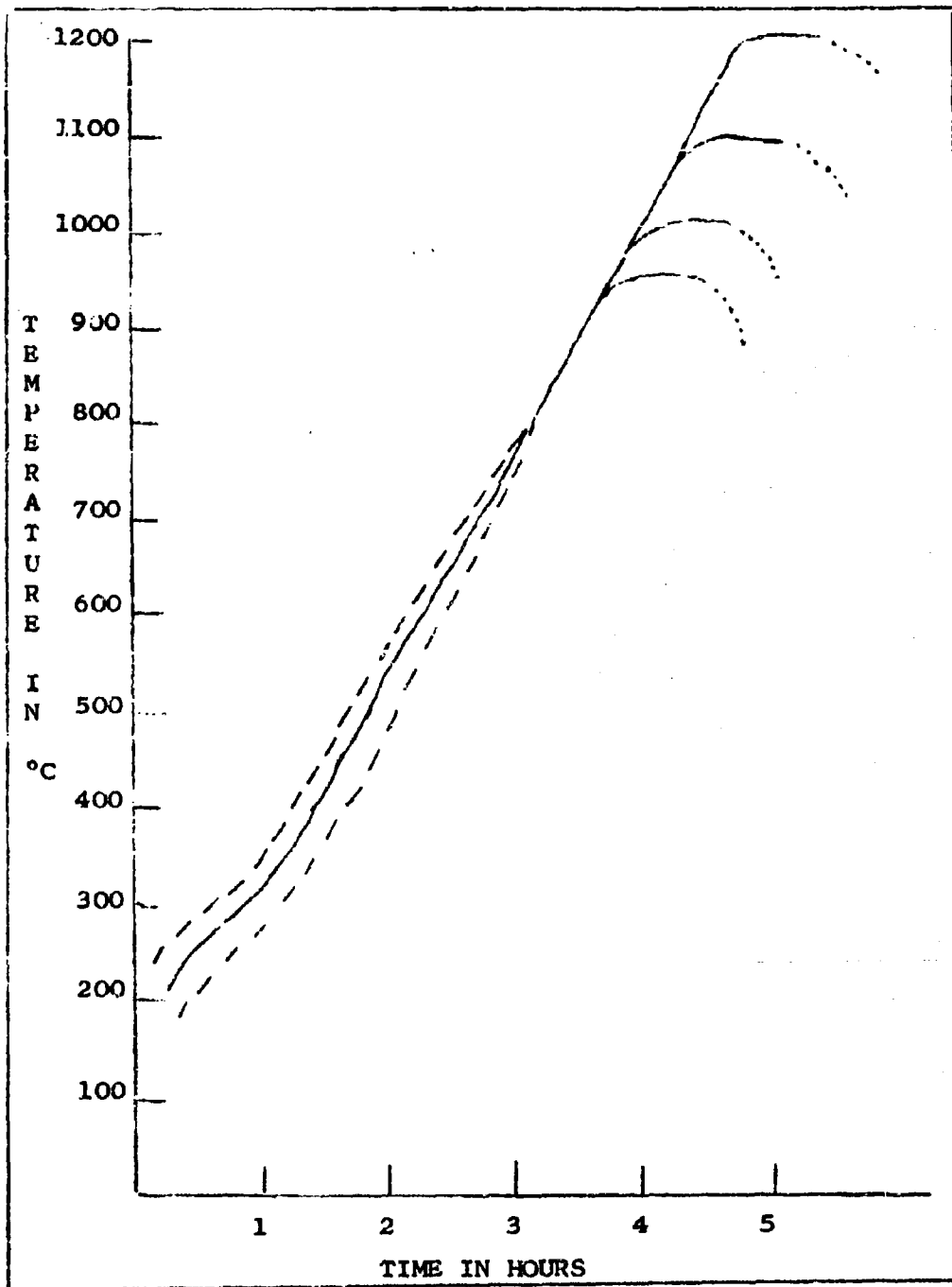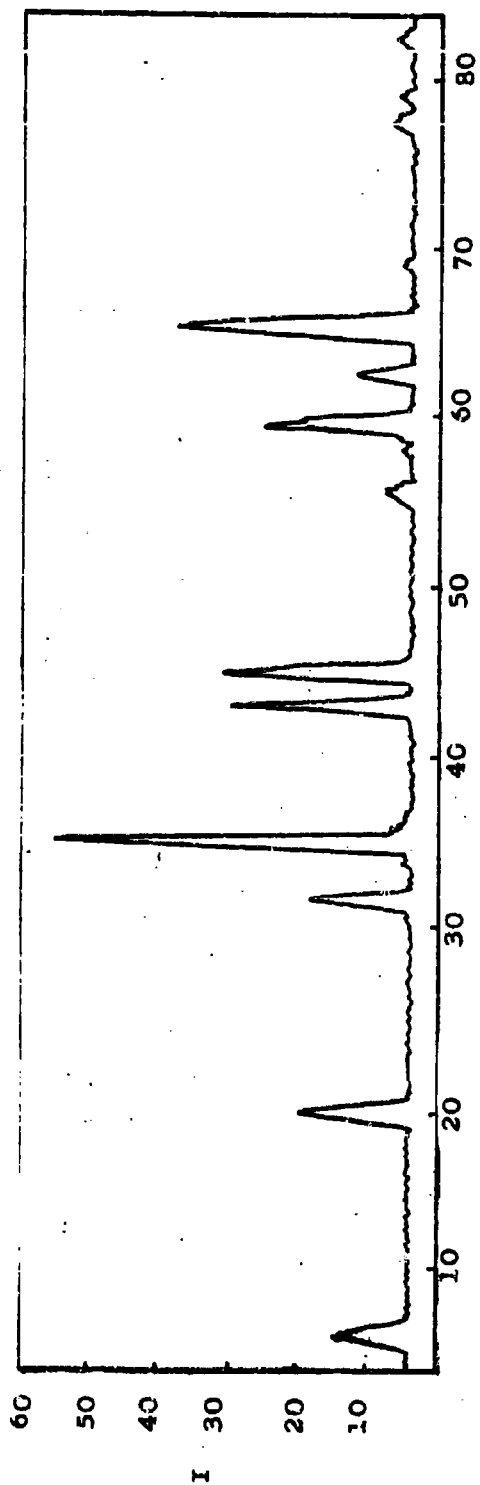
Figure 5 - X-Ray Pattern of Spinel
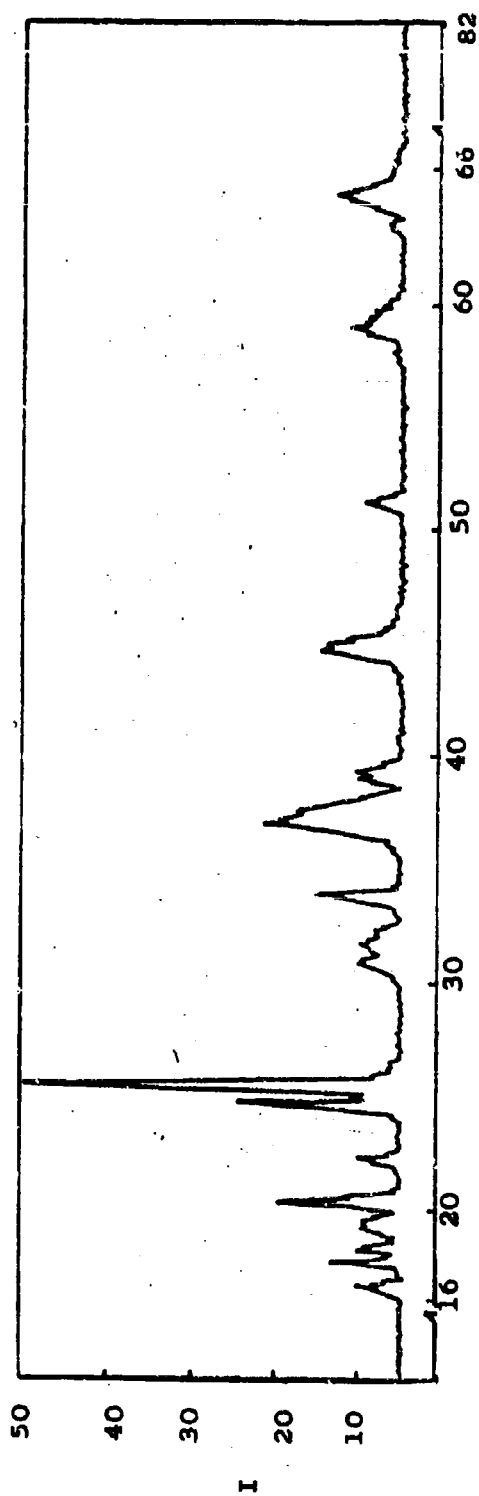
Figure 6.- X-Ray Pattern of Raw Spinel Composition

The x-ray diffraction pattern obtained for composition M, pre-reacted to 1000°C-1200°C, contained the spinel pattern as received for compositions S and A and two additional peaks. The two additional peaks were identified as major peaks of MgO.

The DTA information indicated that the formation of spinel occurred in the region of 910°C. The total width of the reaction peak in terms of temperature was 50°. This information indicated that the transition from starting materials to spinel was completed in the temperature zone 890°C-940°C. The x-ray data supports this statement. The diffraction pattern obtained for all compositions fired to 950°C only contain peaks for the complexed crystal of the two alums. A minimum of 2% of a material must be present in order to be detected by x-ray diffraction. Spinel peaks were not detected indicating that less than 2% spinel could be present. The same condition existed for the starting materials in the pattern obtained for materials pre-reacted to 1000°C-1200°C. Using these limitations the spinel formation was considered 98% complete at 1000°C on the basis of x-ray diffraction. The difference of temperature in detecting the reaction zone by DTA and x-ray diffraction is due to a difference in heating rate used to form the spinel; the faster the heating rate the higher the temperature of formation.

These x-ray patterns were also used to give some indication of the average particle size. The half height-width of the peak at 36° was used for this determination. Ten individual measurements of this width were made and the highest and lowest values obtained were used to determine B_e the effective broadening due to particle size in the relationship $B_e^2 = B_x^2 - B_s^2$. Using relationship $t = N / (B_e \cos \theta)$ and the maximum and minimum values for B_e the average particle size was determined to be 250 Å and 300 Å; thus the average particle size ranged from 250 Å to 300 Å.

A more direct means for measuring particle size and size distribution was the electron microscope. Copper-carbon substrates were procured and prepared in the following manner. An aqueous suspension containing .1% S-1100 composition was vigrously mixed for 1/2 hour in a plastic container and the resultant suspension was sprayed from a glass nebulizer onto substrates held one inch away; the spraying period was 90 seconds. A total of eight substrates were prepared. These were viewed with an Hitachi Electron Microscope (type HU-10). Single crystals were viewed in both light and dark field. Definition of the single particles was best in dark field. Figures 7 and 8 on pages

19 and 20 are electron photomicrographs of single crystal spinel viewed in dark field. Magnification is 20,000X and 10,000X respectively in these figures. Direct measurement of the glass negatives gave maximum diameter of 400 Å and a minimum of 50 Å. The greatest number of diameters measured were between 125 Å and 150 Å. Figure 7 is representative of the particle size distribution. Two photomicrographs had a particle size distribution shown in Figure 8 on page 20. Most of the particles ranged from 50 Å to 100 Å in this view.

The same suspension that was used to prepare the first eight substrates was used to prepare six additional substrates after a lapse of two weeks. The suspension was vigorously stirred prior to spraying. These substrates when viewed in light field indicated that agglomerates of the spinel powders had formed as noted in Figure 9 on page 21. The magnification of this view is 21,600 X. The largest agglomerate found measured approximately 890 Å to 900 Å in diameter and range down to 250 Å; the average is approximately 500 Å. Exact measurement of the diameter was difficult since the agglomerates appeared as spongy masses. The maximum diameter to minimum diameter for the individual particles of spinel was in the order of magnitude of 8:1 or 10:1. This uniformity in particle size made possible optimum sintering conditions.

Samples of magnesium alum, aluminum alum, pre-reacted powder and sintered discs, were submitted to Spectrochemical Laboratories Inc. (8350 Frankstown Avenue, Pittsburgh, Pa.) for chemical analysis. The analyses of these samples appear in Table I on page 22. Based on chemical analysis, the three compositions had actual molar formulas of: S, $1MgO \cdot 1.02Al_2O_3$; A, $1.02Al_2O_3 \cdot 9MgO$ and M, $1MgO \cdot .94Al_2O_3$. All three compositions were shifted toward higher alumina content. This was remedied for subsequent work so as to realize the absolute molar ratios.

Both starting materials were supplied as c.p. grade materials. Chemical analysis indicated that both had a purity of 99.9% excluding the presence of water which is driven off during calcination. The weight loss of approximately 90% associated with the spinel formation caused an increase in the impurity level. Both the pre-reacted powder and sintered samples exhibited a purity of 98.8%, the impurity content being 1.18%. The residual ammonia and sulfate was not significantly higher than any other impurity which remained after pre-reaction.
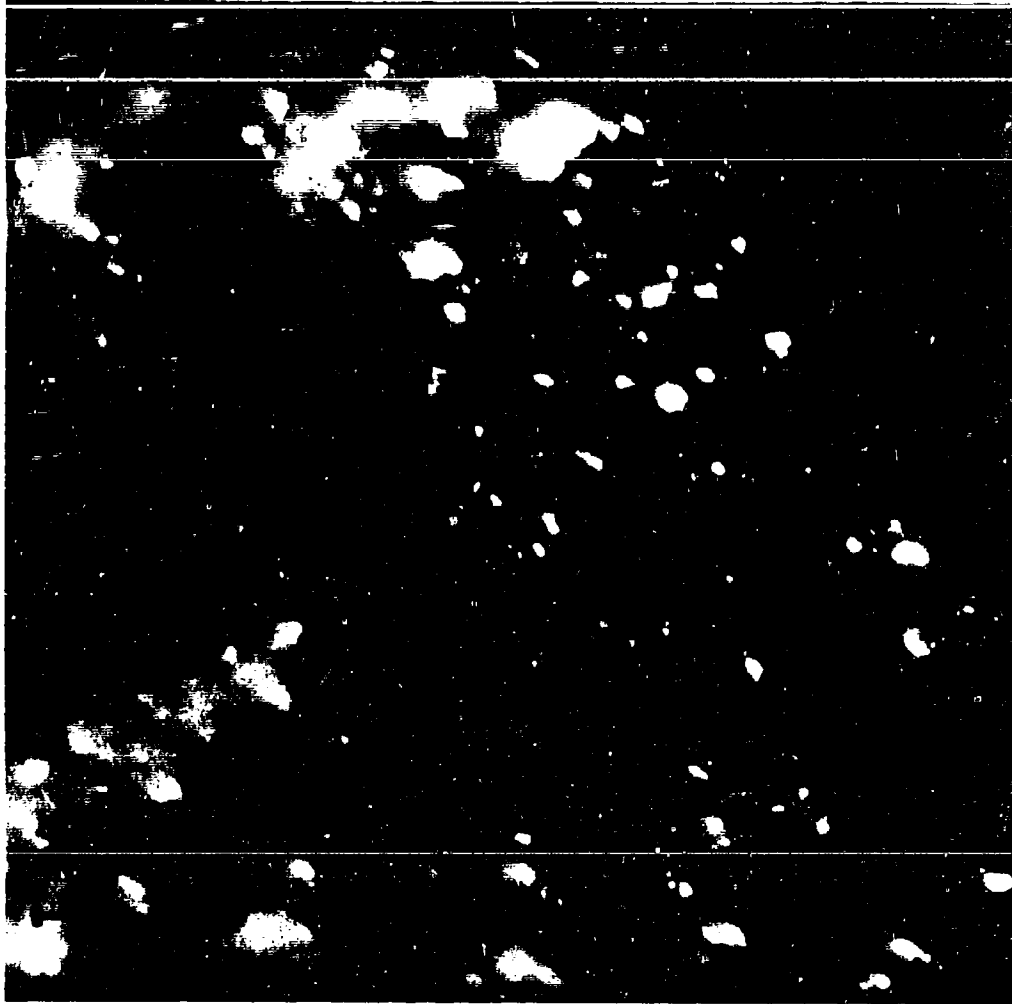
Figure 7 - Photomicrograph of S-1100

Individual Spinel Crystals
in Dark Field (20,000x)
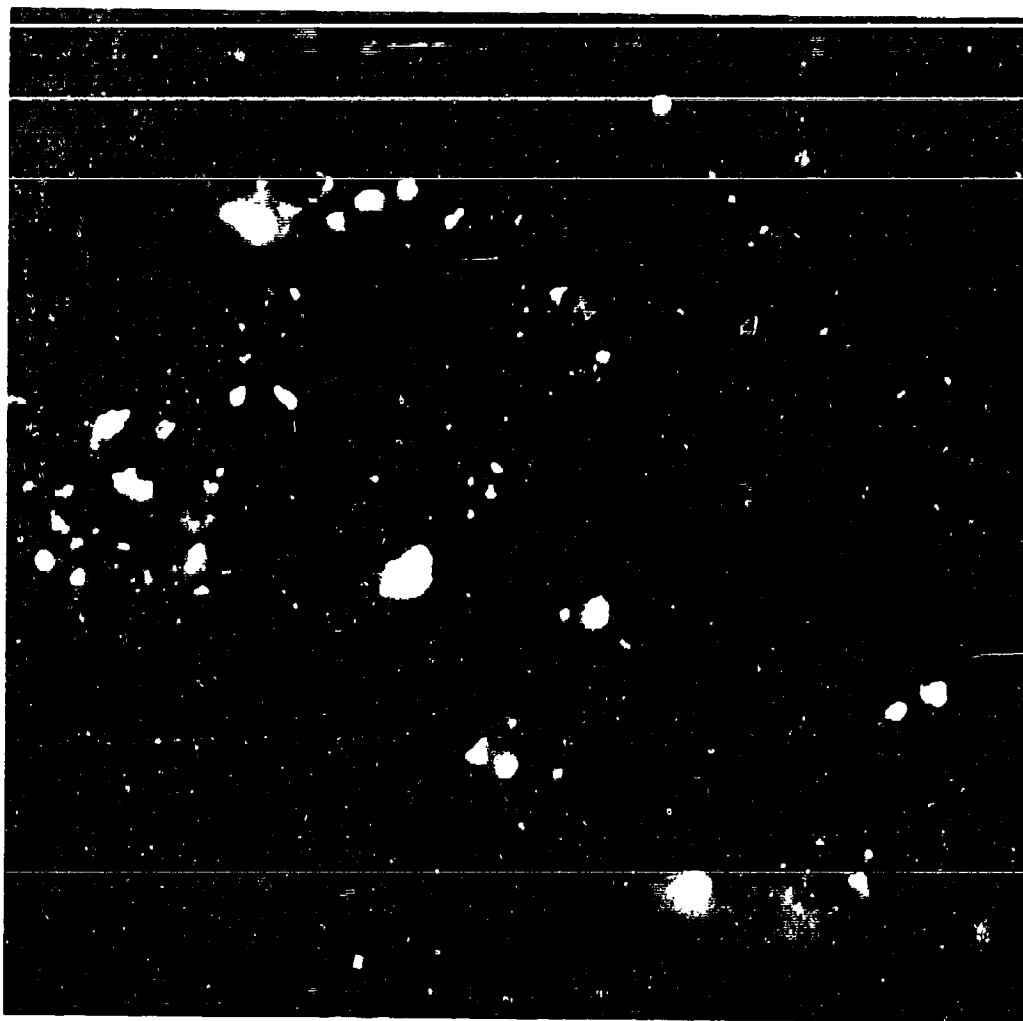
Figure 8 - Photomicrograph of S-1100

Individual Spinel Crystals
in Dark Field (10,000x)
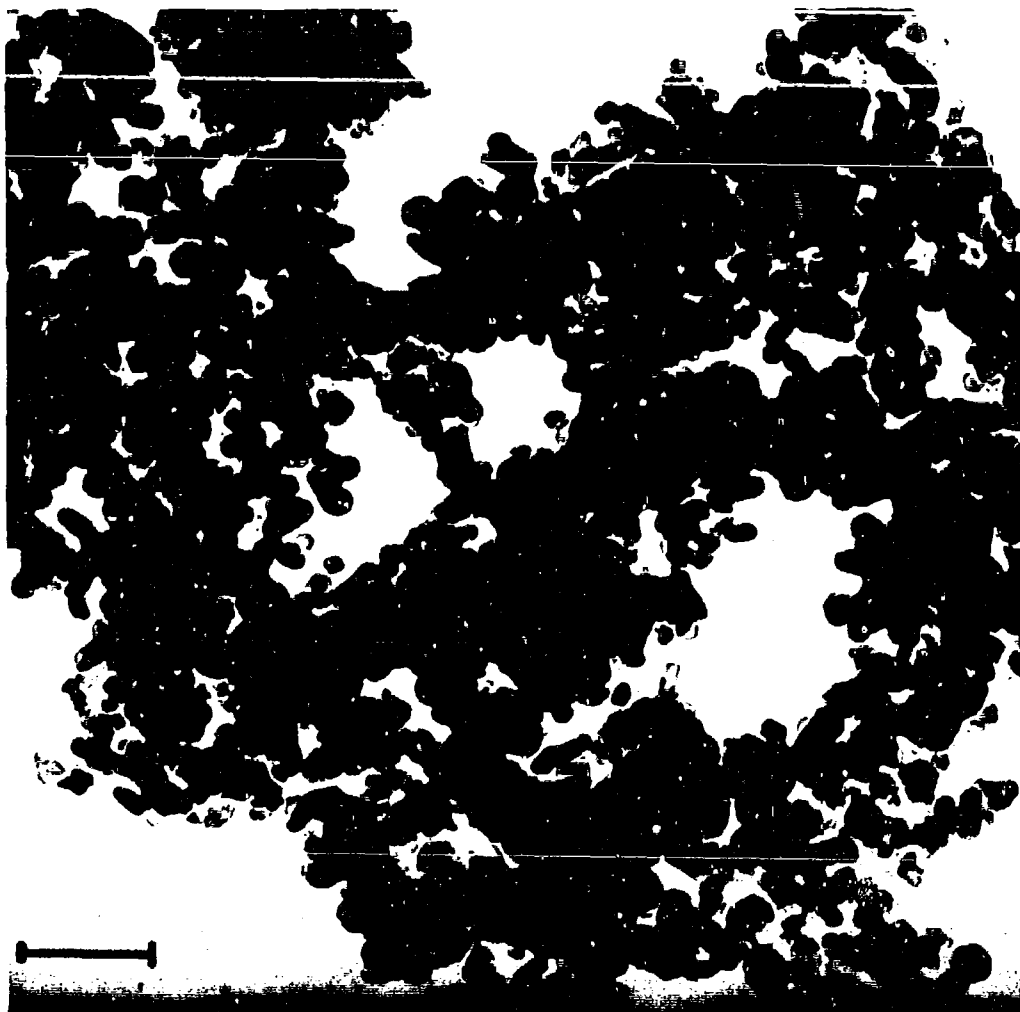
Figure 9 - Photomicrograph of S-1100

Agglomerates of Spinel Crystals
in Bright Field (21,600x)

TABLE I

Analysis of the Alums and Several Compositions

	Al alum	Mg alum	Pre-reacted	Sintered
SiO_2	.005	.03	.12	.17
Al_2O_3	11.92	.06	X	X
Fe_2O_3	.03	.02	.27	.29
Cr_2O_3	.001	*.001	.002	.004
L.O.I. at 500°	62.13	66.58	.24	.13
Na_2O	.001	.001	.18	.08
K_2O	.01	.005	.09	.002
Li_2O	*.001	*.001	.02	.002
CaO	.01	.01	.01	.01
MgO	.10	11.00	X	X
SO_4	42.06	52.55	.25	.11
Cl	*.01	*.01	*.01	*.01
FeO	*.01	*.01	*.01	*.01
NH_3	3.40	8.89		

*Not detected. The number indicates the minimum limit of detection.

XDetermined by composition (composition S: Al_2O_3, 72.47% MgO, 27.34%).

c. **Summary**

The above described procedure has resulted in the production of a pure, fine grained starting material which should be suitable for a sintering study. It is 98.8% pure and the impurities are fairly well known, and the crystallite size ranges from 50 to 400 Å with the average being approximately 150 Å.

B. **Experimental Procedure and Results - Sinterability of the Starting Material**

1. **Processing**

In order to determine the sinterability of the prereacted spinel starting materials it is necessary to form and fire specimens and to evaluate properties which establish the structure such as bulk density and moisture absorption. The eighteen composition-prereaction temperature combinations evaluated and discussed above as prevalent starting materials were studied as fired specimens.

Larger batches of each of the three compositions were prepared and fired to the six prereaction temperatures respectively.

Discs of these eighteen pre-reacted powders were prepared by pressing to a pressure of 10,000 psi in a steel die with a diameter of .634 in. Each disc contained .40 g of pre-reacted powder. Binder and water were not added to the powder for pressing. The punch and die were lubricated with a mixture of stearic acid and carbon tetrachloride. Discs prepared in this manner exhibited good green strength and no evidence of laminations was observed.

They were then sintered in a conventional gas fired kiln to six temperatures: 1370°, 1425°, 1485°, 1540°, 1595°, 1650°C. The firing schedule shown in Figure 4 on page 15 was closely adhered to with a maximum variation of ±5°C at temperatures above 1000°C. All specimens were set in high alumina combustion boats and left uncovered during firing. A setter sand was not used and no adherence between fired samples and the boats was evident. Firing shrinkage, moisture absorption and bulk density were the properties determined to evaluate the sinterability of these materials. The formulas used are as follows:

1. % Fired shrinkage = (given diameter - fired diameter) X 100)/ fired diameter.

2. % Water absorption = [(wet wt.-dry wt.) X 100]/dry wt.
3. Bulk density = (dry wt. X sp. gr. H_2O)/(wet wt. - sus-
   pended wt.).

The specific gravity of water was .9989.

2. Results and Discussion

The results are presented in Tables II, III, and IV on pages
25 through 29 and plotted in Figures 10 and 11 on pages 30 and 31.
The % fired shrinkage for all samples as high ranging from 7.6
to 5.7%. Those for the samples prereacted to 950°C was excessive
and were distorted for all sintering temperatures. The fired
shrinkage of the group of samples with a common pre-reaction tem-
perature and best density values, had a uniform shrinkage within
the respective groups. Thirty percent was the most common value
for the best set of prereaction and sintering temperatures.

The moisture abosrption ranges from a maximum of 0.5% down
to 0.001% over the firing temperature range studied. This range
includes all compositions and any combination of prereaction tem-
perature and sintering temperatures. This indicates the extreme
reactivity and sinterability of this type starting material.
Figure 10 on page 30 shows the effect of preaction temperature
and sintering temperature on this property for the three compo-
sitions. With composition 0.9 MgO.1.0 Al_2O_3, that is deficient
in magnesia, the sintering temperature must be above 1425° to
realize moisture absorptions below 0.02% with minimum variation
over the complete prereaction temperature range. Less variation
is realized by prereacting at 1000°C and above. At a sintering
temperature of 1650°C the moisture absorptions are beginning to
increase slightly. The same results were realized with the stoi-
chiometric compositions but with more stability as noted by the
rather flat curves. It is indicated that at the 1200° prereaction
temperature this property decreases at all sintering temperature.
It may be that higher prereaction temperatures would be advanta-
geous. Composition M, 1.0 MgO·0.9 Al_2O_3, which is deficient in
alumina is a very little more refractory or less reactive as noted
by the increased moisture absorption values vs firing temperature.
Also the effects at lower and the highest sintering temperatures
are exaggerated with respect to the other two compositions. This
very slightly increased refractoriness or decreased reactivity
is also noted by the increase in minimum moisture absorption values
as the magnesia ratio is increased from compositions A to S to M.
In general the prereaction temperature is effective with respect

TABLE II

Properties vs Prereaction and Firing Temperature
Composition A ($0.9MgO \cdot 1Al_2O_3$)

Linear Firing Shrinkage (%)

Sintering Temperature °C						
PREREACTION °C	1370	1425	1485	1540	1595	1650
950	14.8	41.8	42.7	43.7	54.6	48.1
1000	8.7	29.1	35.1	29.1	34.8	36.8
1050	9.4	34.8	29.1	27.0	31.2	29.3
1100	7.6	24.8	21.4	27.3	27.3	29.3
1150	9.0	19.1	31.2	32.6	32.0	29.9
1200	8.5	26.0	29.3	28.8	30.9	31.8

Moisture Absorption (%)

Sintering Temperature °C						
PREREACTION °C	1370	1435	1485	1540	1595	1650
950	.435	.086	.025	.026	.020	.026
1000	.144	.042	.002	.012	.003	.011
1050	.074	.014	.006	.001	.004	.005
1100	.163	.017	.002	.001	.003	.010
1150	.191	.057	.001	.002	.002	.010
1200	.172	.038	.0006	.002	.0006	.005

TABLE II (Cont.)

Sintering Temperature °C

Bulk Density (gr/cc) PREREACTION °C		1370	1425	1485	1540	1595	1650
	950	1.3897	2.9907	2.8906	3.2423	3.2453	3.2227
	1000	2.3033	2.9440	3.3234	3.2550	3.2867	3.1427
	1050	2.8366	3.2076	3.4114	3.5973	3.3691	3.2352
	1100	2.1932	2.9650	3.0876	3.2981	3.3560	3.3254
	1150	2.0354	3.2933	3.1444	3.2992	3.3166	3.2339
	1200	2.2563	2.4793	3.0017	3.3316	3.4075	3.4656

TABLE III

Properties of Prereaction and Firing Temperatures
Composition S (MgO.Al$_2$O$_3$)

Linear Firing Shrinkage (%)

Sintering Temperature °C

PRE REACTION °C	1370	1425	1485	1540	1595	1650
950	10.3	41.2	51.3	57.3	561.	50.9
1000	10.4	13.2	26.5	25.0	24.3	23.?
1050	10.8	32.0	36.3	36.3	39.0	34.8
1100	9.8	28.7	30.4	29.9	30.3	30.1
1150	6.7	16.7	39.8	30.9	33.1	28.3
1200	8.0	23.5	26.0	26.8	34.2	29.9

Moisture Absorption (%)

Sintering Temperature °C

PRE REACTION °C	1370	1435	1485	1540	1595	1650
950	.273	.141	.020	.022	.011	.022
1000	.208	.084	.013	.017	.003	.020
1050	.262	.039	.006	.014	.005	.018
1100	.192	.041	.007	.013	.005	.019
1150	.228	.044	.015	.019	.005	.024
1200	.217	.024	.004	.002	.008	.012

TABLE IV

Properties vs Presintering and Firing Temperature
Composition M ($MgO. 0.9Al_2O_3$)

Sintering Temperature °C

Linear Firing Shrinkage (%)

PRE REACTION °C	1370	1425	1485	1540	1595	1650
950	16.7	44.7	54.5	56.9	56.9	53.8
1000	16.4	28.4	27.3	29.6	26.1	24.3
1050	9.8	26.5	31.2	32.3	29.3	32.0
1100	9.1	25.7	28.6	28.8	27.8	25.5
1150	8.9	26.2	32.3	32.9	34.8	32.9
1200	9.1	27.3	31.8	32.6	32.4	32.3

Sintering Temperature °C

Moisture Absorption (%)

PRE REACTION °C	1370	1425	1485	1540	1595	1650
950	.515	.050	.002	.001	.002	.009
1000	.182	.049	.002	.002	.002	.010
1050	.194	.045	.001	.002	.002	.013
1100	.131	.043	.001	.002	.001	.003
1150	.118	.042	.001	.002	.0005	.002
1200	.223	.010	.0009	.0006	.0005	.006

TABLE IV (Cont.)

Sintering Temperature °C

Bulk Density (gr/cc)	PREB REACTION °C		1370	1425	1485	1540	1595	1650
		950	1.2393	3.0075	3.1631	3.2725	3.4203	3.3298
		1000	2.0768	2.9405	2.9117	3.0114	3.1210	3.1593
		1050	2.0490	3.0238	3.2291	3.3166	3.3333	3.1849
		1100	2.2482	3.0761	3.4412	3.3816	3.1954	3.1695
		1150	2.3431	2.9647	3.3712	3.3721	3.3535	3.5183
		.200	1.9131	3.2326	3.3965	3.4411	3.3964	3.2500

FIGURE 10 - MOISTURE ABSORPTION VS PRE-REACTION
FOR THE SEVERAL COM
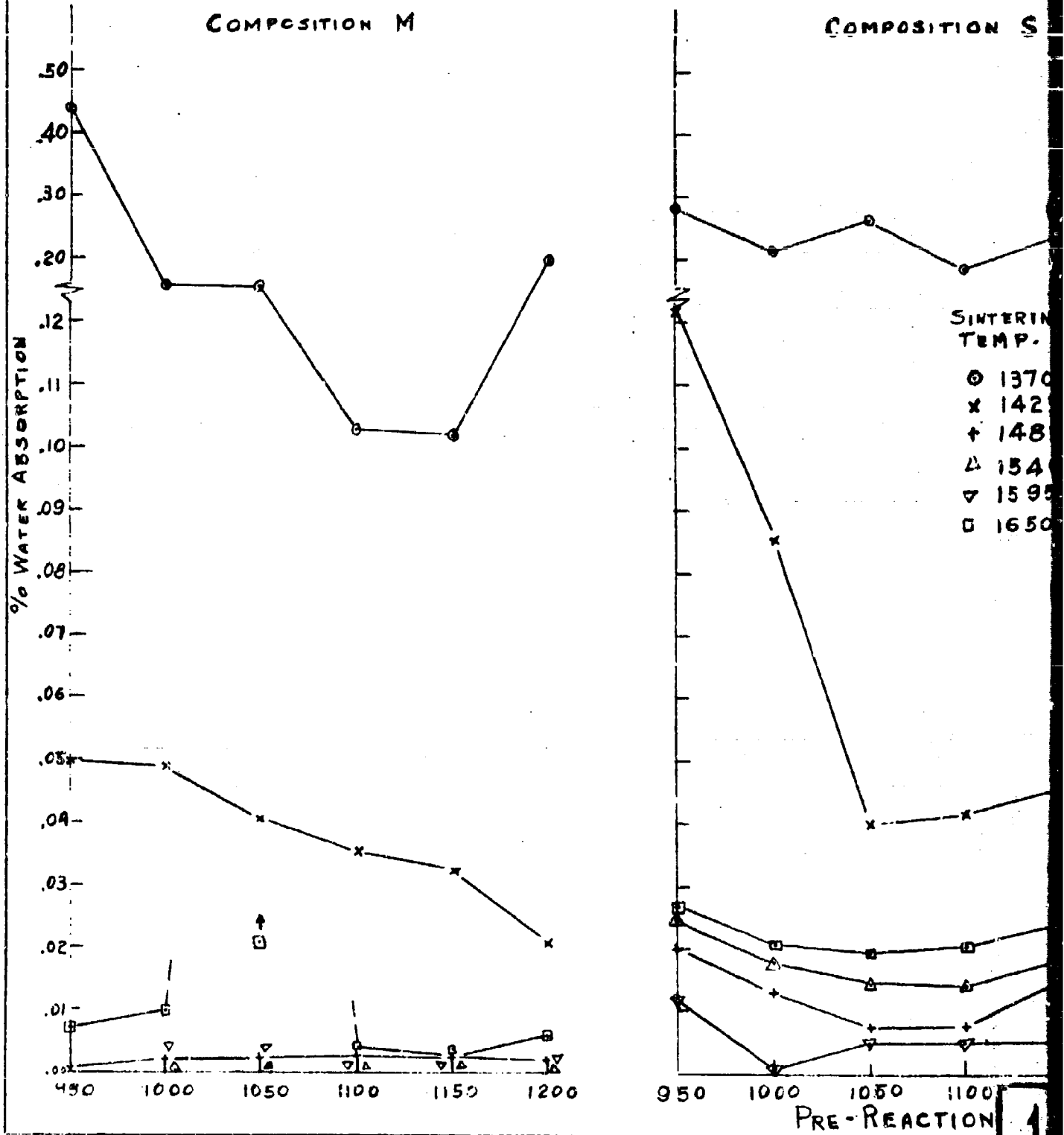
COMPOSITION M

COMPOSITION S

SINTERIN
TEMP.

⊙ 1370
✗ 142
✛ 148
△ 154
▽ 1595
☐ 1650

% WATER ABSORPTION

PRE-REACTION

-REACTION & SINTERING TEMPERATURES
VERAL COMPOSITIONS

ITION S

COMPOSITION A

SINTERING
TEMP.

⊙ 1370°C
✕ 1425°C
+ 1485°C
△ 1540°C
▽ 1595°C
□ 1650°C

1100   1150   1200
ACTION TEMP. °C

950   1000   1050   1100   1150   1200
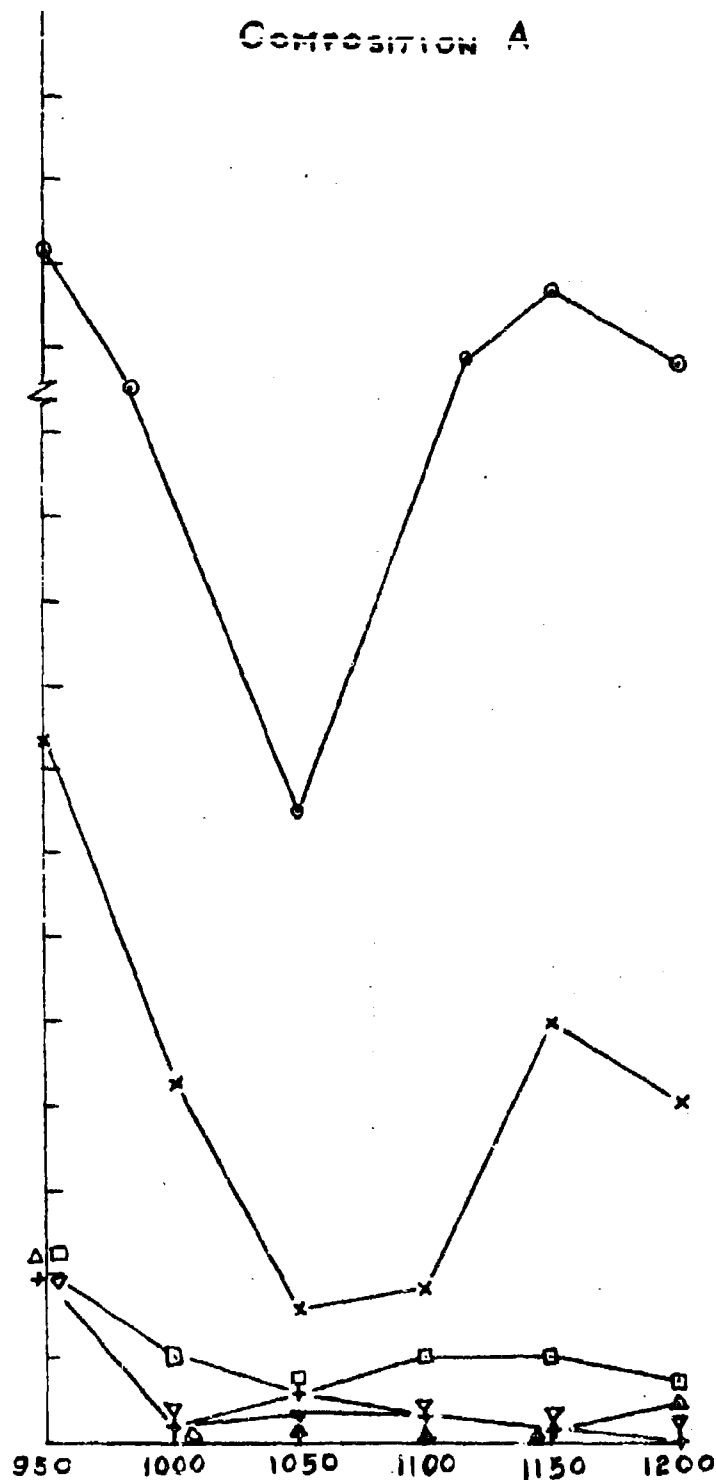
Graphic Representation of Effect of Pre-Reaction
and Sintering Temperatures on Moisture Absorption-Compositions
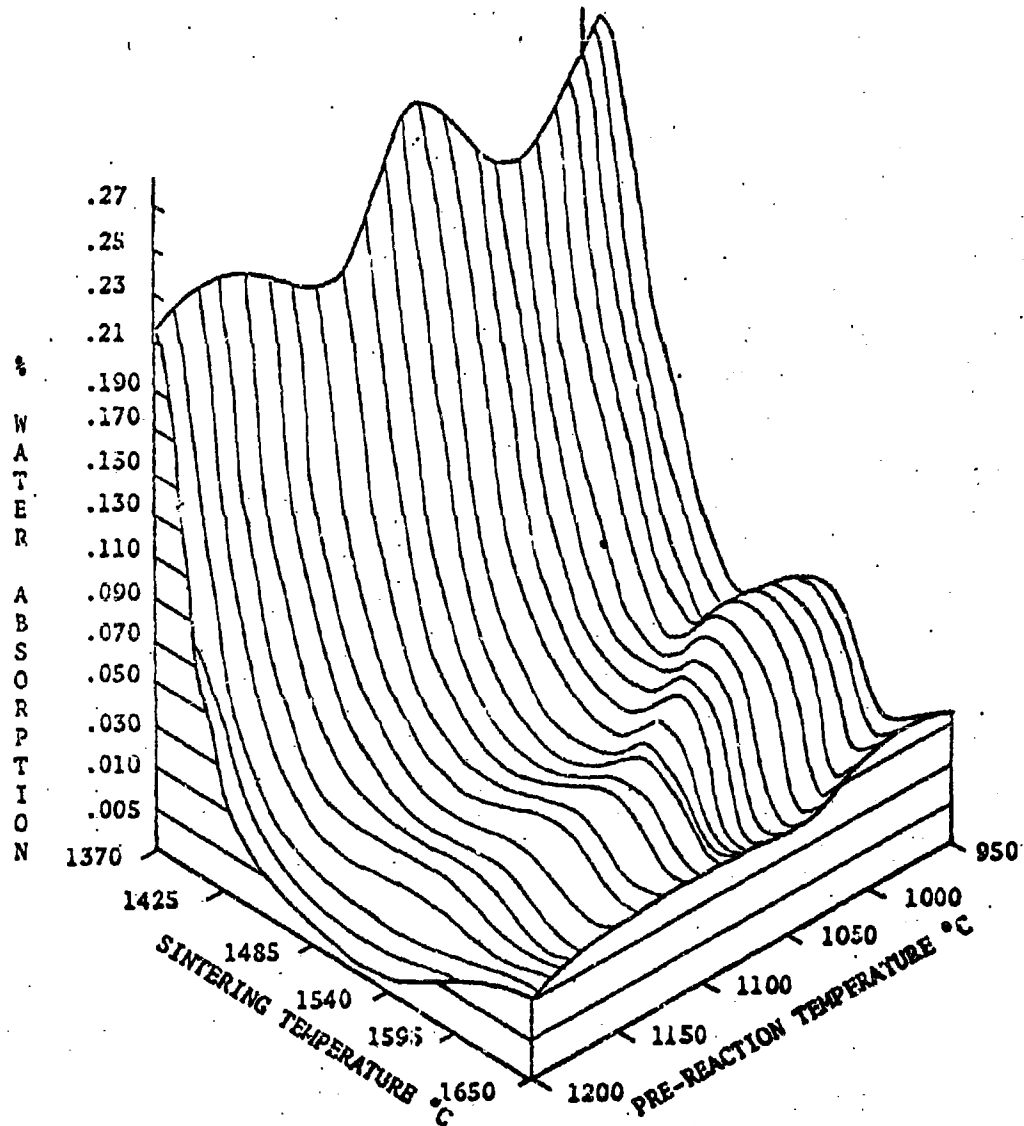
to moisture absorption in that composition difficient in alumina,
while in the others, this is not the case. The overall effect
is presently graphically in Figure 11 on page 31 for the stoi-
chiometric compositions. The differences encountered with re-
spect to composition have been decreased above.

The bulk density ranges from very low values, i.e., 1.39,
to 3.59. The lower values are to be expected because of the
low firing shrinkage exhibited by some specimens. The high
value exceeds that of pure spinel at theoretical density. Only
one such value occurs and is undoubtedly due to experimental
error. Figure 12 on page 33 shows the effect of prereaction
temperature on bulk density for specimens fired at the several
sintering temperatures. For composition A $0.9MgO \cdot 1.0Al_2O_3$ only
the lowest sintering temperature is quite ineffectual. At the
remaining sintering temperatures the prereaction temperature
plays a rather minor role in that curves are quite straight and
more changes in bulk density are due to sintering temperature.
The bulk density ranges from 2.90 to 3.59, this better value
being in error as it exceeds the theoretical density of spinel.
However referring to Table II on page ' it can be noted that
this is an area of high density. Most curves indicate that a
high or the highest density is realized using material prere-
acted to 1050°C. Bulk density above 3.20 can be realized by
sintering specimens at 1540°C and above regardless of prereac-
tion temperature; only one exception is shown.

The stoichiometric composition S performs in a similar manner
however with only a few isolated exceptions the bulk densities
are below 3.2. The highest value reaches 3.53 which is 99.4%
of true density. This is extremely unusual for a composition
sintered in air.

Composition M ($MgO \cdot 0.9Al_2O_3$) which is deficient in alumina,
performs somewhat differently. The bulk densities increase
directly as the sintering temperature at the lower prereaction
temperature with a very slight decrease at the highest one.
At the two highest prereaction temperatures the bulk density
values are high and rather bunched. There is a definite de-
crease in all sintered bulk densities for specimens made of
the 100°C prereacted starting material. In general the overall
effect is somewhat similar to that experienced by Composition A
except that it takes place at higher temperatures. The highest
bulk density realized with this composition is 3.51 which is
98.3% of true density of pure spinel.

FIGURE 12 - BULK DENSITY vs PRE-REACTION
FOR THE SEVE...

COMPOSITION M   COMPO...
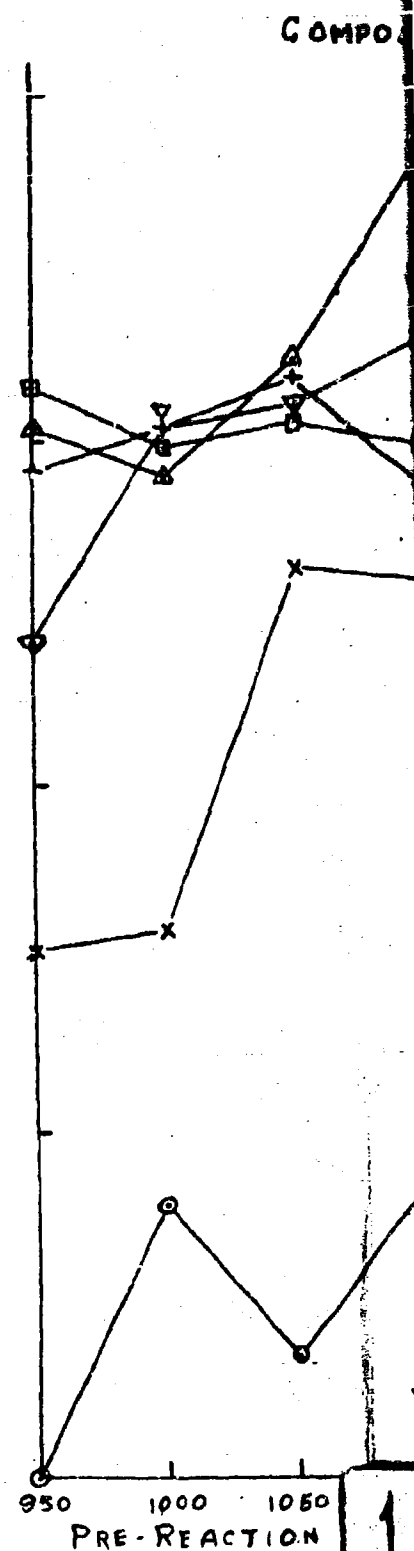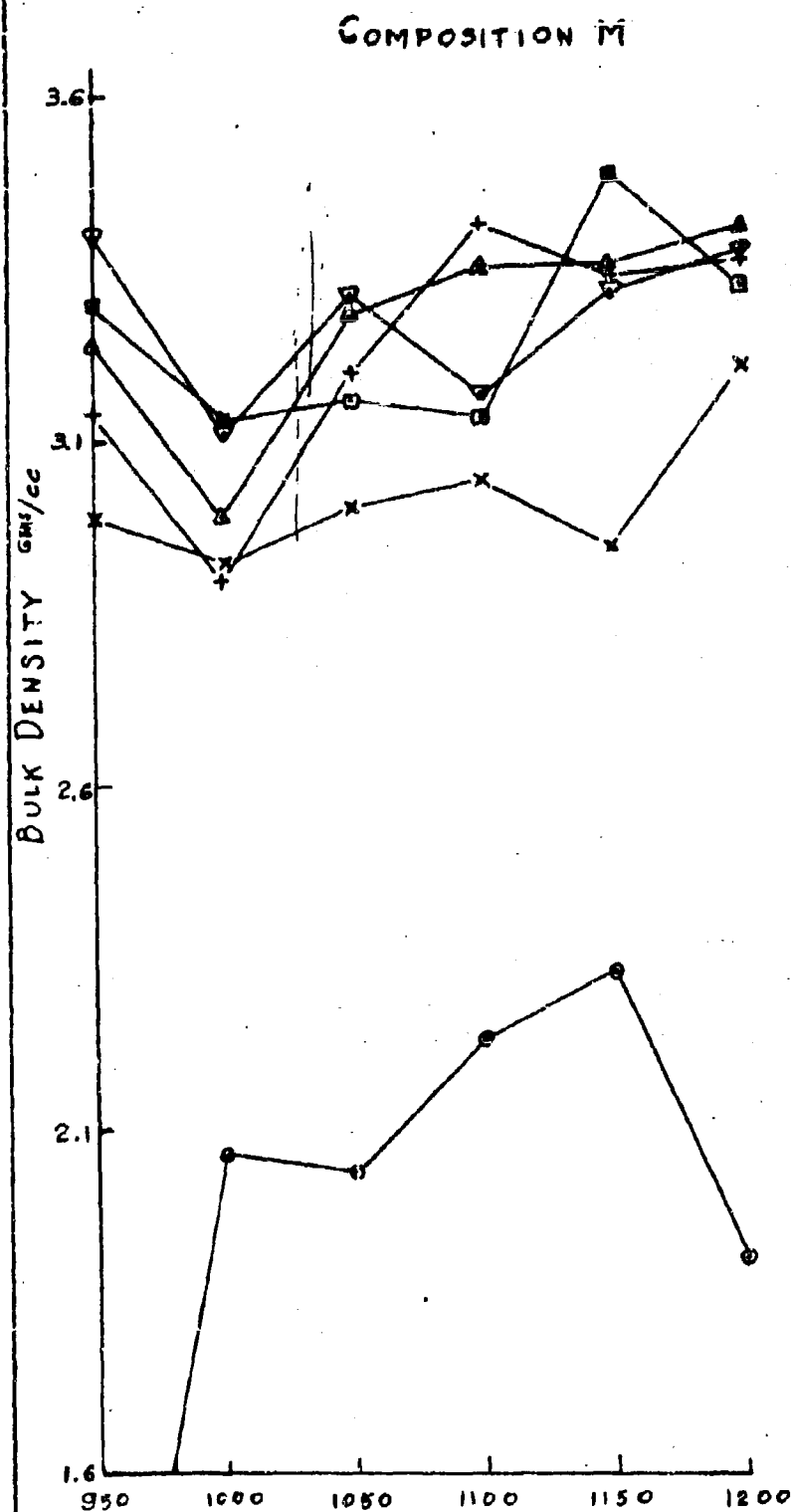
vs Pre-Reaction & Sintering Temperatures
R The several compositions

Composition S

Composition A

SINTERING
TEMP.
⊙ 1370°C
✕ 1425°C
+ 1485°C
△ 1540°C
▽ 1595°C
□ 1650°C

1050   1100   1150   1200

TION TEMP. °C

950   1000   1050   1100   1150   1200

2
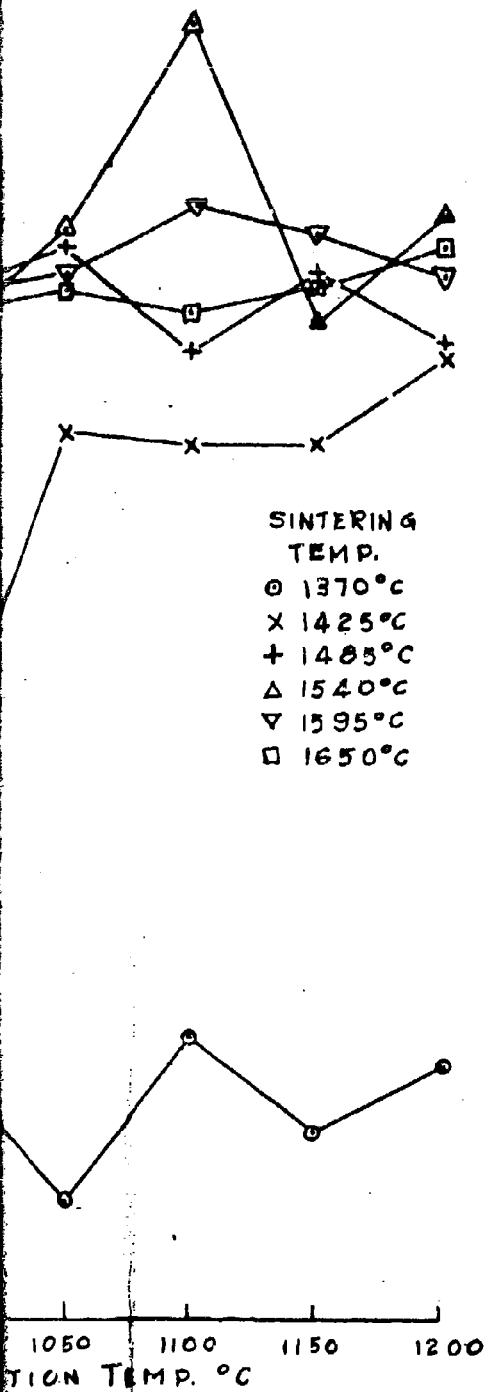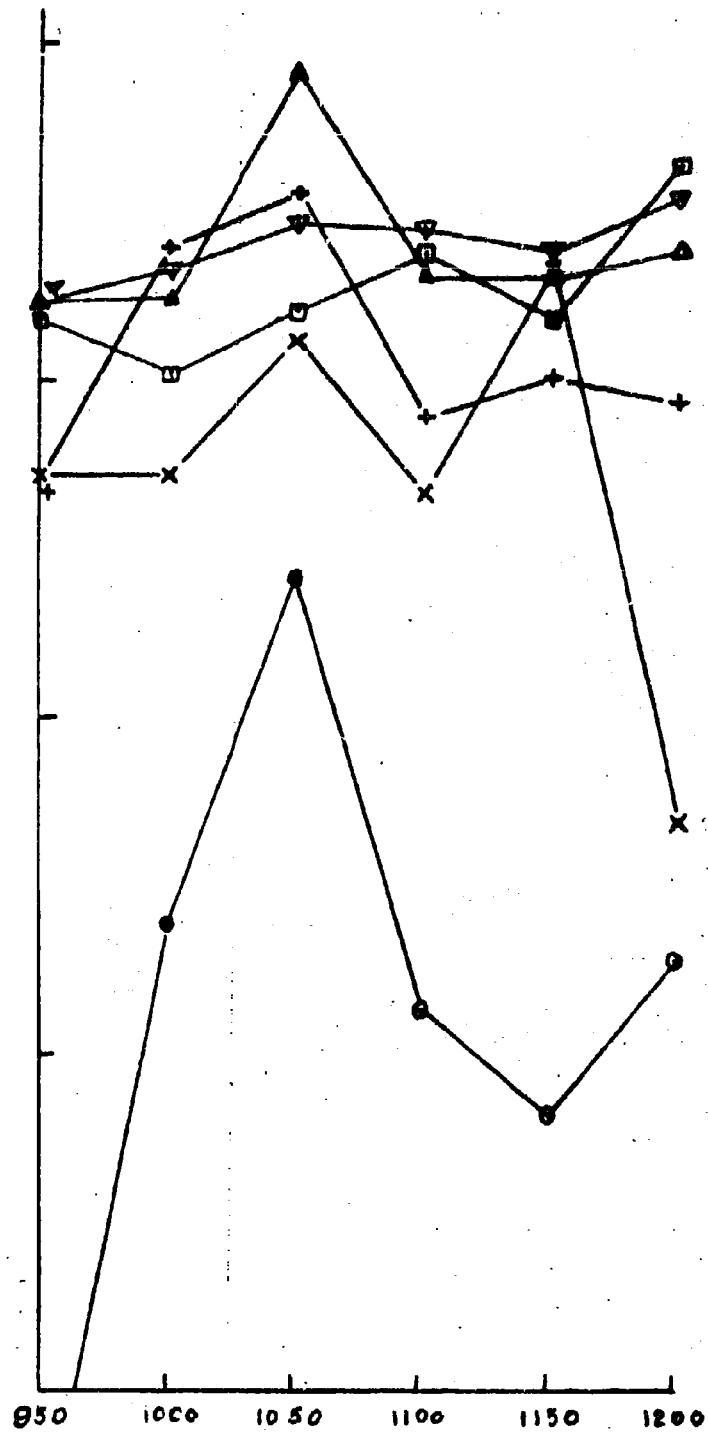
3. Summary

The low moisture absorption and high bulk density and shrinkage indicate that these spinel starting materials are very reactive and sinterable. In general the prereaction temperature is not critical; however the sintering temperature must be 1540 °C or higher to realize the optimum. The magnesia deficient composition appears to be the most reactive. Specimens made of this material exhibit the lowest moisture absorptions and the highest bulk densities over the sintering temperature range. Several specimens approach true density even though sintered in air, however the bulk of the better ones exhibit values in the range 89 to 95%.

F. Summary

The object of this effort is to establish the parameters by which a very reactive and sinterable spinel $MgO \cdot Al_2O_3$ starting material can be made. Pure magnesia and alumina bearing alums were selected as raw materials. They are capable of excellent mixing since they are water soluble and can be mixed as solutions; they melt at moderate temperatures and can again mix as liquids; and finally all but the metal oxides of the respective alums volatilize leaving very small reactive particles to form the spinel. Three compositions were selected: $0.9MgO \cdot 1Al_2O_3$, $MgO \cdot Al_2O_3$ and $1MgO \cdot 0.9Al_2O_3$. The object was to determine whether the excess oxide would function as a sintering aid and/or a grain growth inhibitor.

The alums and the three compositions were studied at temperature by DTA, TGA, X-ray, electron microscope, etc., to determine the reaction temperature range, and to measure reaction, composition, impurities, crystal size, etc. Spinel at 98.3% purity and at a particle size range between 50 and 500 Å was realized by prereacting the composition over the temperature range 950-1200°C.

Eighteen compositions - prereaction temperature combinations of starting materials were prepared as specimens and sintered over the temperature range 1370-1650°C. In general the prereaction temperature is not critical; however the sintering temperature must be 1540°C and higher to realize the lowest moisture absorptions and highest bulk densities. The former property was recorded as low as 0.0006% while one set of specimens realized 99.3% of true density spinel. The compositions deficient in

magnesia appears to sinter slightly better than the others.

The spinel materials prepared as noted above are extremely reactive and sinterable. They possess the necessary character-istics of purity, fine particle size and reactivity for sin-tering and should be utilized for a basic study of the sintering characteristics of pure spinel.

G. Bibliography

1. Allen, W. C., "Solid Solution in the Refractory Magnesium Spinels," A thesis submitted to the Graduate School of Rutgers - The State University, Sept. (1964).

2. Bazilevich, A., "Synthesis of Spinels," Mineral Suir'l. No. 9, 2530 (1934); C. A. 29, 1732 (1935).

3. Bereghnoi, A. A. and Sloneinskaya, E. Z., "Spinel Refrac-tories," Ukrain. Nauk., Issledovatel Inst. Agneuporov i Kislotoriporov No. 45, 78-119 (1939); C. A. 34, 1143 (1940).

4. Castell, H. C., Dilnot, S. and Warrington, M., "Reaction Between Solids," Nature 153.654-4 (1944); C. A. 38, S451 (1954).

5. Chesters, J. H. and Parmelee, C. W., "The Measurement of Reaction Rates at High Temperatures," J. Am. Cer. Soc., 17, 50 (1934).

6. Clark, G. L., Howe, E. and Badger, "Lattice Dimensions of Some Solid Solutions in the System $MgO-Al_2O_3$," J. Am. Cer. Soc. 17 (1) 7-8 (1934).

7. Firth, F. G., "Manufacturing Control Employing X-ray Diffrac-tion Method," J. Am. Cer. Soc., December (1945).

8. Froelich, F., "Artificial Gems," Swiss Patents, 28,888 to 128,891, September 29, 1925; C. A. 23,2791 (1929).

9. Geller, R. F., Yavorsky, P. J., Steierman, B. L. and Creamer, A. S., "Studies of Binary and Ternary Combinations of Mag-nesia, Calcia, Baria, Beryllia, Alumina, Thoria, and Zirconia in Relation to Their Uses as Porcelains," J. Research Natl. Bur. Standards 36, 277-312 (1946); C. A. 40, 5217 (1946).

10. Hanna, Rinoud, "Clastic Moduli of Polycrystalline Magnesia Alumina Spinel," J. Am. Cer. Soc. <u>46</u>, (2) 106 (1963).

1 . Hauffe, K. and Pschera, K., "Concerning the Mechanism of Spinel Formation at Higher Temperatures," Z. anorg. alleg. Chem. <u>262</u>, 147 (1950).

12. Hauptmann, H. and Novak, J., "Lattice Constants of Certain Substances of the Spinel Type." A. Physik, Chem. B15, 365-72 (1932); C. A. <u>26</u>, 2098 (1932).

13. Hedvall, J. A., "On the Reaction Between Cobaltous Oxides and Aluminum Oxide at High Temperatures," A. anorg. allg. Chem. 92, 301 (1915).

14. Holgersson, S., "Crystals of the Spinel and Magnetite Groups," In Ewald, P. P. and Hermann, C., "Strukturbericht," Vol. I, p. 416, akad. Verlag. G. m. b. h. (1931).

15. Huttig, G. F., "Active States Which are passed through During the Chemical Combination of Two Metal Oxides," Z. Elektro Chem. 41, 527 (1935).

16. Jander, W. and Pfister, H., "The Intermediate States which occur During the Formation of Spinel in the Solid State From MgO and Al_2O_3," Z. anorg. alleg. Chem. <u>289</u>, 95 (1938).

17. Jander, W. and Stamm, Wl, "The Inner Structure of Solid Inorganic Compounds at High Temperatures," Z. anorg. alleg. Chem. <u>199</u>, 165 (1931).

18. Kordes, E. and Becker, H., "Spinel Mixed Crystals in the System $MgAl_2O_4$," Z. anorg. allg. Chem. 258, 227 (1949).

19. Kriegel, W. Wurth, Hayne Palmour III, and Dong M. Choi, "The Preparation and Mechanical Properties of Spinel," Department of Army Project #59901007. Final report submitted to the Department of Engineering Research North Carolina State of the University of North Carolina, July, (1964).

20. Nakai, T. and Fukami, Y., "Systems Composed of Silica, Alumina and Magnesia and Cordierite," J. Soc. Chem. Ind. Japan <u>39</u>, Suppl. binding 231-2; C. A. <u>30</u>, 7055 (1936).

21. Navias, Louis, "Preparation and Properties of Spinel made by Vapor Transport and Diffusion in the System $MgO-Al_2O_3$," J. Am. Cer. Soc., 44 (9) 434-46 (1961).

22. Noda, T. and Hosegawa, M., "Effect of the Addition of Salt Vapor on the Synthesis and the Crystal Growth of Spinel," J. Soc. Chem. ind. Japan 43, Suppl. binding 72-3 (1940); C. A. 34, 5333 (1940).

23. Noguchi, C., "Synthesis of Spinel: II, Re-examination of Natural and Synthetic Spinels," J. Japan, Cer. Assoc., 54 (624) 56-59 (1946); Refr. biblio. 1947-1956, p. 1150-b.

24 Passerini, L., "Investigations of Spinels II. The Compounds $CaAl_2O_4$, $MgAl_2O_4$, $ZnAl_2O_4$, $ZnCr_2O_4$, $ZnFe_2O_4$ and $MnFe_2O_4$," Gazz. Chim. ital. 60, 389-99 (1930); C. A. 24, 4439 (1930).

25. Posnjak, E., "Lattice Dimensions of Spinel ($MgAl_2O_4$)," J. Am. Sci. 10, 528-30 (1928); C. A. 23, 3140 (1929).

26. Roy, D. M., Roy, Rustum, "The System $MgO-Al_2O_3-H_2O$ and Influence of Carbonate and Nitrate Ions on the Phase Equilibria," Am. J. Sci. 251 (5) 237-61 (1953).

27. Rudorff, W. and Reuter, B., "The Structure of Magnesium and Zinc Vanadium Spinels," Z. anorg. Chem. 253, 194 (1947).

28. Ryshkewitch, Eugene, "Oxide Ceramics," Academic Presses, New York and London, (1960).

29. Schikore, W. and Redlich, G., "Contribution to the knowledge of the Luminescence of Spinels," Z. anorg. Chem. 257, 96 (1948).

30. Sullivan, William, F., "The Formation of Spinels at Low Temperature," A thesis submitted to the faculty of the Graduate School of Rutgers - The State University of New Jersey, September, 1953.

31. Suzuki, S., "Magnesia Spinel," J. Japan Ceram. Assoc. 47, 302-9 (1939; C. A. 34, 2550 (1940).

32. Suzuki, S. and Fujita, Y., "Refractory Materials for Sight-Metal Metallurgy," J. Japan Ceram. Assoc. 49, 466-73 (1941); C. A. 44, 8080 (1950).

33. Tanaka, Y., "Reactions in the Solid State at Higher Temperatures. VII. The Reaction Between Magnesium Oxide and Aluminum Oxide in the Solid State," J. Chem. Soc. Japan 62, 477-9 (1941); C. A. 35, 7861 (1941).

34. Verneuil, A., "Artificial Production of Ruby by Fusion," Compt. Rend., 135, 791-94 (1902).

35. Verwey, E. J. W. and Heilmann, E. L., "Physical Properties and Cation Arrangement of Oxides with Spinel Structures. I. Cation Arrangement in Spinels," J. Chem. Phys. 16, 174 (1947).

III. DEVITRIFICATION STUDIES

A. Introduction

This phase is devoted to the devitrification approach of the prereacted raw materials technique. The method entails melting a complete, more complex composition, which results in mixing on an atomic basis, then retaining the random or glass structure at room temperature by quenching the melting into water; this procedure is identified as fritting. This material is comminuted to a controlled particle size distribution and formed into specimens by conventional forming methods. During the subsequent firing operation a crystalline phase or phases devitrify and the remainder of the composition forms a glassy bond. The resulting body is vitrified or impervious. This procedure is identified as the one glass or one frit approach and some work was discussed in the last Final Report noted above. A two frit approach is described below.

B. Two Frit Approach

1. Introduction

This aspect of the study deals with the development of cordierite bodies prepared from two devitrifiable glasses. One glass is of the theoretical cordierite composition, and the other is a low melting glass in the $CaO-MgO-BaO-Al_2O_3-SiO_2$ system. The object is to prepare a body with sufficient cordierite to dominate the thermal expansion, and to develop a liquid phase to densify the body.

2. Technical Approach

In the earlier work reported in the Final Report, Contract Now 65-0199-d, dealing with the one frit system, it was shown that the theoretical cordierite composition devitrifies completely into crystalline cordierite. However, the bodies produced from this frit do not densify to any appreciable extent because the diffusion rate is too low at these temperatures for solid state sintering and also because a liquid phase is not being formed except as the melting temperature of cordierite is approached and this results in melting. This problem was approached by adding a low melting glass to the base cordierite glass. This low melting glass had to meet the following requirements: the additive glass must, 1) wet the cordierite, 2) contain ions which can go into solid solution in the crystalline cordierite, 3) be able to dissolve the cordierite crystal to a slight extent, 4) be added in sufficient quantity to densify the body, but not greatly increase the overall thermal expansion of the body, and 5) devitrify upon cooling, or subsequent heat treatment, to reduce the amount of glass in the final body. To satisfy these requirements, it was reasoned that a low melting frit, possessing a similar composition to the cordierite frit, was necessary as a densifying glass. Thus, compositions in the $BaO-CaO-MgO-Al_2O_3-SiO_2$ system with alumina-silica ratios similar to those of cordierite were chosen as the low melting glasses. It was reasoned that in the final firing, the cordierite glass would melt to form a fluid and reactive liquid phase. The cordierite crystals should be slightly soluble in the $BaO-CaO-MgO-Al_2O_3-SiO_2$ glass, and the alkaline earth ions should go into solid solution into the open cordierite structure. This interaction at the crystal-glass interface should reduce the compositional gradient

across the interface, and result in a gradually changing com-
position with a gradually changing thermal expansion from the
center of the cordierite crystal to the center of its surround-
ing glass phase. Thus, the stresses introduced by heating and
cooling the sample would not be concentrated at the interfaces,
but would be distributed over a wide area within the sample.
This should effectively reduce, or even eliminate, thermally
induced fracture within the body. This plus the overall low
thermal expansion anticipated for this type composition should
result in high thermal shock resistance.

As a starting point, compositions were chosen which lie
in and about the primary field of cordierite in the $MgO-Al_2O_3-SiO_2$ system. In order to reduce the melting temperature of
these glasses, the magnesia was replaced by equal amounts of
magnesia, baria, and calcia. Their locations are in the $RO-Al_2O_3-SiO_2$ system as shown in Figure 13 on page 42. It was
reasoned that glasses of this system and composition would sat-
isfy the five requirements necessary for compatible densifica-
tion of the crystalline cordierite.

These ten glasses and the glass of the theoretical cor-
dierite composition were prepared by melting the total compo-
sition, quenching, and then grinding to a fine particle size.
These glass powders were then used as the raw material in the
fabrication process. Specimens were prepared by dry pressing
and then firing to maximum density. These eleven individual
frit compositions were evaluated for bulk density, true density,
moisture absorption, firing range, melting temperature, devi-
trifying crystalline phases, thermal expansion, and phase re-
actions occurring.

Composite bodies were prepared with ten, twenty, and thirty
percent weight additions of low melting frits to the phase cor-
dierite frit. The two components were thoroughly mixed and
specimens were then prepared by dry pressing. Bodies were fired
and then evaluated for density, true density, moisture absorption,
firing range, melting temperature, thermal expansion, crystalline
phases present, electrical properties, transverse strength, mi-
crostructure, and thermal shock resistance.

Figure 13

Location of Additive Glasses in the
RO-Al$_2$O$_3$-SiO$_2$ System and their Coefficients
of Linear Thermal Expansion

44% SiO$_2$
28% Al$_2$O$_3$
28% RO

5.33 . C-F

5.42 . Cb-98

5.43   4.90   4.56
C-B   C-C   Cb-910

4.91   4.54
Cb-9   C-A

5.44   4.54   4.31
C-D   Cb-96   C-B

62% SiO$_2$
10% Al$_2$O$_3$
28% RO

62% SiO$_2$
28% Al$_2$O$_3$
10% RO
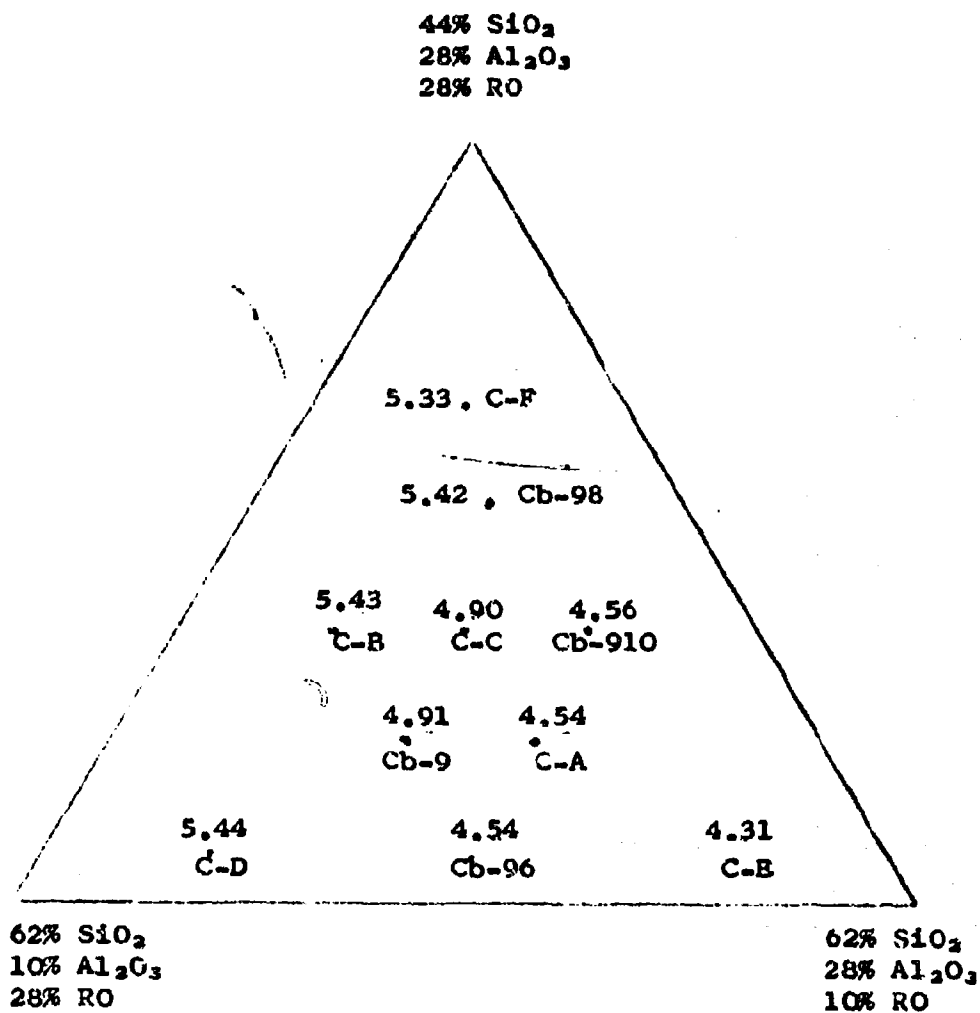
3. Experimental Approach

The compositions of the cordierite glass and the bonding glasses are presented in Table V on page 44. The raw materials used are as follows: silica, Supersil #5 Micron, Pennsylvania Sand Corporation; alumina A-14, Alcoa Corporation; magnesia, magnesium carbonate, Magcarb L, Merck Chemical Company; baria, barium carbonate, Reagent Grade, Fisher Scientific Company; and calcia, calcium carbonate, Analytical Reagent, Mallinckrodt Chemical Works.

The proper amounts of each ingredient were weighed out and then mixed dry in a twin shell blender for one hour. Each batch was calcined to 1500°F in fire clay crucibles in a gas-fired kiln, in order to reduce the volumn of material. The calcined batch was then passed through a 200 mesh screen to break up agglomerates and then repacked into the fireclay crucibles. These were fired to 2730°F in an oxygen-gas pot furnace in six hours. At this temperature, all glasses were of sufficient fluidity to be fritted into cold water. After quenching, each glass was milled in an alumina mill with alumina pebbles for 48 hours. This ground glass was screened through a 200 mesh screen and this powder was the prereacted raw material ready for further processing.

In the preparation of specimens of the individual glasses, a 5% Superloid solution (ammonium alginate) was mixed into the glass powder using a mortar and pestle. Specimens were pressed into discs, one and two inches in diameter, one half inch thick, at a pressure of 10,000 psi.

In the preparation of the composite bodies, the proper amounts of each ingredient were weighed to make 250 gram batches and each was placed in an alumina mill with alumina pebbles and 1000 ml of methanol then ground for 48 hours. After this the material was removed from the mill and dried overnight at 250°F. A 5% Superloid solution was then mixed into the batch with a mortar and pestle and discs, two inches in diameter and one half inch thick, and bars, four inches in length and one half inch in width and breadth, were pressed at 10,000 psi.

Specimens of the ten low melting glass frits in the form of one inch diameter discs were fired from 1600°F to 2300°F at 100°F intervals in individual firings. The firing cycle was five hours from start to maximum temperature plus an hour soaking period. Specimens of the composite bodies at the same size were

TABLE V

Compositions and Properties of the Cordierite and Bonding Glasses

Compositions	C-O	C-A	C-B	C-C	C-D	C-3	C-F	Cb-98	Cb-91	Cb-96	Cb-9
SiO_2	51.4	58.0	55.0	55.0	61.0	61.0	49.0	58.0	55.0	52.0	61.4
Al_2O_3	34.8	22.0	19.0	22.0	13.0	25.0	25.0	19.0	25.0	23.0	18.3
MgO	13.8	6.7	8.7	7.7	8.7	4.7	8.7	6.7	7.7	8.3	6.8
BaO	-	6.7	8.7	7.7	8.7	4.7	8.7	6.7	7.7	3.3	6.8
CaO	-	6.7	8.7	7.7	8.7	4.7	8.7	6.7	7.7	8.3	6.8

Properties of Glasses

	C-O	C-A	C-B	C-C	C-D	C-3	C-F	Cb-98	Cb-91	Cb-96	Cb-9
Firing Temp. (°F)[1]	1800	1800	1800	1700	1700	1800	1700	1700	1700	1700	1700
Density (gr/cc)[1]	2.65	2.65	2.83	2.73[5]	2.72[3]	2.63[3]	2.80[3]	2.75	2.65	2.50	2.67
Firing Temp.[2]	2200	2200	2250	2250	2100	2200	2250	2200	2100	2000	2100
Coef. Linear Therm. Exp.[4]	-	4.54	5.43	4.90	5.44	4.31	5.33	5.42	4.54	4.54	4.91
Power Factor (%) (1 Mc)	-	-	-	.459	-	.419	-	-	-	.472	-
Power Factor (%) (10 Mc)	-	-	-	.353	-	.325	-	-	-	.390	-
Power Factor (%) (1 Mc)[5]	-	-	.151	.160	-	.131	-	-	-	.141	-
Power Factor (%) (10 Mc)[5]	-	-	.102	.110	-	.101	-	-	-	.119	-
True Density (gr/cc)[6]	2.625	-	2.774	-	-	-	-	-	-	-	-
True Density (gr/cc)[5]	2.519	-	2.848	-	-	-	-	-	-	-	-

1. At which 0.00% moisture absorption is realized.
2. At which moisture absorption remains at 0.00% and density is retained.
3. Increases slowly with temperature.
4. Between room temperature and 630°C.
5. After devitrifying the glass specimens.
6. All true densities were determined by the picometer method.

fired from 2300°F to 2675°F at 25°F intervals in individual firings. The heating cycle was the same as utilized in the firing of the indi·idual glasses. All firings were carried out in an electric furnace, Hevi-Duty Electric Company Model C-07-Pt which utilized silicon carbide resistance elements. The temperature rise was held constant at 400°F per hour.

Moisture absorptions and bulk densities were determined conventionally. Thermal expansion properties were determined using a conventional Fizeau Interferometer which was heated to 650°C at a rate of 5°C/min. The small pyramidal specimens were made of each glass and the composite bodies. True density was determined using standard picnometers. Transverse strength was determined using specimen 4 inches in length and approximately 1/2 inches square.

Several analytical methods were used to study reactions and structures. Differential thermal analysis was made using a Fisher Differential Thermalyzer, Model 260P using alumina as a standard and a heating rate of 10°C/min. X-ray analysis was used to determine the crystalline phases present in all compositions as well as petographic methods. For the latter method specimens were polished with silicon carbide grinding paper and 0.5 micron gamma alumina, and were etched in a 5% solution of H_2SiF_6 for 30 minutes. A Zeiss polarizing light microscope was used to study the structure and photomicrographs were taken at 700X. Electron microscope pictures were taken at 5000X using the carbon replica method.

The two inch diameter discs were used to determine electrical properties. Values were determined on several of the additive glasses as well as the composite bodies. Air drying silver electrodes were painted on the specimen. A capacitance bridge and a Booton "Q" meter Type 160A were used to attain data from which power factor and dielectric constant were calculated. All data was measured at room temperature and between 1 Kc and a little above 10 Mc.

4. Results and Discussion

a. Glasses

Two of the glasses C-0, the cordierite glass and C-A, one of the additive glasses, were analyzed for particle size distribution before specimens were formed. The results are as follows:

Particle Size Range	C-O	C-A
Above 50 microns	0.00%	0.9%
40 to 50 microns	0.1	0.6
30 to 40 microns	0.5	1.8
20 to 30 microns	5.1	1.4
10 50 20 microns	14.5	10.4
5 to 10 microns	24.8	18.3
3 to 5 microns	18.4	23.1
2 to 3 microns	14.1	17.3
1 to 2 microns	11.4	13.8
0.5 to 1 micron	1.9	8.1
0.3 to 0.5 micron	4.5	2.5
Below 0.3 micron	4.9	0.9

Table V on page 44 presents the bulk density and moisture absorption values obtained for the individual low melting glasses over a series of firing temperatures. It can be seen that the bulk density varies from 2.60 for composition Cb-96 to 2.93 for composition C-B. Also, all compositions attained a 0.00% moisture absorption and possessed extended firing ranges.

The significant factor in determing the bulk density variation and the length of the firing range appears to be the amount of alkaline earth oxides present. In general, the bulk density increases as the amount of alkaline earth oxides increases. Further, the temperature at which maturity is first realized decreases as the amount of alkaline earth oxides increases. Both these phenomena can readily be explained. First, the bulk density increases because the crystalline phases formed have open structures permitting additional alkaline earth oxides to be incorporated since these ions can go into the structure in solid solution, thus, increasing the density. Second, an increase in the

amount of alkaline earth ions increases the fluxing action in this type system, thus the glass would be formed in greater amounts at lower temperatures. This can be seen by comparing Composition C-R which possesses a bulk density of 2.6% and a firing range of over 400°F, and contains 14% by weight alkaline earth oxides, to Composition C-B which contains 26% by weight of alkaline earth oxides and possesses a bulk density of 2.83 and a firing range of over 450°F.

The coefficients of linear thermal expansion between room temperature and 650°C range from 4.31 for additive glass C-E to 5.44 for C-D. This property tends to increase as the RO content increases as can be seen in Figure 13 on page 42. The other properties reported in Table V on page 44 will be discussed along with those of the composite bodies.

Figure 14 on page 48 shows the differential thermal analysis curves for the cordierite glass, C-O, and the representative curve for low melting glasses, C-A, C-B, C-C, C-D, C-E, Cb-96, Cb-98, Cb-910, and Cb-9. The low melting glasses possessed identical differential thermal analysis curves.

The reaction takes place in the low melting glasses from room temperature to 750°C. The elongated, slightly endothermic peak from room temperature to 750°C is associated with drift within the instrument. From 750°C to 850°C, there is an endothermic peak associated with nucleation within the glass. Above 850°C, there is an increasing endothermic peak which is associated with the softening of the glass. Actually, two phenomena are occurring, the glass is softening and crystallization is taking place. The softening is an endothermic reaction, while the crystallization is an exothermic reaction. However, the softening of the glass takes up so much heat that it masks the peak which occurs with the release of heat associated with the crystallization. Both microscopic analysis and X-ray analysis confirm that there is crystallinity above 850°C; however, the amount is very small. Thus, these glasses are quite unusual in that they devitrify and soften at about the same temperature.

In the case of the cordierite glass, no reaction occurs until 780°C. The elongated, slightly exothermic peak is associated with the softening of the glass. Actually, two pheomena are occurring, the glass is softening and crystallization is taking place. The softening is an endothermic reaction, while the crystallization is an exothermic reaction. However, the softening of the glass takes up so much heat that it masks the peak

Figure 14

Differential Thermal Analysis of
Cordierite Glass and Additive Glass
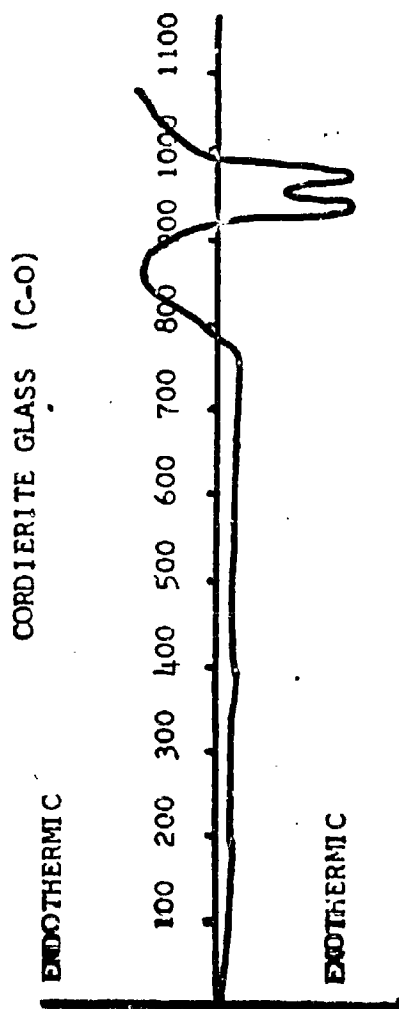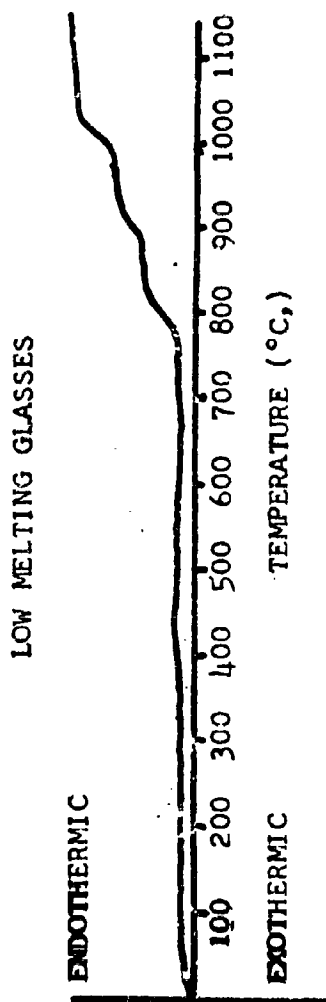
which occurs with the release of heat associated with the crystallization. Both microscopic analysis and X-ray analysis confirm that there is crystallinity above 850°C; however, the amount is very small. Thus, these glasses are quite unusual in that they devitrify and soften at the same temperature.

In the case of the cordierite glass, no reaction occurs until 780°C. The elongated, slightly exothermic peak is associated with drift within the instrument. The endothermic peak from 780°C to 915°C is associated with nucleation of the glass. From 915°C to 960°C there is a strong exothermic peak which results from the crystallization of the mu-phase or cordierite from the glass. From 960°C to 1010°C, there is another strong exothermic peak associated with the phase transformation of the metastable mu-phase to the stable alpha-phase. These results are in good agreement with those presented by Tyrrell, Gibbs, and Shell.

The ten low melting glasses and the theoretical cordierite composition glass were investigated by X-ray diffraction analysis to determine the crystalline phases present after devitrification. In the case of the low melting glasses, two crystalline phases, Ba-C and an unknown phase, were found to devitrify upon heat treatment. Ba-C is a complex barium magnesium aluminosilicate first reported by Wisely.[2] The presence of the unknown phase was indicated by five diffraction peaks located at angles of 22.0°, 25.8°, 28.0°, 29.6°, and 36.9°. The other diffraction peak associated with the compound are either not strong enough to be distinguishable from the background or they may be masked by the numerous diffraction peaks of the Ba-C phase. It is reasoned that the unknown phase is a complex alkaline earth aluminosilicate that has not yet been identified. In the case of the theoretical cordierite composition, crystalline cordierite was the only crystalline phase present.

Several of the additive glasses were evaluated for power factor as glasses and after devitrification. As glasses this property ranges from .419% to .493% at 1 Mc and from .325 to .390% at 10 Mc. These rather high values are to be expected of the random structure of the glass. These values decrease at 10 Mc. This is undoubtedly the minimum point in the power factor frequency curve. The values decrease in the devitrified specimens. This is due to some of the loss producing ions which were in the randomly oriented or glass structure, being bonded in crystals when their contribution to electrical losses is minimized. The power factor again decreases at 10 Mc for the same reason.

The true density of the cordierite glass C-O before and after devitrification was determined to be 2.625 and 2.519 gr/cc respectively. These values are in good agreement with published values. The decrease in density from the random to the oriented structure is quite unusual however this is more apt to be the case of the open type crystalline structure characteristic of a very low thermal expanding crystalline phase. The additive glass composition C-B increases from 2.774 gr/cc as a glass to 2.848 gr/cc as the devitrified body. This is more characteristic of ceramics structures with higher thermal expansion. Further the true density of the bonding glass C-B is 2.848, when devitrified on firing. Specimens made of this glass exhibit a bulk density of 2.83. These specimens are 99.3% their true density and thus exhibit only 0.7% void volume. This is characteristic of the prereacted raw material approach when only one glass is involved.

b. Composite Bodies

As discussed above the ten additive glasses studied were mixed individually with the cordierite glass, C-O at 10, 20 and 30% respectively. Specimens were prepared as discussed above and fired over a termpreature range in which the lowest temperature resulted in slightly porous specimens, and the highest generally displayed evidence of overfiring. The physical and electrical properties are shown in Table VI on pages 50 through 52.

At cordierite glass 90% and bonding glass 10% the maturing temperatures for all composite bodies ranges from 2575 to 2625°F and the firing range is 50 to 100°F.

The bulk-density values range from 2.35 for the addition of composition C-D to 2.49 for the addition of composition C-F. At the firing temperature required to attain maximum density, all bodies exhibited a 0.00% moisture absorption. The firing range, the temperature range over which maximum density and a 0.00% moisture absorption are attained, is at least 50°F for all composite bodies prepared with the 10% addition of low melting glass. The variation in the bulk density between the different compositions can in general be attributed to the variation in the bulk densities of the additive glasses. The attainment of the 0.00% moisture absorption and the 50°F firing range indicate that the additive glass possesses a viscosity at the firing temperature which is of sufficient fluidity to density the body, yet it does not change in viscosity rapidly such as to result in an overfired body.

TABLE VI

Compositions and Properties of Composite Bodies

Glass Compositions C-C	C-A	C-B	C-C	C-D	C-E	C-F	Cb-98	Cb-910	Cb-96	Cb-9
	Cordierite Glass 90% - Bonding Glass 10%									
Firing Temp. (°F)[1]	2625	2575	2575	2575	2600	2575	2600	2600	2600	2600
Density (gr/cc)[1]	2.40	2.41	2.44	2.35	2.31	2.49	2.42	2.43	2.40	2.38
Firing Temp.	2675	2675	2675	2675	2675	2675	2675	2675	2675	2675
Density[2]	2.49	2.49	2.49	2.42	2.49	2.51	2.44	2.45	2.42	2.40
Coef. Therm. Exp.[3]	1.55	1.37	1.64	1.59	1.53	1.55	1.65	1.59	1.44	1.41
Modulus of Rupture (psi)	16,500	14,700	14,000	15,000	16,700	15,100	15,800	16,600	16,200	15,000
Dielectric constant (1 Kc)	5.10	5.07	5.10	4.95	5.11	5.13	5.09	5.08	5.18	-
Dielectric constant (1 Mc)	4.61	4.61	4.70	4.46	4.62	4.70	4.60	4.61	4.78	-
Power Factor (%) (1 Kc)	.340	.353	.318	.385	.336	.340	.312	.341	.312	-
Power Factor (%) (L Mc)	.330	.357	.370	.345	.335	.345	.375	.328	.290	-
True Density (gr/cc)				2.478						

TABLE VI (Continued)

Glass Compositions C-O	C-A	C-3	C-C	C-D	C-E	C-F	Cb-98	Cb-910	Cb-96	Cb-9
	Cordierite Glass 80% - Bonding Glasses 20%									
Firing Temp. (°F)[1]	2550	2500	2500	2500	2500	2525	2525	2525	2525	2525
Density (gr/cc)[1]	2.40	2.41	2.41	2.30	2.36	2.45	2.39	2.40	2.40	2.30
Firing Temp. (°F)[2]	2625	2625	2525.	2600	2650	2600	2625	2600	2625	2625
Density[2]	2.38	2.29	2.32	2.28	2.49	.244	2.40	2.43	2.44	2.29
Coef. Therm. Exp.[3]	1.68	1.57	1.75	1.86	1.64	1.73	1.75	1.67	1.61	1.83
Transverse Strength (psi)	14,000	13,800	12,300	12,600	14,300	12,900	13,000	15,000	15,100	13,400
Dielectric constant (1 Kc)	5.09	5.08	5.09	4.91	5.20	5.13	5.06	5.06	5.15	-
Dielectric constant (1 Mc)	4.55	4.58	4.67	4.44	4.75	4.64	4.61	4.52	4.74	4.75
Power Factor (%) (1 Kc)	.331	.323	.309	.380	.350	.322	.243	.322	.335	-
Power Factor (%) (1 Mc)	.311	.345	.363	.340	.361	.332	.389	.356	.315	.300

- 52 -

TABLE VI (Continued)

Glass Compositions C-O	C-A	C-B	C-C	C-D	C-E	C-F	Cb-98	Cb-910	Cb-96	Cb-9
		Cordierite Glass 90% - Bonding Glass 30%								
Firing Temp. (°F)[1]	2375	2300	2300	2300	2375	2300	2325	2400	2375	2375
Density (gr/cc)[1]	2.36	2.43	2.42	2.35	2.35	2.45	2.35	2.36	2.33	2.30
Firing Temp.[2]	2500	2450	2450	2425	2525	2500	2475	2500	2500	2475
Density[2]	2.36	2.24	2.40	2.01	2.37	2.21	2.37	2.38	2.34	2.31
Coef. Therm. Exp.[3]	1.73	1.89	1.81	2.11	1.23	1.91	1.94	1.83	1.77	2.07
Transverse Strength (psi)	-	11,800	10,050	-	11,420	-	11,900	-	13,700	-
Dielectric Constant (1 Kc)	-	5.10	5.07	-	5.14	-	5.07	-	5.17	-
Dielectric Constant (1 Mc)	-	4.54	4.60	-	4.70	-	4.65	-	4.75	-
Power Factor (%) (1 Kc)	-	.353	.291	-	.299	-	.253	-	.291	-
Power Factor (%) (1 Mc)	-	.362	.301	-	.341	-	.340	-	.271	-

1. At which 0.05% moisture absorption is realized.
2. Maximum before overfiring.
3. Between room temperature and 150°C.
4. Picnometer density.

The coefficients of linear thermal expansion are low ranging from 1.37 to 1.65 "/"/°C. The composition of the bonding glass does not effect this property directly. The variation may to be due to interaction of the glasses.

For composite body compositions, 80% cordierite glass - 20% bonding glass, the minimum maturing temperature ranges from 2500 to 2550°C while the maximum ranges from 2600 to 2625°C. This is the firing range and covers between 100 and 125°C over which the maximum moisture absorption is 0.05% and the bulk density is essentially constant. The bulk density ranges from 2.28 to 2.44 gr/cc at the minimum maturing temperature and tends to remain essentially the same at the maximum firing temperature. Variation in composition of the bonding glass appears to have little effect on density of the composite bodies. The coefficients of linear thermal expansion increases slightly for those for the 90% - 10% compositions with the values ranging from 1.57 to 1.86 "/"°C.

For composite body compositions, 70% cordierite glass - 30% bonding glass, the minimum maturing temperature ranges from 2300 to 2375°F while the maximum ranges from 2450 to 2525°F. This is a firing temperature range of approximate 150°F over which 0.05% moisture absorption is the maximum and the bulk density remains essentially constant. This latter property ranges from 2.30 to 2.45 gr/cc and remains essentially constant through the maximum firing temperature for each composition. There are several indications of overfiring as identified by decreased bulk density at the maximum firing temperature and by that composition containing C-B glass. Variations in composition of the bonding glass appears to have little effect on density of the composite bodies. The coefficients of linear thermal expansion are again increased slightly to between 1.73-2.11 "/"/°C for compositions containing the 10 bonding glass. In general an increasing amount of additive glass has the following effects:

1. The bulk density decreased slightly. The reason for this is not obvious as cordierite which is the lower in density decreases and the bonding glasses which are higher in density are decreasing. It may be that the greater glass content entraps more voids thus decreasing the density.

2. The firing range increases. This property increases from 50°F for the 10% addition to 150°F for the 30% addition. The glass obviously is quite viscous and the higher contents lower the firing temperature well below that when the cordierite crystalline phase starts to be dissolved into the glass.

3.   The maturing temperature decreases.   It is decreased
fror approximately 2575°F minimum at the 10% bonding glass
addition to approximately 2475°F at the 30% addition.   This is
to be expected because of the increased glass content whose
melting temperature is approximately 2300°F.

4.   The maximum maturing temperature decreases.   This also
is to be expected as the glassy phase developed tends to dissolve
the cordierite crystalline phase and the more glass present the
easier it can dissolve cordierite at lower temperatures.

The true density of the 90% Cordierite - 10% C-D bonding glass
is 2.478; its bulk density alone fired to 2600°F, the maximum
maturing temperature, is 2.42.   This is 97.6% of true density;
that is, the specimen contains 2.4% pore volume.   At its min-
imum firing temperature, 2575°F, the bulk density is 2.35; that
is 92.7% of true density.   The former valve is very high for this
type composition while the latter is more or less normal.   This
increase in pore volume as noted by decreasing density is un-
doubtedly due to the two glass system in which the frits were
mixed as larger individual particles.   The coefficients of linear
thermal expansion in the temperature range fo 650°C range
from: 1.37-1.65 for all compositions at 90% cordierite glass -
20% bonding glass; and 1.23-2.40 at 70% Cordierite glass - 30%
bonding glass.   Though these ranges of values overlap, each bond-
ing glass at increasing contents caused the coefficients to in-
crease.   This is shown in Figure 15 on page 56 in which the
linear expansion vs temperature relationship of bonding glass C-A
at several addition levels is presented.   The curve for the cor-
dierite glass C-O after devitrification is also presented.   This
latter material is characterized by a low negative thermal ex-
pansion between room temperature and approximately 200°C which
decreases as the additive glass content is increased and actually
disappears at a 30% addition of the bonding glass C-A.   This
behavior is cordierite has been reported.   The magnitude of ex-
pansion at any additional level varies directly with the magni-
tude of the expansion of the bonding glass.

Transverse strength values for those compositions containing
10% addium glass average 15,600 psi and range from 14,000 to 16,
700 psi.   The high value is realized with bonding glass Compo-
sition C-E which contains the lowest RO and highest value silica
contents.   Values decrease as alumina and silica contents de-
crease.   The same behavior is exhibited with those compositions
containing 20% additive glass with one exception namely compo-
sition C-E which is slightly low.   The average value drops to

Figure 15
Thermal Expansion vs. Temperature of Several
Cordierite Compositions
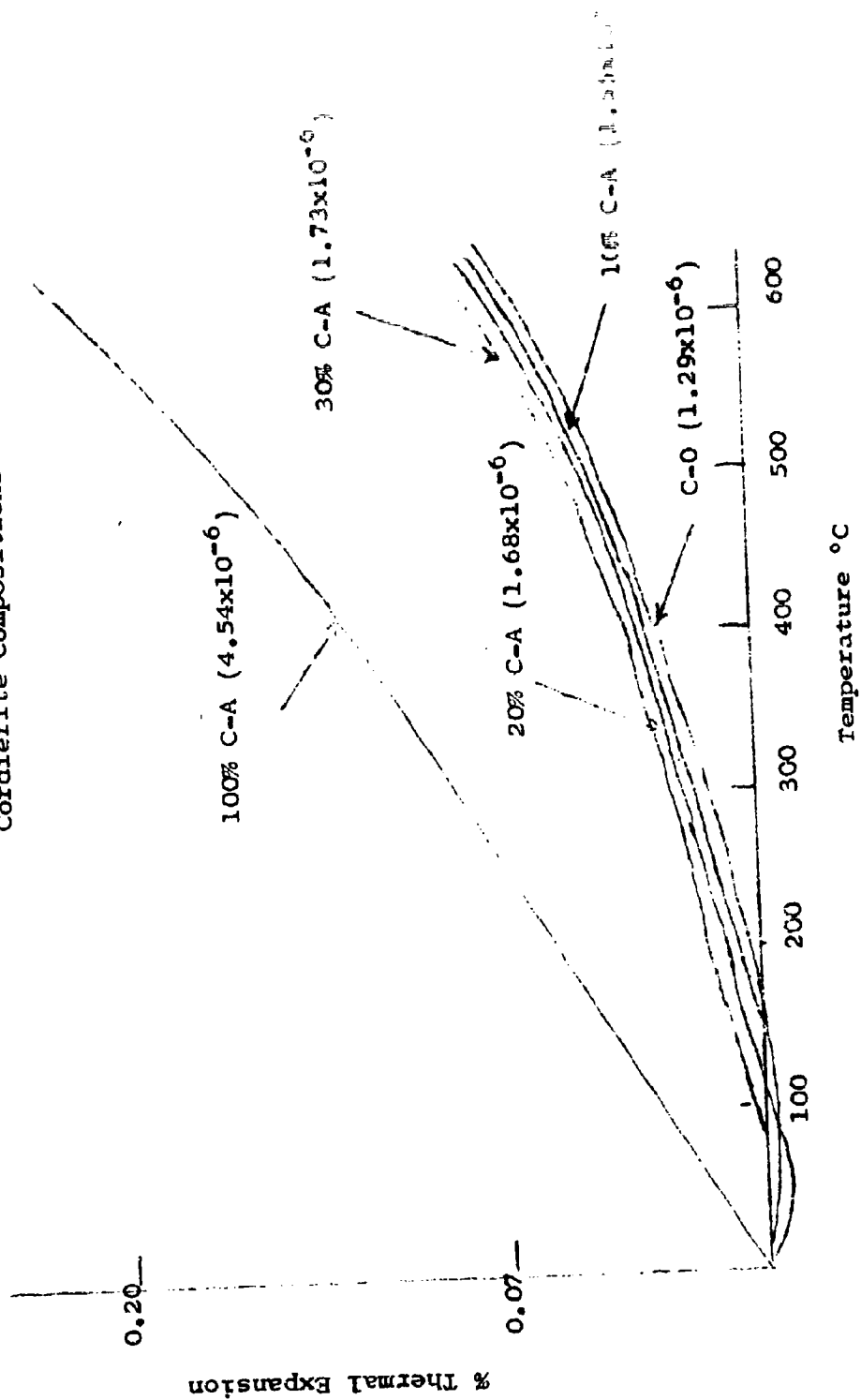
13,700 psi. Those compositions containing 30% additions of
glass exhibit an average transverse strength value of 11,900
psi. In general the higher values are found in the low RO
part of the compositional diagram of the bonding glasses. Thus
with a value of 11,900 psi at the 30% glass composition, a de-
crease in glass content to 20% results in increasing the trans-
verse strength by 13.5% and a decrease to 10% bonding glass in-
creases at the 31.1% at an average value of 15,600 psi.

The electrical properties proved to be quite uniform
throughout the effort. The average dielectric constant for all
compositions varies from 5.09 to 5.11 at one Kc and from 4.63
to 4.65 at 1 Mc. This behavior is to be expected because the
densities are higher and quite uniform and the glass; phases
are alkaline earth aluminosilicates. The frequency effect is
also to be expected. At 1 Kc the power factor decreases as the
glass content increases from .336% to 10% bonding glass to .297%
at 30%. Normally the reverse effect is expected; however, the
general background with cordierite type compositions is that the
losses are generally quite high. They are quite low here, how-
ever the effect of the increased cordierite content tends to
make itself felt. At 1 Mc the power factor is very uniform with
average values ranging from .331 to .343% and varying directly with
the bonding glass content from 10 to 30%. Thus the elec-
trical losses are low and quite uniform. This is due to the
alkaline earth type glasses developed and the rather high and
uniform densities of the composite bodies.

As noted in Table I on page -22 and discussed above, several
of the bonding glasses were evaluated for power factor as mon-
olithic glasses and as devitrified bodies. All three bonding
glasses thus evaluated exhibit powers higher than the composites
bodies with an average value of .450% at 1 Mc. This is due to
the fact that all the loss producing ions are in the glass or
random structure where they can contribute to losses. When
devitrified by a second heat treatment it dropped to .144% which
is considerably below that of the composite body. This is due
to a considerable amount of the loss producing ions being bonded
in the devitrified crystalline phase. Thus the power factors of
the bonding glasses evaluated are higher than those of the com-
posite bodies containing them but when they are devitrified the
values are much lower. It is anticipated that the failure of
the composite bodies to realize the low power factors of the de-
vitrified bonding glasses which are present in them, is due to
the presence of the cordierite crystalline phase.

c. Structural Analysis of Composite Bodies

Selected samples of several compositions were polished and etched with H_2SiF_2 and photomicrographs of the structure taken at 600X. Figure 16 on page 59 present these for: compositions containing 90% cordierite and 10% bonding glasses C-A and C-D respectively; compositions 80% cordierite and 20% bonding glass C-D; and compositions containing 70% cordierite and 30% bonding glasses C-E and Cb-98 respectively. The structure is similar in all cases. The cordierite crystals are well developed and range from 355 microns in size; they are identified as the light gray material. The Ba-C phase occurs in crystals 1-8 microns in size which are sparely dispersed and increased in content as does the bonding glass content; it is identified as the white crystals. The glass is well dispersed and is also found in finger shape pockets up to 3 microns in length and one micron wide. It is anticipated that the small black areas are regions where the glass has been etched out. The larger, rounded block areas are voids, many of which are due to poor dispersion of the binder; some are up to 10 microns in diameter. The glass content in the composite body increases as the bonding glass content. The following point count analysis indicates that there is little reaction between the two glasses and the content of the respective phases are approximately the same after firing.

Point Count on the Composite Bodies

	90% C-O 10% C-A	80% C-O 20% C-D	70% C-O 30% C-E
Cordierite	85.81%	72.68%	64.51%
Secondary Phases	10.16	18.92	28.56
Voids	4.03	8.40	6.93
Per Cent Cordierite			
Exclusive of Voids	89.4%	79.3%	69.3%

Comparing the three composite bodies, it is seen that the additive glass plays the same role in all compositions. It is used primarily to densify the body with the added advantage of being low melting, having excellent wetting properties with

Figure 16

Photomicrographs of Composite Bodies Containing
Additions of Low Melting Glass

10% C-A

600x ——10 Microns

10% C-D

600x ——10 Microns

20% C-D

600x ——10 Microns

20% C-D

600x ——10 Microns

30% C-E

700x ——10 Microns

30% Cb-98

600x ——10 Microns
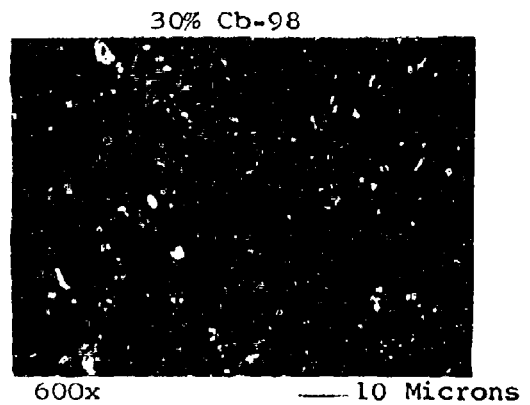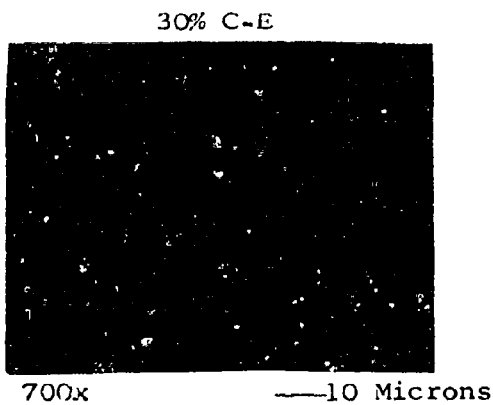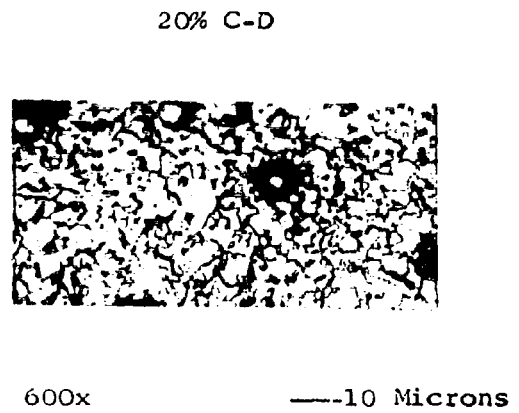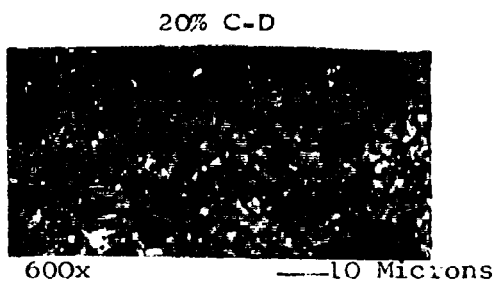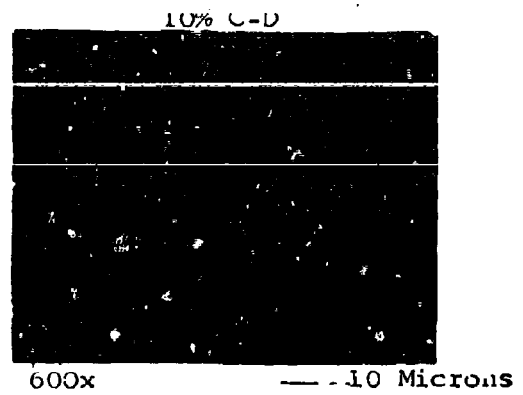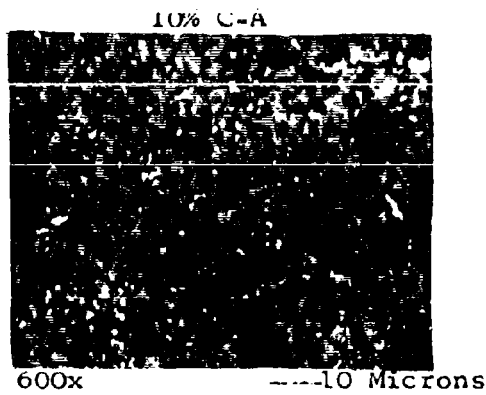
regard to the cordierite, and devitrifying to some extent to reduce the glassy content of the body. As the amount of added glass incorporated in the body is increased, the glass content and the BA-C crystalline content increases a proportional amount in the final fired bodies. The cordierite content decreases as the added phases increase, however in the fired body it is only slightly lower than the content incorporated. This is attributed to the slight amount of solubility or interaction of the cordierite in the glass,

Figures 17A and B on pages 61 and 62 are electron photomicrographs of two areas of the composite body prepared with a 20% addition of the low melting glass C-D. They show the microstructure magnified 10,000 times. Since, as was shown by the light microscope, the average grain size of the cordierite crystals is three to five microns, it was necessary to focus on smaller grains in order to contain a whole grain within the field of view. The grain size shown is not indicative of the average grain size of the cordierite in the final fired body. Holes approximation 0.01 micron in size can be seen scattered throughout the cordierite grains. It is reasoned that these holes are submicroscopic pores. By the nature of their spherical shape, it is reasoned that when the glass frit is prepared, very small gas bubbles were trapped within the glass particles. In the firing of the composite body, these spherical pores can act as nucleation sites for the devitrification process. After the grain boundaries are formed, they begin to move through the grain in an attempt to reduce the grain boundary surface area. If there is sufficient energy associated with the grain boundary, it will sweep past the pores leaving them in the interior of the grain. The grain boundary may also sweep through the grain carrying the pores along with it. Both cases are seen in these photographs. Pores are seen at the interior of the grains and are collected at the grain boundaries. The pores trapped in the interior are very difficult to remove since they must migrate by diffusional means to the grain boundary where they will be sunk. They may also be due to the function of many very small crystals on devitrification with selective directional grain growth result in the formation of pores at the intersection of several crystals. The remainder of the process would be as described above.

The presence of the bonding glass is noted by the lighter areas which surround each grain. It can be seen that the glass is well dispersed and coats each grain individually. This would

Figure 17A

Electron Micrograph of Composite Body
80% Cordierite - 20% Bonding Glass C-D
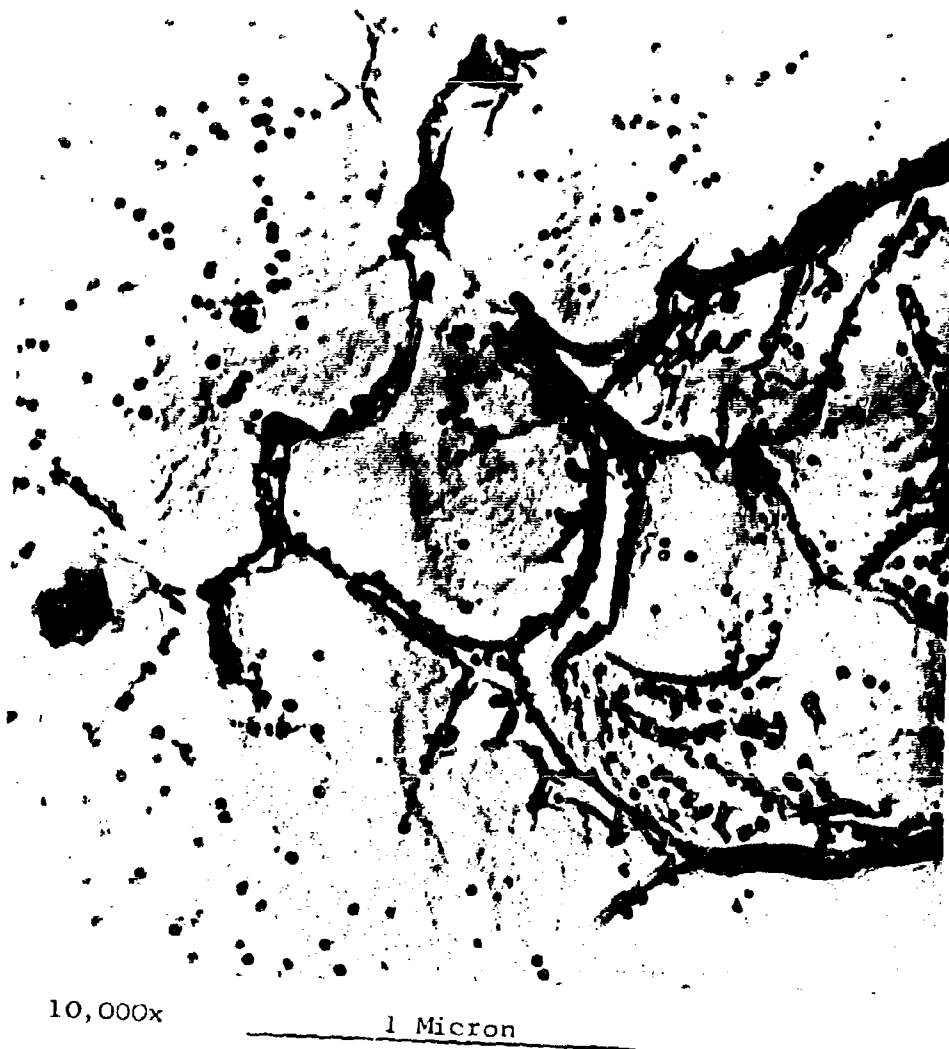
10,000x   1 Micron

Figure 17B

Another Area of 17A

Electron Micrograph of the Composite Body
Prepared with a 20% Addition of Composition C-D

10,000x   1 Micron

further indicate that excellent wetting has occurred and that the glass is effective as a sintering agent. The glass has sufficient fluidity to be well dispersed throughout the body, and the wetting action pulls the grains together by capillary forces to sinter the body. The presence of the rounded grain boundaries adjacent to the glassy phase indicates that there is some solubility of the cordierite grains in the glass.

These photographs show graphically that the additive glass has satisfied all the requirements set forth in this study. The glass was required to be fluid at low temperatures, effectively wet the cordierite, not hinder cordierite development, and act as a sintering agent of the reactive liquid type. It is quite apparent that additive glasses of the type utilized in this study are necessary and beneficial in producing dense cordierite bodies.

Thus a structural study as determined by electron microscopy shows that cordierite is devitrified into crystals ranging from approximately 1-5 microns in size and that voids or pores are present in these crystals. These are due either to gas entrapment during fritting or sintering of many very small devitrifiable crystallites during firing. A second phase Ba-C is devitrified in small amounts from the bonding glasses and occurs in sizes ranging from 1-8 micron scattered throughout the body. The glassy phase wets the crystals and there is indication that some reaction takes place. It occurs on the surface of the crystals and in finger-like pockets. The percentage of phases present, that is, cordierite and others as per pointcount analysis is a function of the raw composition. The crystal size and glass pocket sizes are approximately the size as the original glass particle sizes.

d. Thermal Shock Study

Cordierite compositions are characterized by their low thermal expansion which results in rather high thermal shock resistance. All thermal shock test procedures result in qualitative data only. The criterion of failure takes on one of several forms: appearance of the first crack, decrease in transverse strength, specimens breaking into several pieces, etc. The object of this phase of the work was to attempt to establish a quantitive test procedure to evaluate the cordierite compositions made from two frits.

The theoretical background of stress-strain effects must be considered for a perfectly elastic body, the applied stress is an unique function of the strain. Since the variation of the stress-strain ratio is not time dependent, these ideal solids do not show elastic after-effects. However, all materials are non-ideal solids and they exhibit stress-strain relationships which deviate from perfect elastic behavior. Zener[3] introduced the formal theory and physical interpretation of anelasticity using a mechanical model proposed by van Rotger.[4] When a force is applied to this model, called a standard linear solid, an instantaneous elastic deformation occurs, followed by a time dependent delayed elastic deformation. Upon removal of the load, there is an instantaneous recovery of the elastic deformation followed by a time dependent delayed elastic recovery. This relationship between stress and strain can be shown mathematically by:[60]

$$T_E \frac{ds}{dt} + s = M_*(T_s \frac{dE}{dt} + E)$$

where:

T_E = relaxation period at constant strain
T_S = relaxation period at constant stress
s = stress
E = strain
t = time
M_* = modulus govering final equilibrium achieved at time ∞

This relationship approaches the elastic behavior displayed by most ceramic materials, however, it is not a complete representation.

In a non-linear solid, a periodically applied stress will result in a periodic strain lagging behind the stress. The tangent of the phase angle indicating this lag is one measure of internal friction. Internal friction is a dimensionless quantity used to describe the ability of a material to dissipate mechanical vibrational energy. Tan δ, the tangent of the angle by which the strain lags the stress, can be expressed mathematically as:[2]

$$\tan \delta = (\tan \gamma) \max. \frac{W}{1+W^2} T^2$$

where:　T = mean relaxation time
　　　　W = frequency
　　　　= angle by which the strain lags stress.

It can be seen that the energy loss per cycle is a maximum
when the period of vibration is just equal to the relaxation
time for the process. Various process can lead to delayed
anelastic deformation and the resultant energy loss. These
include heat diffusion, chemical diffusion, stress induced
ion jump, viscous flow, viscoelastic effects, and internal in-
homogeneities as proposed by Reid[5] and Marino[6]. Reid[5] is cur-
rently investigating the contribution of cracks and other in-
ternal disorders by internal friction techniques and Marino[4]
is currently investigating the detection of crack propagation
by internal friction techniques.

　　　When ceramic materials are subjected to a rapid change
in temperature, stresses are developed which result in a weak-
ening or fracture of the ceramic body. The effect of the of
thermal stress has a material dependence with regard to thermal
conductivity, elastic modulii, porosity, homogeneity, and duct-
ility. There is also a physical dependence such as stress level,
stress distribution, stress duration, size, shape, temperature
gradient, and surfact heat transfer. Thus, there has been no
satisfactory quantitative representation of thermal shock re-
sistance because of the complex nature of the subject. In
the simple case where the materials are assumed to be ideally
elastic, fracture occurs when the surface stress reaches the
critical level. Assuming rapid rates of heat transfer, the
temperature gradient necessary for fracture in the ideal case
is given by:[97]

$$T_f = \frac{f\,(1 \cdot \mu)\ S}{E\ a}$$

where:

　　　T_f = temperature gradient for fracture
　　　E = modulus of elasticity
　　　a = coefficient of linear thermal expansion
　　　f = stress required for fracture
　　　μ = Poisson's Ratio
　　　S = shape factor.

Other relationships which consider surface heat transfer, size, porosity, thermal conductivity, and stress duration are derived to give a better approximation for τ_f, the temperature gradient required for fracture. However, the conditions are still not ideal and there is no quantitative measure with regard to the degree of failure. A ceramic body which has undergone thermal shock may exhibit a large volume of cracks, but there is no actual physical separation. Therefore, the temperature gradient required for fracture does not consider a body which has thermally induced cracks, but which hasn't physically failed. A truer measure of thermal shock would be the temperature gradients necessary to induce failure, or physical separation, rather than one which measures fracture or cracking.

This leads into the object for this section of the study. Cordierite bodies will be quenched at temperature gradients below the temperature gradient required for failure. The internal friction of each bar will be measured in an attempt to correlate the increase in internal friction values with the amount and degree of thermally induced cracking within the cordierite body. The object of this study is to show that thermally induced cracks, which certainly detract from the integrity of the body, are present much below the failure temperature gradient. Also, it will be shown that a semiquantitative measure of the volume of cracks through internal friction measurements can be attained.

Specimens were prepared from individual compositions of the composite bodies containing 10, 20, and 30% additions of composition C-E and a 10 and 30% addition of composition CB-96. Bars, 3" x 1/2" x 1/4", were dry pressed under a pressure of 10,000 psi utilizing a 5% Superloid solution as a binder. These bars were fired to maturity in a six hour firing cycle with a one hour soaking period at the maximum temperature. All bars were ground to a size of 2.500 ± 0.01" x 0.080 ± 0.005" x 0.120 ± 0.005" using a standard ceramic machining process. Steel armatures in the form of one-sixteenth of an inch diameter flat discs were attached to the bars using Testors Model Cement, Formula B, in order to provide energy coupling between the specimen, the audio generator, and the pick-up system.

The apparatus utilized to determine the resonant frequency and the internal friction values for the individual bars is shown in Figure 18 on page 67. This consists of Acoustic Spectrometer, Model V, Nametre Corporation, and Flexural Adjustable Transducer, Nametre Corporation, and Electric Counter, Model

Figure 18

Apparatus for Internal Friction Measurements

Transducer and Sample

Audio Spectro- meter

Electronic Counter
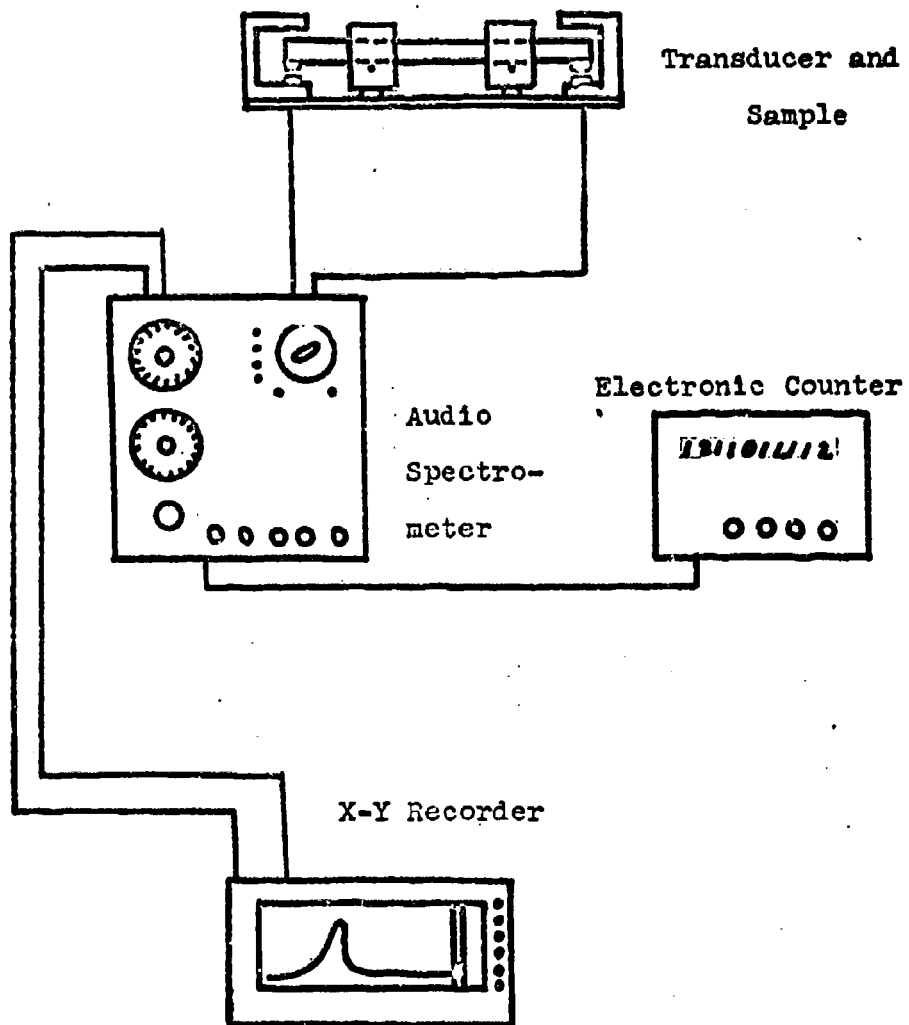
X-Y Recorder

524C, Hewlett-Packard Corporation, and a X-Y Recorder, Model 97-U, Houston Instrument Company.

The bars were inserted in the transducer with both ends free by setting the bar on thin wire supports at the nodal points (0.22 length from each end). The driving and receiving end of the specimens are subjected to a static magnet field produced by the Alnico V core of the coil within the transducer. Superimposed on this static field at the driving end is an oscillating magnet field generated by the acoustic spectrometer. The oscillating field induces eddy currents in the steel armature, which in turn are pulled and pushed by the oscillating, inhomogeneous, magnet field, thereby exerting an oscillating force upon the specimen. At the detecting end, the specimen is subjected also to a stationary magnetic field. Vibrations therefore induce eddy currents at this end. The field of these eddy currents is then detected by the pick-up at this end and transferred through the audio spectrometer to the X-Y recorder.

The weight of the steel armature results in a shift of the resonant frequency to a lower value than that which would be recorded for the bar alone measured by another technique. A calibration curve was obtained by plotting frequency versus armature weight. This plot was found to be linear, and through regression analysis an equation for the line was determined. From the relationship:

Measured Resonance Frequency = True Resonance Frequency - (4100.659) (Weight of armature in grams + glue), the true resonance frequency can be determined.

The determination of Young's modulus can be calculated from the following formula:[8]

$$Y = \frac{0.9464 \ f^2_r L^4 \ p}{a^2}$$

Where:

Y = Young's Modulus (dyness/cm.^{2})
L = length (cm.)
p = density (gm./cm.^{3})
a = thickness (cm.)
f_r = resonance frequency (cycles/sec.)

When the bar is driven at its resonance frequency, the amplitude
of vibration is at its maximum. At the maximum amplitude, as
determined from the X-Y recorder, the resonance frequency is
read from the electronic counter. This frequency is the reson-
ance frequency for the bar with the armatures attached, and it
is corrected to determine the resonance frequency of the bar
alone. This value, along with the values for length, thickness,
and density of the bar are inserted in the formula to obtain a
value for Young's Modulus. The values determined are shown in
Table VII.

The value of internal Friction can be calculated from the
formula:[4]

$$\text{Internal Friction} = Q^{-1} = \frac{\Delta f}{\sqrt{3}\ f_r}$$

where:

f_r = corrected resonance frequency of bar

f = the change in impressed frequency necessary to change
the amplitude from half-maximum on one side of the
critical frequency to half-maximum on the other side.

The bar is driven at its resonant frequency and the amplitude
of vibration is recorded on the X-Y recorder. The bar is then
driven at a significantly lower frequency to determine the am-
plitude of the background. A line is recorded equidistant
between the maximum amplitude and the background on the chart
paper in the X-Y recorder. Utilizing the frequency scatter in
the audio spectrometer, the bar is driven at the frequency which
coincides with the frequency of one-half the maximum amplitude
on both sides of the resonant peak. The values were determined
by using the electronic counter, and they were inserted into the
formula for internal friction as $f = f_1 - f_2$, where f_1 and f_2
are the frequencies associated with the half widths of the reson-
ant peak. The bar was then driven at it resonance frequency and
the value determined by the electronic counter. These three
frequency values were then inserted in the formula, and the value
of internal friction was determined. The values are shown in
Table VII on page 70.

TABLE VII

Young's Moduli and Internal Friction for Selected Ceramics
Including Several Two Glass Cordierite Compositions

Ceramic Bodies	Modulus dynes/cm.^{2}
Sintered Alumina Body (5% Porosity)................	$3.6C \times 10^{12}$
Sintered Magnesia Body (5% Porosity..............	2.10×10^{12}
Sintered Zirconia Body (5% Porosity).............	1.52×10^{12}
Composite Cordierite Body (90% C-O 10% C-R)......................	1.28×10^{12}
Silica Glass......................................	0.72×10^{12}
Pyrex Glass.......................................	0.69×10^{12}
Mullite Porcelain.................................	0.69×10^{12}
Steatite Porcelain................................	0.69×10^{12}
Cordierite Porcelain..............................	0.56×10^{12}

Additive Glass	Young's Modulus	Internal Friction (Q^{-1})
10% C-E	1.28×10^{12} dynes/cm.^{2}	1.37×10^{-4}
20% C-E	1.26×10^{12}	1.42×10^{-4}
30% C-E	1.12×10^{12}	1.92×10^{-4}
10% Cb-96	1.28×10^{12}	1.49×10^{-4}
30% Cb-96	1.13×10^{12}	1.91×10^{-4}

For the thermal shock test, the bars were placed in an electric kiln and heated to 300, 500, 700, 900, and 1100°C in individual firings of four hours with a holding period of two hours to stabilize the temperature. At the end of the holding period, the bars were quickly removed from the kiln and dropped into a 1000 ml beaker of boiling water. After drying overnight, armatures were cemented on the bars in the predescribed manner. Young's modulus and internal friction values were determined for all the thermally shock bars in the manner previously described.

Table VII on page 70 presents Young's moduli and internal friction values for selected ceramic compositions and for several two glass cordierite compositions. The Young's modulus values for the cordierite compositions are in keeping with fundamentals in that the higher glass compositions exhibit lower values, as are the internal friction values which increase as the glass content increases. From the values for the ceramic bodies it was established that the apparatus was operating correctly. Table VIII on page 72 shows the internal friction Young's modulus values for selected compositions exposed at several quenching gradients or thermal shock conditions. Figure 19 on page 73 shows the thermally induced cracking at the various quenching temperatures for the composite body prepared with a 30% addition of low melting glass Cb-96. When investigated under a microsocope, the cracks were found to be less than three in width. Water based dyes of fluorescein and methyl violet were unable to penetrate into the cracks. It was necessary to use Dubl Chek Penetrant Dp-52, Belmont Chemicals, for visual observation of the cracks. However the penetrant in the cracks was not of sufficient contrast to allow photographic reproduction. The figure is a drawing rather than a photomicrograph. The crack population was drawn to scale; but the width of the cracks is greatly exaggerated.

For those compositions studied the internal friction values are quite low ranging from 137 to 192 x 10^{-4} with the values increasing with the bonding glass content. After the 200°C quenching test all compositions exhibit a slight increase in value, then all decrease progressively as the quenching temperature. This general behavior is anticipated as the formation of the cracks, their size, shape, and number increase the internal friction. The behavior after the 200°C quenching cycle, that is a decrease in internal function, may be due to "thermal conditioning" a process analogous to the tempering of glass which results

TABLE VIII

Internal Friction and Young's Modulus of
Compositions Exposed to Several Quenching Gradients

Internal Friction ($\times 10^{-4}$)

Additive Glass	Per cent Addition	Quenching Gradient (°C)					
		0	200	400	600	800	1000
C-E	10	1.37	1.36	1.83	9.30	15.24	19.07
	20	1.42	1.18	5.71	8.64	10.32	11.36
	30	1.92	1.74	8.16	10.37	14.66	15.25
CB-10	10	1.49	1.36	1.86	12.68	14.66	22.49

Youngs Modulus ($\times 10^{12}$ dynes/cm^2)

C-E	10	1.28	1.28	1.28	1.25	1.24	1.24
	20	1.26	1.27	1.24	1.24	1.23	1.20
	30	1.12	1.12	1.12	1.09	1.08	1.01
Cb-96	10	1.28	1.26	1.26	1.23	1.20	1.16
	30	1.13	1.13	1.10	1.10	1.06	1.06

Figure 19

Thermally Induced Cracking
Composite Body Containing 30% of Bonding Glass Cb-96

200° C. Thermal Gradient

400° C. Thermal Gradient

600° C. Thermal Gradient

800° C. Thermal Gradient

1000° C. Thermal Gradient

1000° C.   End View

- 74 -
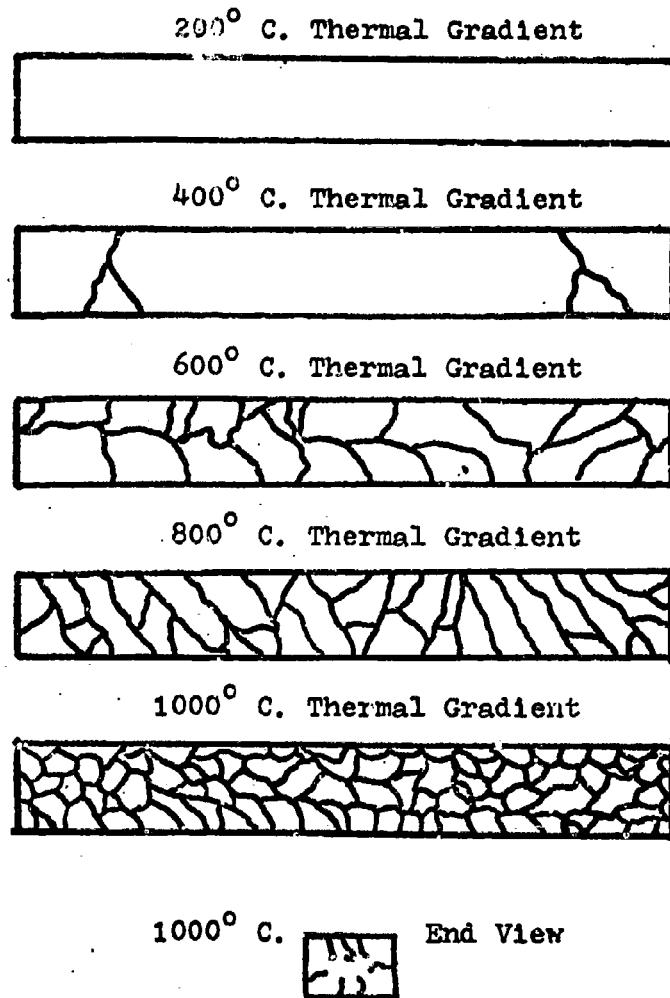
in increased strength; this is undoubtedly due to a compressive
layer induced in the surfaces of the composite bodies by rapid
cooling or quenching. This mechanism has resulted in increas-
ing transverse strength up to 80% in some compositions.

From Table VIII on page 72 it can be seen that while the
internal friction values increases, the Young's modulus values
decrease with increasing temperature gradients above 200°C.
The increase in crack population increases the internal friction
values and decreases the Young's moduli values. Reid[3] proposed
that the mechanism which gives rise to the increasing internal
friction values is a mechanical damping of the wave by the crack
interfaces. The decrease in Young's modulus is attributed to
the loss of rigidity of the bar from the cracks and a scatter-
ing of the wave at the crack interfaces. With both of these
postulated mechanisms, the internal friction value and the
Young's modulus are dependent upon the crack population. The
numerical contribution of individual cracks to an increase in
internal friction values or a decrease in Young's modulus has
not been determined; however, it is anticipated that with a com-
plete knowledge of crack population, width, length, and config-
uration, the numerical contribution of each crack to internal
friction and/or Young's modulus values can be determined.

The composite bars prepared for this study were found to
be able to withstand a thermal gradient of 1000°C without
physical separation. However, with a 400°C gradient, they were
found to exhibit small diameter cracking. These cracks would
have a severe detrimental effect on the strength characteristics
of the bodies. Thus, in reality, there must be at least two
significant temperature gradients in a discussion of thermal
shock; the temperature gradient necessary to propagate a crack,
and the gradient necessary to physical failure. The distinc-
tion becomes important in radome materials. The primary function
of the radome is a housing for the radar apparatus possessing
sufficient homogeneity for radar transmission. If the crack
population is of such a nature and volume to allow radar trans-
mission, then the effect thermal gradient that these composite
bodies can withstand is above 1000°C.

This study has shown that the effects of thermal shock may
be measured quantitatively below the temperature gradient at
which physical separation or failure occurs. There is indica-
tion that a low temperature quench induced thermal conditioning
which is measureable by a decrease in internal friction values.

Also, it has been found that small diameter cracks are present
above a quenching gradient of 500°C in the composite bodies,
and that the population of these cracks increases with an in-
creasing thermal gradient. There appears to be a direct cor-
relation between the crack population and the values determined
for internal friction and Young's modulus.

There are many important ramifications of this study which
deserve further comment. First, the decrease in internal fric-
tion at the low temperature quench may be a measure of the
effectiveness of thermal conditioning. Second, the numerical
contribution to internal friction values by the crack population
can be calculated. Third, the significance of the temperature
gradients, one for crack propagation and the other for physical
separation, deserves further study. And finally, internal
friction measurements may be sued as a numerical criteria for
thermal shock resistance.

5. Summary

In this aspect of the study, cordierite bodies exhibiting
low thermal expansions and extended firing ranges were developed
using an intimate mixture of two devitrifiable glasses in their
fabrication. One frit was of the theoretical cordierite com-
position, and the second of a low melting glass in the BaO-CaO-
MgO-Al$_2$O$_3$-SiO$_2$ system. The function of the cordierite glass was
to devitrify wholly into cordierite during the final firing
operation, thus maximizing and controlling the cordierite content.
In the case of the additive glass, the function was to: 1) supply
a low melting liquid phase for sintering or densification, 2)
effectively wet the cordierite phase, 3) allow ions from the glass
to go into solid solution in the crystalline cordierite, 4)
slightly dissolve the cordierite, and 5) subsequently devitrify
to some extent to reduce the glassy content of the body. The
experimental work has shown that both glasses performed as de-
signed and satisfied their basic requirements.

The bodies prepared were studied with respect to structure,
properties resulting from the structure and composition. Micro-
structural analysis showed the bodies to be fine grained (3 to
5 microns) with a relatively homogeneous distribution of glass
and possessing a small pore volume (approximately 5%). Some of
the glass content appeared as elongated firings like concentra-
tions. Electron microscopy showed that the glassy phase wets
and slightly dissolves the cordierite phase. X-ray analysis de-
termined that cordierite was the principle crystalline phase and

Ba-C was the minor crystalline phase and that a solid solution was evident in the cordierite structure.

The bodies possessed high density approximately 95% of true density, a 0.00% moisture absorption, low thermal expansions (1.37 to 2.11 x 10^{-6}) extended firing ranges (50 to 150°F), high transverse strengths (11,000 to 17,000 psi), good electrical properties (dielectric constant 4.63, power factor 0.0033, at 1 Mc/sec), high Young's modulus (1.1 to 1.3 x 10^{12} dynes/cm^2), low internal friction (1.3 to 1.9 x 10^{-4}), and a high thermal shock capability ($\triangle$ T = 1000°C). In all cases the firing range increased and the values of the physical properties were diluted with an increasing amount of additive glass.

In an analysis of thermal shock resistance, the values of internal friction and Young's modulus were measured at various temperature gradients. Above a 200°C quench, the internal friction value increased and the Young's modulus value decreased with an increasing thermal gradient. The change in values was directly attributed to small thermally induced cracks whose population was a function of the thermal gradient.

6. Bibliography

1. Tyrrell, M. E., Gibbs, G. V., Shell, H. R., "Synthetic Gardierite," Bulletin 594, Bureau of Mines, U. S. Dept. of Interior, Washington, D. C., (1961).

2. Wisely, H. R., "Phases in the Quaternary System Bao-Mgo-Al$_2$O$_3$-SiO$_2$," Doctoral Thesis, Rutgers, The State University, New Brunswick, N. J., (1952).

3. Zener, C., Elasticity and Anelasticity of Metals, The University of Chicago Press, Chicago 1948.

4. von Rotger, H., "Elastic Relaxation Behavior of Simple and Mixed Alkali Silicates and Borax," Glass Tech. 31, 54-60 (1958).

5. Reid, D., Final Report Contract NOw-65-0294-d, Rutgers, The State University, New Brunswick, N. J., June 1966.

6. Marino, A., Personal Communication.

7. Kingery, W. D., Introduction to Ceramics, John Wiley & Sons Inc., New York-London, 1960.

8. Matusik, F. J., "Structure, Composition, Bond Strength," Ceramic Age 80, 40-50 (1964).

A complete bibliography on "Cordierite" appears in Progress Report No. 3, Contract NOw-64-0040-d.

C. Comparison of Several One and Two Glass Compositions

In the Final Report of Contract NOw 65-0199-d dated December 1, 1964 to December 15, 1965, which contains the results of earlier effort on this research program "Studies of Ceramic Processing," the results of the work on the one glass approach of this prereacted materials process were reported. In this approach the total composition is fritted. It is so designed that after comminuting the frit, and forming specimens, a crystalline phase devitrifies during firing resulting in a composite body. Two compositions identified as C-8 and C-13 proved to be the best. The raw composition of the former is 35% MgO, 23% Al$_2$O$_3$ and 32% SiO$_2$; the latter composition is 10% MgO, 35% Al$_2$O$_3$ and 55% SiO$_2$. Table IX on page 78 compares the properties and astructure of several one-glass compositions to those of several of the better two-glass compositions. The structures are comparable for those of approximately the same cordierite content, i. e., C-8 and 80-20; and C-13 and 90-10. This includes crystal size and content, void size and content, and size and shape of the larger glassy areas. This is further illustrated by comparing the photomicrographs for compositions C-8 and C-13 in Figure 8 on page 20 with those for the two-glass compositions shown in Figure 16 on page 59. In Figure 8 the large light gray crystals are forsterite; the dark gray firings-shaped areas enclosed by dark lines are glass; and the inducing gray matrix is cordierite. The large voids are due to binder burnout. The glass appears to be better distributed and to exhibit fewer larger areas in the one-glass composition.

In general the properties are very similar and the only outstanding difference is in the firing range. For the one-glass compositions it is only 30°F, while for the two-glass system it is a minimum of 50°F at the lowest glass content and increases with the content of the additive glass to 150°F at 30%. This may be due to the fact that both the crystalline

TABLE IX

Comparison of Properties of Several One and Two Glass Compositions

	One Glass Compositions		Two Glass Compositions		
	C-8	C-13	90% C-0 10% C-A	80% C-0 20% C-D	70% C-0 30% C-E
Cordierite (%)	72.6	86.3	85.8%	72.7	64.5
Secondary Phases (%)	19.3	8.6	10.2	18.9	28.6
Voids	8.1	5.1	4.0	8.4	6.9
Cordierite Crystal Size	2-4	2-4	3-5	3-5	3-5
Secondary Crystal Size	$3-10^2$	$3-10^3$	$1-8^1$	$1-8^1$	$1-8^1$
Glass Average Size	3x1	3x1	3x1	3x1	3x1
Void Size[4]	5+	5+	10	10	10
Density (gr/cc)	2.45	2.41	2.??	2.30	2.25
Moisture Absorption (%)	0.10	0.00	0.00	0.00	0.00
Firing Temp.(°F)	2525	2600	2625	2500	2375
Firing Range (°F)	30	30	50	100	150
Coef. Lin. Ther. Exp. ($\times 10^{-6}$)	1.97	1.69	1.55	1.86	1.73
Transverse Str. (psi)	13,300	15,500	16,500	12,600	11,470
Firing Range (°F)	30	30	50	100	150

1 - Ba-C   2 - Forsterite   3 - Mullite   4 - Large voids due to binder burnt

phase and the glassy phase are magnesium aluminosilicate compositions. These phases in the two-glass system are of different composition and made separately.

D. One-Glass Compositions in the BaO-MgO-Al$_2$O$_3$-SiO$_2$ System

1. Introduction

As noted above the two-glass approach to the devitrified type composition definitely has a desirable long firing range; however the microstructure tends to suffer in that both the bonding glass and that which produces cordierite on devitrifying, is added as dilute particles whose average particle size is approximately 5 microns with an appreciable percentage up to 44 microns. On firing this immediately results in larger cordierite crystals and glass pockets or volumes. This results in an improved structure with respect to conventional cordierite compositions but leaves much to be desired. Further improvement will result in improving the engineering properties. By applying the one-glass approach the complete composition can be mixed thoroughly on an atomic basic and devitrification will occur much more uniformly resulting in greatly improved structure. The earlier effort with the one glass system suffered because both the glass and the cordierite were magnesium aluminosilicates. This resulted in considerable interaction of the two phases resulting in greater crystal growth and conversely, rapid solution of the crystals in the glass. The success of the one glass system depends on the proper design of the glassy phase with respect to cordierite.

The object of this phase is to study the one-glass system of the devitrification approach to prereacted raw materials. Special emphasis will be placed on glass composition and on the mechanics of devitrification and sintering in this type system. Improved structure will result in improved engineering properties.

2. Technical Approach

Compositions evaluated in the two glass system could not be used here. Several were prepared, but as single glasses they started to melt or overfire before the cordierite devitrified, resulting in very poor bodies whose properties could not be determined. One of the investigators has had appreciable experience in low loss statistics. The best fluxing compositions are within the BaO·Al$_2$O$_3$·SiO$_2$ system. The approximate composition of such a fluxing system or glassy phase was calculated and used

Figure 20

Photomicrographs of
One-Glass Compositions C-8 and C-13

Composition C-8
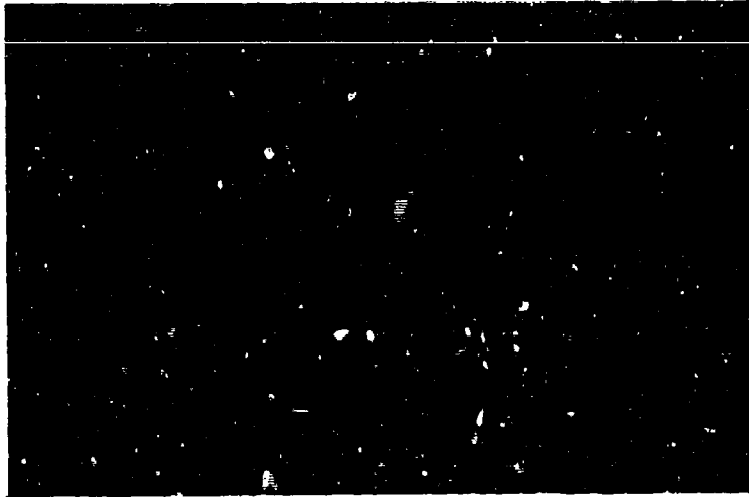
Composition C-13
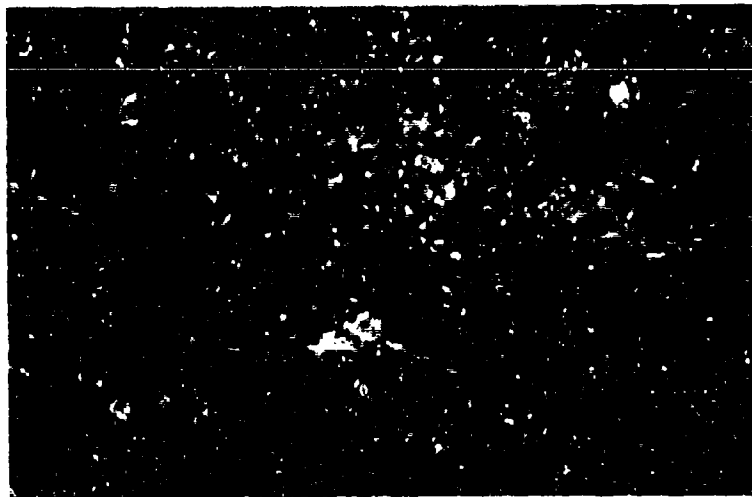
700x   ——10 Microns

for this work. The initial composition investigated was selected as to contain 80% cordierite and 20% of this $BaO.Al_2O_3 \cdot SiO_2$ system. Variations were made in the composition of the bonding glass and several percentage of the cordierite compositions were used including 80 and 90%. The oxide compositions of the three additive glass and cordierite selected for study are shown in Table X on page 82 along with the finer frit compositions investigated. Included is the additive or bonding glass-cordierite ratios. The properties evaluated were essentially those described in earlier sections.

3. Experimental Approach

Batch compositions were calculated to give the desired weight percents of each constituent. 2000 gm batches were mixed and blended in a twin-shell blender for one hour. The material was then packed into fire clay crucibles and calcined to 1800°F in a gas fired kiln. In the calcining operation the temperature was raised from room temperature to 1800°F in four hours and soaked for one hour. The purpose of the calcining operation was to reduce the bulk of the batches by driving off the CO_2. The calcined material was then passed through an 80 mesh screen to break up agglomerantes and repacked into fire clay crucibles, and fritted. All compositions melted between 2700 and 2760°F. They were heated to melting in 5 to 6 hours and held at the temperature of desired fluidity for 1/2 hour, then poured into cold water. A second approach eliminated the calcining step and involved adding material to the heating batches as its bulk decreased. The end product was found to be the same for both approaches.

The fritted glasses were dried at 250°F overnight. They were then ground dry for 48 hours in an alumina mill with a controlled size distribution of alumina grinding media. After dry grinding, distilled water was added to aid in removal of the material and to pass it through a 325 mesh screen. After drying the agglomerates were passed through 80 mesh.

The glass powder was mixed with 5% by weight distilled water in an alumina mortar and pestle, then passed through a 16 mesh screen to produce granules which would uniformly fill the die cavity. For pressing, hardened steel dies were used and a pressure of 10,000 psi was applied by means of a hand operated hydraulic press. The cavity was de-aired during the pressing operation. Discs one inch in diameter by 3/8" thick and bars 3" x 1/2" x 1/2" were pressed and then allowed to dry at room

TABLE X

Compositions of Additive Glasses, Cordierite and Frits

	Additive Glasses			Cordierite
	GI	G2	G3	Co
BaO	25.8	38.7	12.9	-
MgO	-	-	-	13.7
Al$_2$O$_3$	11.2	11.2	11.2	34.9
SiO$_2$	63.0	50.1	75.9	51.4

	Frit Compositions				
	20% Glass-80% Co			10% Glass-90% Co	
	G1	G2	G3	G1	G2
BaO	5.2	7.5	2.6	2.6	3.9
MgO	10.9	11.0	11.0	12.3	12.3
Al$_2$O$_3$	30.1	30.2	30.2	32.5	32.5
SiO$_2$	53.8	51.1	55.3	52.6	51.3

temperature for two days before being fired. Firing was carried
out in an electric resistance furnace on a schedule of 5 hours
to reach temperature plus a one hour soaking period.

Several properties were determined. Percent moisture absorp-
tion and bulk density procedures were discussed above. Firing
range was established by determining the firing temperature in-
terval over which the bulk density was constant and moisture
absorption did not exceed 0.05%. Qualitative cordierite for-
mation was determined by major peaks intensities as determined
by x-ray analysis. Coefficient of linear thermal expansion was
measured by the interferometric method over the temperature
range 25-625°C with a heating rate of 50°C per minute. Trans-
verse strength values were measured with an Instron Tensil
Tester using a 2 inch span. These latter two properties were
determined for all compositions fired to that temperature which
resulted in maximum cordierite formation.

4. Results and Discussion

All compositions and results are presented in Table XI on
page 84. This table is set up so as to reflect an increase of
silica at the expense of baria form left to right. The effect
of firing temperature on moisture absorption, bulk density and
x-ray intensity is presented in Figure 21 on page 85. All com-
positions but 20G3-80Co fired to 0.00% moisture absorption
from 2150°F to their respective overfiring temperatures. This
exception which contains a 20% addition of the glass having the
lowest baria content, did not become impervious until 2600°F.
It is anticipated that the resulting higher silica content makes
a more refractory glass which does not behave very well as a
diversifier. The bulk density of this composition increases
slightly between 2300 and 2650°F as the moisture content de-
creases.

The bulk densities of these compositions range from approx-
imately 2.3 to 2.8 gr/cc over the entire firing range. For the
individual compositions, the densities curves are fairly smooth.
Their magnitude at the 80% cordierite level vary directly with the
baria content which is to be expected because of the high density
of the oxide. Further, the maximum maturing temperature decreases
as the silica content decreases. This is due to the decrease in
the glass former or silica and resulting increase in the glass
modifier namely, baria. The same is true for 90% cordierite
level except that the density difference is not significant.
From the moisture absorption and bulk densities the firing range
for all compositions varies from 150-300°F.

TABLE XI

Compositions and Properties of the One Glass Series

Compositions (Weight %)

	20G	20G1	20G2	10G1	10G2
BaO	2.58	5.10	7.54	2.58	3.97
MgO	10.96	10.94	10.98	12.33	12.33
Al_2O_3	30.16	30.10	30.16	32.53	32.53
SiO_2	55.30	53.80	51.12	52.56	51.27

Properties (still must include firing range)

Firing Temp. (°F)		20G	20G1	20G2	10G1	10G2
1950	M.A.[1]			0.00		
	B.D.[2]			2.71		
2150	M.A.		0.00	0.00		0.00
	B.D.		2.43	2.60		2.52
2250	M.A.		0.00	0.00	0.00	0.00
	B.D.		2.44	2.62	2.52	2.54
2300	M.A.	1.98	0.00			
	B.D.	2.32	2.49			
2350	M.A.		0.00		0.00	0.00
	B.D.		2.52		2.51	2.52
2400	M.A.		0.00			
	B.D.		2.57			
2450	M.A.	1.37			0.00	0.00
	B.D.	2.36			2.52	2.51
2550	M.A.				0.00	
	B.D.				2.87	
2600	M.A.	0.00				
	B.D.	2.42				
2650	M.A.	0.00			0.03	
	B.D.	2.42			2.59	

Transverse Strength (psi)

	20G	20G1	20G2	10G1	10G2
	15,800	16,100	13,200	21,200	20,500

Coef. Linear Thermal Exp. ($\times 10^{-5}$/"/"/°C)

	20G	20G1	20G2	10G1	10G2
	1.62	1.68	1.81	1.57	1.46

Figure 21-Properties vs. Firing Temperature of One Frit Bodies
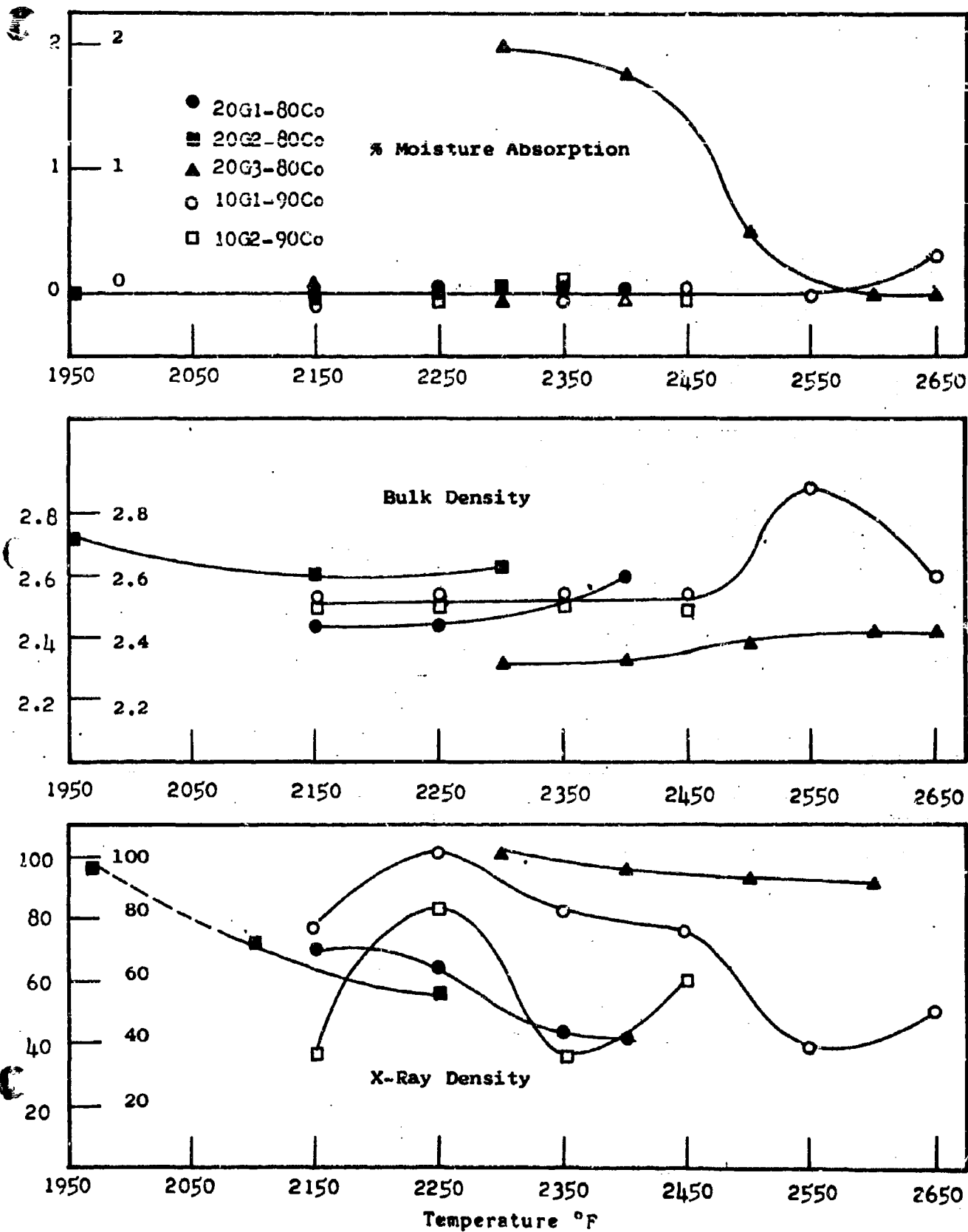
The most promising of all the compositions studied, 10G1-90Co was investigated for true specific gravity. It was found that an average value of 2.58 was realized. Comparing this to the bulk density for the same composition (2.52) it was found that the fired samples had reached 97.6% of true density. This means that the closed pore volume is less than that obtained for the two-frit compositions and helps to explain (in the following discussion) the increase in physical properties that the one-frit compositions have over the two-frit compositions. It is felt that the increased true specific gravity is due to the inherent nature of the one-frit process since the entire composition is being mixed on an atomic basis.

The extent of cordierite formation was not as constant with temperature as was bulk density. X-ray diffraction techniques using the powder method were used to identify the crystalline phases present and this relative amount. In all cases cordierite was found as the dominant crystalline phase. There were indications of secondary crystalline phases; however these were difficult to distinguish. In general, there appeared to be maximum cordierite formation at and around 2250°F, however, there was one firing temperature at which the maximum amount was realized in each composition. Above each critical temperature there was a decrease in all the cordierite peak intensities and below these temperatures the samples had not yet reached maturity. For compositions containing 10% glass there was appreciable cordierite formation over the temperature ranges as shown in the figure. Specifically, composition 10G1-90Co had the largest amount of cordierite formed over the largest temperature range while still maintaining a constant bulk density at a 0.00% moisture absorption. Through composition 10G2-90Co did not develop as much of the cordierite phase it did behave in a similar manner to the 10G1-90Co composition. Again, the 10G2-90Co composition had more BaO than that of the 10G1-90Co composition.

Of the compositions corresponding to 20% glass the 20G3-80Co composition developed an appreciable amount of cordierite from 2300 to 2650°F; however, as mentioned earlier the moisture absorption did not reach 0.00% until 2600°F. Here, due to the refractoriness of the glass the crystalline cordierite was able to remain stable over a high temperature range without any appreciable solution of the crystalline phase in the glass. On the other hand composition 20G1-88Co reported as having a firing range of from 2150 to 2350°F behaved differently. Upon

x-ray examination it was found that the samples fired to 2150°F had a larger amount of cordierite present than those fired at 2350°F. It is felt that at 2350°F there was considerable solution of the cordierite phase in the relatively low melting bonding glass. It is due to the higher baria content which reacts with the cordierite to dissolve a considerably amount and form a lower firing body.

Specimens of composition 20G2-80co fired to 1950°F did not develop any of the stable high temperature form of cordierite. However, the dominant crystalline phase was the metastable low temperature form, -cordierite. Rankin and Merwin Ternary System: MgO-Al$_2$O$_3$-SiO$_2$," Am. Jour. Sci., 45 4 301 (1918) reported the inversion of the metastable low temperature form,
μ cordierite, to the stable high temperature form, μ cordierite, as taking place between 1740 and 2100°F. They also reported a 4.7% volume increase which accompanies the inversion. This could account for the decrease in bulk density from 1950 to 2150°F. Thus this composition has the lowest maturing temperature and range; the largest amount of glass; and the greatest solubility of cordierite. It also has the highest baria content. This explanation is applicable to this entire series.

For the evaluation of physical properties specimens wei used of each composition fired to that temperature which resulted in 0.00% moisture absorption, highest bulk density and greatest cordierite development. The transverse strength ranged from 13200-21,200 psi with the 90% cordierite compositions resulting in values over 20,000 psi. The 80% cordierite compositions ranged from 13,200-16,100 with the highest values realized at the intermediate baria content. The coefficients of linear thermal expansion between room temperature and 625°C were lowest for the 90% corierite compositions with an average value of 1.46 x 10^{-6}. At the 80% cordierite level the values were slightly higher ranging from 1.62-1.81 with these values increasing as the baria content increased. Figure 22 on page 88 is a typical expansion vs temperature curve for this type composition.

The macrostructure of the compositions studied was excellent except for possibly two of the 20% glass compositions, namely 20G1-80Co and 20G2-80Co. Specimens of these compositions exhibited glossy surfaces and in fact some were quite translucent. This was undoubtedly due to a high glass content with less of the crystalline phase. This was confirmed by x-ray investigation.

Figure 22

Typical Thermal Expansion vs. Temperature
Curve for the One Class Type Composition

Temperature °C
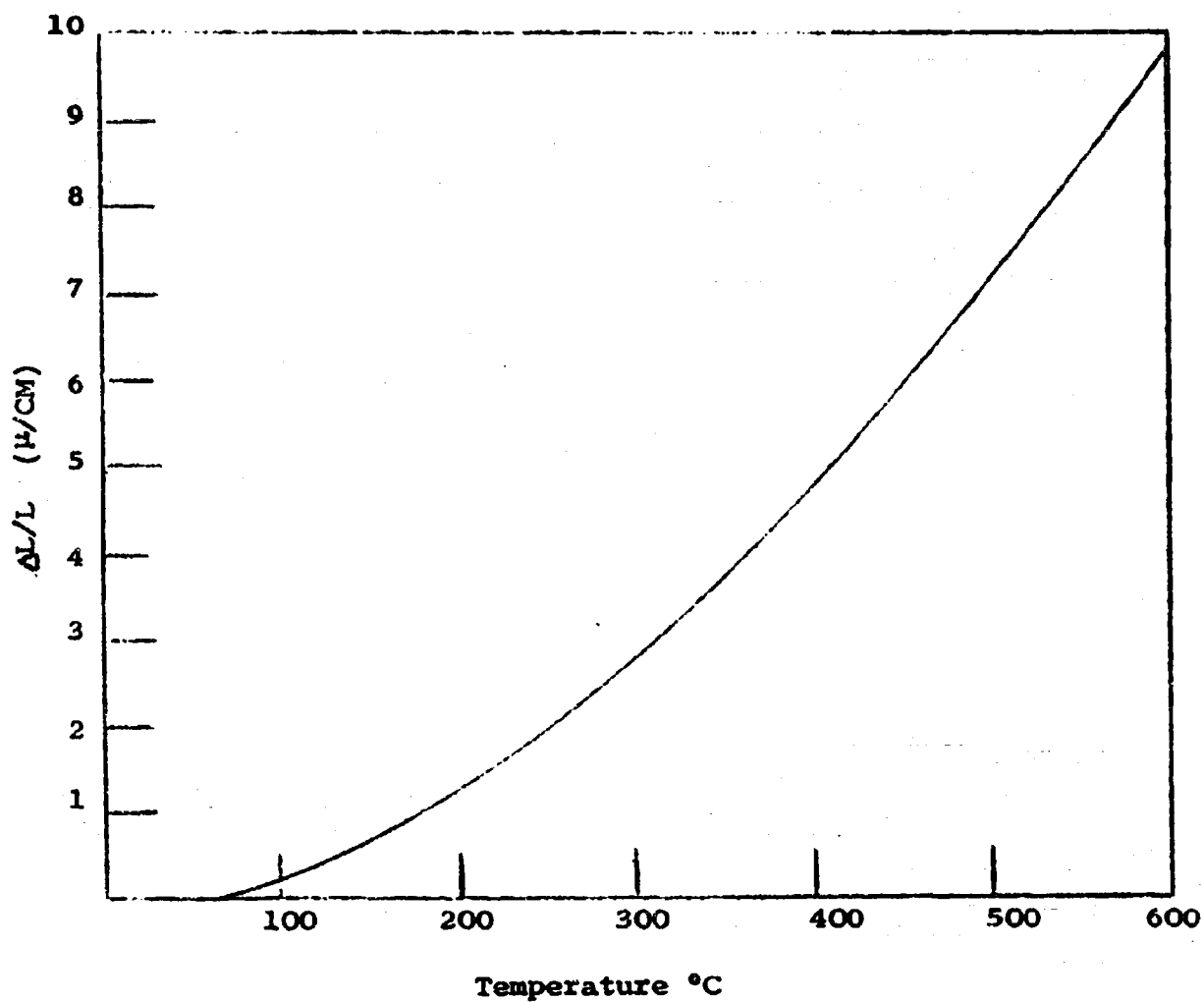
On the other hand, both the exterior surfaces and fractured
surfaces of all the other compositions were extremely dense
and uniform with no translucency. Though some solution
of the cordierite phase did take place in all compositions
fired above the maximum cordierite formation temperature no
slumping or rounding of the corners was observed, except in
the 20% glass compositions which exhibited some translucency.
The macrostructure of the 10% glass compositions was extremely
good. There was no visible difference between samples fired at
2150 and 2450°F. However, some bloating of samples of 10G1-
90C1 was observed on firing to 2550°F.

The microstructure was investigated by means of both light
and electron microscopes. Specimens were etched at 5 minute
intervals from 5 to 40 minutes in a 5% solution of H_2SiFe in
order that the individual grains might be seen. Unfortunately,
little could be seen in any of the specimens examined, using a
light microscope at 400X to 700X. This was due two things:
one, the inability of the etchant to preferentially attack the
bonding glass and, two the extremely small size of the crystals.
It was determined using the electron microscope (transmission
technique) that most of the crystals were of the order of the
1μ in size. The porosity in the specimens was minor and thorgh-
out the bulk of the specimens. Some difficulty was throughout
in determining true density (picometer), however from this and
the electron microscope work it is anticipated that the bulk
density of the best composition are greater than 98% of true
density.

5. Summary

The devitrification approach to the prereacted raw mater-
ials technique shows promise in the development of cordierite
compositions utilizing the one-glass system. Increased strength,
low thermal expansion and improved microstructure has resulted.

The extent of cordierite formation depends a great deal on
the composition and amount of the glassy phase. This effort
dealt with compositions in the $BaO \cdot MgO \cdot Al_2O_3$ SiO_2 system. There
was no difficulty in producing bodies of any of the compositions
studied which had a constant bulk density while remaining at
0.00% moisture absorption over an extended firing temperature
range. In general, for glasses containing less BaO, more re-
fractory bodies were obtained. As the BaO content increased
both higher densities and low maturing temperatures were realized;

this was accompained by a decreased cordierite formation. For the high BaO glass compositions, especially for the 20% additions, glass crystal reactions were taking place after the formation of cordierite which led to the solution of some of the crystalline phases. By proper choice of the composition and amount of the glassy phase the glass to crystal reaction can be controlled to the point where a sufficient amount of crystalline cordierite is present to control the overall expansion of the body while still remaining imprevious with a constant bulk density over an extended temperature range. Transverse strengths to 21,000 psi were realized along with coefficients of linear thermal expansion as low as 1.46×10^{-6}.

E. Summary

In the initial investigation of the devitrification approach to the raw materials technique compositions in the ternary system $MgO-Al_2O_3-SiO_2$ were investigated. The complete compositions were melted in a single fritting operation. It was found that a composition far removed from the theoretical cordierite composition was necessary to form bodies having 0.00% moisture absorption and at least 25°F firing range while still maintaining an appreciable amount of the crystalline phase to control the thermal expansion (Final Report Now 64-0040-d and Section C above). Properties are summarized in Table V on page 44. In that study the best body exhibited the following physical properties;

1. Firing range 30°F
2. Maximum transverse strength of 15,500 psi
3. Coefficient of linear thermal expansion (1.69×10^{-6} "/"/°C)
4. Firing temperature of 2600°F

In an effort to improve on the overall physical properties of the initial effort with the one frit system, a two-frit approach was investigated as discussed in Section B above. This approach utilized the addition of a low-melting, devitrifiable glass (10, 20 and 30% additions) to the cordierite glass in order to maximize the cordierite development, extend the firing range and mature the body. The Properties of the best bodies are shown in Table V on page 43:

1. Firing range as high as 150°F
2. Maximum transverse strength of 16,600 psi
3. Coefficient of linear thermal expansion below 1.55×10^{-6} "/"/°C
4. Firing temperature of 2525°F

However, it should be pointed out that the extended firing range
of 150°F was only realized in bodies containing a 30% addition
of the low-melting glass. For these bodies the thermal expansions
were greater then 1.77×10^{-6} "/"/°C with the majority being approx-
imately 1.95×10^{-6} "/"/°C while having decreased strengths in the
neighborhood of 11,900 psi. In other words, the compositions
which had thermal expansions below 1.55×10^{-6} "/"/°C and strengths
of 15,600 psi corresponded to compositions having a 10% addition
of the low-melting glass. These latter compositions had firing
ranges of only 50°F, though this is an adequate firing range for
commercial use. This means that as the firing range increased
for the two-frit compositions the physical properties became
poorer.

The results compare quite favorably; however the specimens
prepared by two-glass systems exhibit a slightly greater firing
range and strength, and a slightly lower coefficient of linear
thermal expansion. This is undoubtedly due to the fact that
the 3 to 30 micron particles of the cordierite glass resulted in
larger agglomerations of crystals which are not attacked as
readily by the glassy phase. The photomicrographs show slightly
improved or more desirable structure for the one glass specimens;
however this type composition studied, $MgO-Al_2O_3-SiO_2$, results
in the shorter firing range, etc.

These findings indicated that the one glass approach should
be studied more thoroughly as it was anticipated that the micro-
structure could be improved giving rise to still a further in-
crease in physical properties while having a firing range much
greater than 50°F. The $BaO-MgO-Al_2O_3-SiO_2$ system was chosen for
this investigation based on the reasons stated in section D.

It was found that a firing range of 150°F could be obtained
with no difficult while the physical properties were considerably
improved. Transverse strength values greater than 20,000 psi
and thermal expansions as low as 1.46×10^{-6} "/"/°C were realized.
A more detailed comparison of the physical properties of the one
and two-frit systems is given in Table X on page 80. This in-
crease in physical properties is again a direct result of the
improved microstructure of the one-frit system.

Since all of the individual particles in the specimens
before firing were of the same composition and of a smaller size,
(-325 mesh instead of -200 mesh used in the two-glass system) dur-
ing the devitrification process the nucleating sites for the
cordierite phase are uniformly dispersed through the body. There-
fore, as the crystallization grain growth developed there was't

A large composition gradient from the center of each crystal to the glassy phase surrounding the crystals. This allows the two phases to be very compatible with each other decreasing the glass-crystal reactions taking place after the crystals are formed at and around the maximum cordierite formation temperature. Hence, an extended firing range is realized. The glass which does not crystallize also acts to inhibit the growth of the cordierite crystals not to the point of decreasing the amount of cordierite formed but only to the point of controlling the crystal size. This means that there are many small crystals being formed rather than a few larger ones which are separated by pockets of glass and secondary crystalline phases.

The following table is a summary of the pertinent properties of pure cordierite, the best as prepared by the two glass approach, and by the one glass approach. The advantages of the one glass approach are obvious.

Summary of Properties of the Best Cordierite
Composition Prepared by the Two-Glass and
One-Glass Systems and Compared to Pure Cordierite

	Pure	2 glasses	1 glass
Firing Temp. °F (specimens tested)	2600	2500-2600	2150-2450
Firing range		50%	150-300°F
% Moist. Absorp.	11.20	0.00	0.00
Bulk Density	2.52x	2.40	2.52
Coef. of Exp. ($\times 10^{-6}$ "/"/°C)	1.29	+1.55	21.46
Transverse Strength		16,600	21,200
Crystal size		3 to 10	1
Void content (%)		7	2-4
% of True Density		92-96[xx]	97.6[xxx]

[x] Attempts to fire to higher density resulted in overfiring.
[xx] Highest value only for very limited part of firing range.
[xxx] Essentially uniform for complete firing range.

DOCUMENT CONTROL DATA - R&D

(Security classification of title, body of abstract and indexing annotation must be entered when the overall report is classified)

1. ORIGINATING ACTIVITY *(Corporate author)*	2a. REPORT SECURITY CLASSIFICATION
Rutgers, The State University New Brunswick, New Jersey 08903	2b. GROUP

3. REPORT TITLE

STUDIES OF CERAMIC PROCESSING

4. DESCRIPTIVE NOTES *(Type of report and inclusive dates)*

Final; December 1, 1964, to December 15, 1965

5. AUTHOR(S) *(Last name, first name, initial)*

Smoke, E. J., Fleischner, P. L., Jacobs, W. G., and Mangino, D. R.

6. REPORT DATE December 16, 1965, to February 15 1967	7a. TOTAL NO. OF PAGES 90	7b. NO. OF REFS 43
8a. CONTRACT OR GRANT NO. NOw 66-0205-d	9a. ORIGINATOR'S REPORT NUMBER(S)	
8b. PROJECT NO.		
c.	9b. OTHER REPORT NO(S) *(Any other numbers that may be assigned this report)*	
d.		

10. AVAILABILITY/LIMITATION NOTICES

Distribution of This Document is Unlimited.

11. SUPPLEMENTARY NOTES	12. SPONSORING MILITARY ACTIVITY Naval Air Systems Command

13. ABSTRACT

The object of this program is to improve the structure of ceramics by processing. The overall temperature range of interest is 1800°F to above 3000°F. In the high portion of the range, 3000°F and above, spinel $MgO-Al_2O_3$ is presently under study. The parameters have been established for preparing suitable starting materials. Pure alums which by proper heat treatment result in the formation of ultra fine, pure magnesia and alumina, have been studied along with the formation of spinel. DTA, TGA, X-ray, electron microscopy, etc., have been utilized. Three compositions are of particular interest namely, $0.9MgO \cdot 1.0Al_2O_3$, $1.0MgO \cdot 1.0Al_2O_3$ and $1.0MgO \cdot 0.9Al_2O_3$. They have been studied as starting materials prereacted over the temperature range 950-1200°C and as bodies made of these prereacted materials and fired over the range 1370-1650°C. The intermediate temperature range 2600-3000°F, was studied utilizing the presintering approach to the prereacted raw materials technique and the results were reported in earlier reports. The low range, 1800-2600°F, was studied using the devitrification approach of the prereacted raw material technique. Cordierite is the crystalline phase of particular interest because of its low thermal expansion. The one-glass and the two-glass approaches have been studied. Processing, structure and properties are presented and compared.

DD FORM 1473 and properties are presented and compared.

14. KEY WORDS	LINK A		LINK B		LINK C	
	ROLE	WT	ROLE	WT	ROLE	WT
sinter						
prereaction						
devitrification						
presintering						
structure						
composite						
cordierite						
alumina						
bonding glass						
fluxing						

INSTRUCTIONS

1. ORIGINATING ACTIVITY: Enter the name and address of the contractor, subcontractor, grantee, Department of Defense activity or other organization (corporate author) issuing the report.

2a. REPORT SECURITY CLASSIFICATION: Enter the overall security classification of the report. Indicate whether "Restricted Data" is included. Marking is to be in accordance with appropriate security regulations.

2b. GROUP: Automatic downgrading is specified in DoD Directive 5200.10 and Armed Forces Industrial Manual. Enter the group number. Also, when applicable, show that optional markings have been used for Group 3 and Group 4 as authorized.

3. REPORT TITLE: Enter the complete report title in all capital letters. Titles in all cases should be unclassified. If a meaningful title cannot be selected without classification, show title classification in all capitals in parenthesis immediately following the title.

4. DESCRIPTIVE NOTES: If appropriate, enter the type of report, e.g., interim, progress, summary, annual, or final. Give the inclusive dates when a specific reporting period is covered.

5. AUTHOR(S): Enter the name(s) of author(s) as shown on or in the report. Enter last name, first name, middle initial. If military, show rank and branch of service. The name of the principal author is an absolute minimum requirement.

6. REPORT DATE: Enter the date of the report as day, month, year; or month, year. If more than one date appears on the report, use date of publication.

7a. TOTAL NUMBER OF PAGES: The total page count should follow normal pagination procedures, i.e., enter the number of pages containing information.

7b. NUMBER OF REFERENCES: Enter the total number of references cited in the report.

8a. CONTRACT OR GRANT NUMBER: If appropriate, enter the applicable number of the contract or grant under which the report was written.

8b, 8c, & 8d. PROJECT NUMBER: Enter the appropriate military department identification, such as project number, subproject number, system numbers, task number, etc.

9a. ORIGINATOR'S REPORT NUMBER(S): Enter the official report number by which the document will be identified and controlled by the originating activity. This number must be unique to this report.

9b. OTHER REPORT NUMBER(S): If the report has been assigned any other report numbers (either by the originator or by the sponsor), also enter this number(s).

10. AVAILABILITY/LIMITATION NOTICES: Enter any limitations on further dissemination of the report, other than those imposed by security classification, using standard statements such as:

(1) "Qualified requesters may obtain copies of this report from DDC."

(2) "Foreign announcement and dissemination of this report by DDC is not authorized."

(3) "U. S. Government agencies may obtain copies of this report directly from DDC. Other qualified DDC users shall request through

_____."

(4) "U. S. military agencies may obtain copies of this report directly from DDC. Other qualified users shall request through

_____."

(5) "All distribution of this report is controlled. Qualified DDC users shall request through

_____."

If the report has been furnished to the Office of Technical Services, Department of Commerce, for sale to the public, indicate this fact and enter the price, if known.

11. SUPPLEMENTARY NOTES: Use for additional explanatory notes.

12. SPONSORING MILITARY ACTIVITY: Enter the name of the departmental project office or laboratory sponsoring (paying for) the research and development. Include address.

13. ABSTRACT: Enter an abstract giving a brief and factual summary of the document indicative of the report, even though it may also appear elsewhere in the body of the technical report. If additional space is required, a continuation sheet shall be attached.

It is highly desirable that the abstract of classified reports be unclassified. Each paragraph of the abstract shall end with an indication of the military security classification of the information in the paragraph, represented as (TS), (S), (C), or (U).

There is no limitation on the length of the abstract. However, the suggested length is from 150 to 225 words.

14. KEY WORDS: Key words are technically meaningful terms or short phrases that characterize a report and may be used as index entries for cataloging the report. Key words must be selected so that no security classification is required. Identifiers, such as equipment model designation, trade name, military project code name, geographic location, may be used as key words but will be followed by an indication of technical context. The assignment of links, roles, and weights is optional.

DD FORM 1473 (BACK)
1 JAN 64